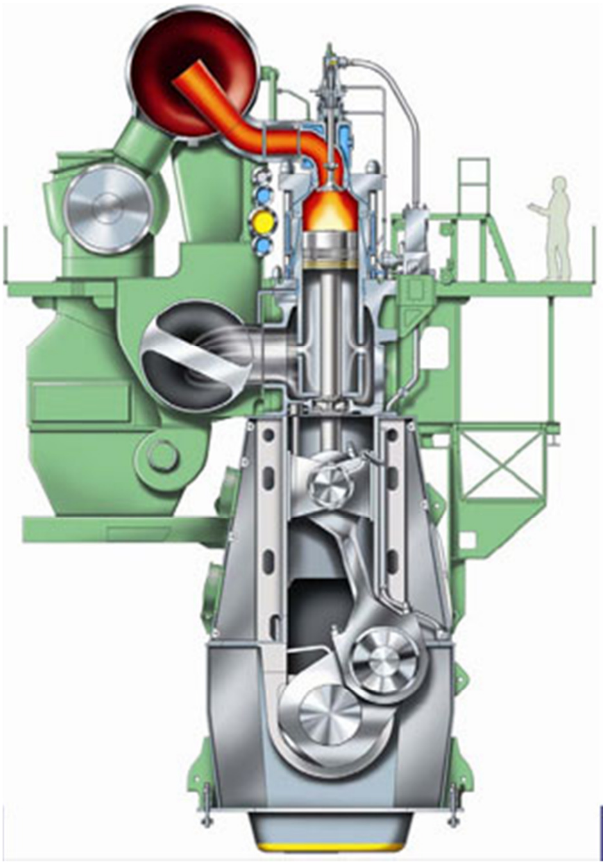

This thesis entitled:

Evaluation of Selective Catalytic Reduction for Marine Two-Stroke Diesel Engines

is submitted in partial fulfillment of the requirements for

the Master of Science degree from

Aalborg University

Thermal Energy and Process Engineering

Lenka S. Chladova

10 December 2010

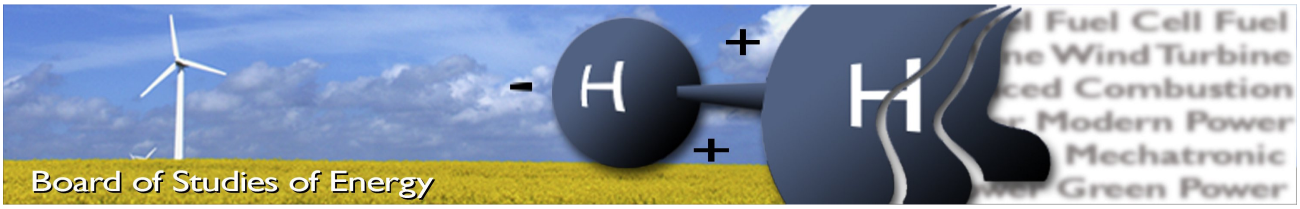

Title: **[Evaluation of Selective Catalytic Reduction for Marine Two-Stroke Diesel Engines]**
Semester: **[10]**
Semester theme: **[Thesis]**
Project period: **[]**
ECTS: **[]**
Supervisor: **[Tom Condra]**
Project group: **[]**

SYNOPSIS: Due to an increased emphasis on the reduction of emissions from commercial cargo ships, there has been increased interest in applying emissions reduction technology to marine vessels. This paper investigates the application of selective catalytic reduction (SCR) for the purpose of reducing NOx emissions from a large bore slow speed marine diesel engine of the type that would be typical of a PANAMAX containership. Selective catalytic reduction, which relies on a catalyst to promote a reduction reaction between NO and NH3, is is a well-established technology that has seen wide application in the shoreside power generation industry, but for which there have been relatively few applications to marine low speed diesel engines. This paper investigates the feasibility of applying a selective catalytic reactor to a large containership propulsion engine by developing a program for sizing SCR units for various applications. The program is evaluated for an MAN K90 MC-C and K98 MC-C engines, and the relevant system parameters such as catalyst dimensions, flow rates, Urea consumption, and NOx reduction profiles are presented.

Lenka S. Chladova

[Name 1]

[Name 2]

[Name 3]

[Name 4]

[Name 5]

[Name 6]

Copies:	[1]
Pages, total:	[84]
Appendix:	[45]
Supplements:	[0]

By signing this document, each member of the group confirms that all participated in the project work and thereby that all members are collectively liable for the content of the report.

ABSTRACT

Due to an increased emphasis on the reduction of emissions from commercial cargo ships, there has been increased interest in applying emissions reduction technology to marine vessels. This paper investigates the application of selective catalytic reduction (SCR) for the purpose of reducing NOx emissions from a large bore slow speed marine diesel engine of the type that would be typical of a PANAMAX containership. Selective catalytic reduction, which relies on a catalyst to promote a reduction reaction between NO and NH3, is is a well-established technology that has seen wide application in the shoreside power generation industry, but for which there have been relatively few applications to marine low speed diesel engines. This paper investigates the feasibility of applying a selective catalytic reactor to a large containership propulsion engine by developing a program for sizing SCR units for various applications. The program is evaluated for an MAN K90 MC-C and K98 MC-C engines, and the relevant system parameters such as catalyst dimensions, flow rates, Urea consumption, and NOx reduction profiles are presented.

ACKNOWLEDGEMENTS

I am deeply grateful to the many people who have helped me to see this project to fruition.

First and foremost, I would like to thank Henrik Trolle Jacobsen and Francesco Castellino at Haldor Topsoe for their invaluable support and enthusiasm.

I would also like to thank Kevin Krick at American President Lines for providing me with a source of usable emissions data and Micheal Miller at Avogadro Group for the guidance that he provided regarding emissions testing.

TABLE OF CONTENTS

Abstract i

Acknowledgements iii

Table of Contents v

List of Figures vii

1 Introduction 1

1.1 Problem Statement 2

1.2 Limitations 2

2 Background 4

2.1 Environmental Impacts of Shipping and NO_X Emissions 4

2.2 NO_X Generation Abatement from Marine Low-Speed Diesel Engines 5

2.2.1 Low-Speed Diesel Engines and Exhaust Systems 5

2.2.2 Fuel description and combustion 6

2.2.3 Mechanisms of NO_X Formation 7

2.2.4 NO_X formation in low-speed Diesel Engines 9

2.2.5 NO_X Reduction Technology 12

2.2.6 Regulatory Requirements 15

2.3 Selective Catalytic Reduction 16

2.3.1 Chemical Reactions 16

2.3.2 Decomposition of Urea 17

2.3.3 Selective Catalytic Reduction 17

2.3.4 Oxidation of SO_2 18

2.3.5 Catalyst Function and Description 18

2.3.6 Mechanisms of Catalysis 20

2.3.7 Reaction Kinetics 21

2.3.8 Influence of Catalyst Microstructure 22

2.3.9 Catalyst Deactivation 24

2.3.10 Overall Mass Transfer and Bulk Fluid Motion 25

2.3.11 Convective Mass Transfer 27

2.3.12 Intraporous Mass Transfer 28

2.3.13 Catalyst Selection 30

2.3.14 SCR for Marine Applications........31
3 Model........36
3.1 Program Description........36
3.1.1 Governing Equations:........37
3.1.2 Programming concept........38
3.2 Model Assumptions........39
4 Model Description........41
4.1 Module 1: Calculation of exhaust gas flow rate........41
4.2 Module 2:........44
4.3 Module 3:........45
4.4 Module 4: Urea consumption and storage requirements........47
4.5 Module 5: Diffusion Coefficients........49
4.6 Module 6: Catalyst properties........50
4.7 Module 7: SCR Reactor........53
5 Results........58
6 Discussion........65
6.1 Feasibility of Application of SCR........67
7 Conclusions........69
8 Recommendations for future work........70
Selected Bibliography........71
Appendices........74

LIST OF FIGURES

Figure 1 - Comparison of Transportation Modes' Emissions Contribution. (1) 4
Figure 2 - Cross-Section of a K90MC-C Low-Speed Diesel Engine 5
Figure 3 - Effect of burned gas conditions on relative contributions to NO_x from the thermal, N_2O intermediate, and N_2O extension mechanisms. (13) 12
Figure 4 - Schematic of a Typical SCR System. (21) 16
Figure 5 - Example of Typical Honeycomb type Catalyst. (27)... 20
Figure 6 - Catalytic cycle for the SCR reaction over vanadia/titania. (23) 21
Figure 7 - Examples of Catalyst Pore Properties. (20)... 23
Figure 8 - Transport of Species within Catalysts of Different Structure. 26
Figure 9 – Effect of Vanadia Content on NO_X Reduction and SO_2 Oxidation. (23) 33
Figure 10 - Schematic of a Proposed Layout for an SCR Unit for a Marine Low-Speed Diesel Application. (27)... 35
Figure 11 - Installation of Honeycomb Catalyst Blocks. (27) 35
Figure 12 - NO_X Reduction Profile for an 11K90MC-C Marine Low-Speed Diesel Engine........ 59
Figure 13 - NO_X Reduction as a Function of Engine Load.. 61
Figure 14 - Required Reactor Length as a Function of Exhaust Temperature. 62
Figure 15 - Required Reactor Length as a Function of Reynolds Number. 63
Figure 16 - Required Reactor Length as a Function of Channel Width. 64

1 INTRODUCTION

For the past 40 years, low-speed diesel engines have been the propulsor of choice for large merchant vessels. In addition to their reliability and durability, low-speed diesel engines have the significant advantage of low fuel consumption relative to the power produced. Compared to other methods of propulsion, low-speed diesel engines have the additional advantage of being able to burn low-quality, and therefore lower cost, residual fuels with relative ease. This, combined with the overall efficiency of waterborne transport, has enabled low-speed diesel powered vessels to offer consumers a low cost and efficient method of moving goods and materials.

However, recent years have seen an increase in concern regarding the effect that commercial shipping is having on the environment and one of the issues that has received the most attention is the effect that airborne emissions from marine vessels are having on the environment.

Similar to other technologies that rely on combustion engines for power, the primary exhaust constituents of concern that are generated by ships' engines include CO_2, NO_X, SO_X, and particulate matter. However, relative to other combustion technologies, the emissions from low-speed diesel engines of the type that would typically be used for ship propulsion are characterized by increased levels in the emission of both the oxides of sulfur and nitrogen (SO_X and NO_X). Of the two, SOx is relatively easy to control by reducing the sulfur content of the fuel that is being burned. The reduction of NOx emissions, on the other hand, is much more problematic because the formation of NOx is a function of high local temperature within the combustion chamber.

Although there are a number of technologies that have been shown to reduce the emission of NO_X from low-speed diesel engines, there has not, until recently, been an incentive for shipowners to install the additional equipment aboard their vessels. However, with the adoption of recent regulations, the application of NOx reduction technologies will soon be compulsory for vessels operating in many of the world's busiest trading routes.

Shipboard installations of NOx reduction equipment are made complex by a series of considerations which are unique to the marine environment. These include the very significant constraint of limited space available for installation and the storage of raw materials, as well as other considerations such as the need for ease of operation and simplicity of maintenance, overall reliability, and increased resistance to damage from vibration and moisture.

Of the NO_X reduction systems currently available, one of the most promising is the installation of a Urea-based selective catalytic reduction (SCR) system which relies on the oxidation of NO_X over a titania-vanadia based catalyst. The principle advantages of the Urea based SCR systems are the high conversion rates that are attainable as well as the fact that SCR units do not appreciably increase the fuel consumption of the engine nor do they alter the engine’s basic operating principle so that it can operate at peak efficiency for each loading condition.

While there has been considerable experience with the application of Urea based SCR systems to large scale power plants and likewise to mobile truck applications, there have been relatively few marine installations. Even fewer of these have been installed on vessels with low-speed diesel engines and have tended to be relegated to the smaller bore engines.

The purpose of this paper is therefore to investigate the feasibility of using SCR technologies as the primary method of NO_X reduction for low-speed diesel propelled merchant vessels. By considering the extreme case of applying an SCR unit to a containership with a large-bore engine that is typical of a PANAMAX containership power plant, this project will explore the feasibility of using selective catalyst reduction to address the NO_X reduction requirements for the large end of the low-speed diesel prime movers that are available today.

1.1 PROBLEM STATEMENT

In order to determine whether selective catalytic reduction is a feasible option for the reduction of NOx emissions from shipping, a program is developed to investigate the size and efficacy of a suitable SCR unit for a large bore low speed diesel engine.

The model is then applied to an MAN B&W 11K90MC-C engine which is the same engine for which in-service NO_X emissions measurements have been made by Miller et.al. (8) while aboard a PANAMAX containership

In order to aid with the evaluation of feasibility of the application, the paper will also present a general discussion of the topics related to NO_X generation from low-speed diesel engines, available NO_X reduction technologies, the basic theory behind selective catalytic reduction, and the considerations and limitations of applying an SCR system to a marine vessel.

1.2 LIMITATIONS

The computational model that is presented in this work is intended as a flexible sizing tool which can be used to evaluate the main operating parameters of a variety of low speed diesel engine profiles. The model is based upon a one dimensional lumped parameter model which is utilizes the analogy between heat and mass transfer to evaluate the concentration profile through a single stream mass exchanger.

The model is designed to be flexible but the exhaust gas model is specifically designed to calculate the exhaust gas flow from two stroke low speed marine diesel engines which operate on a variable speed basis.

Computations are executed using a combination of published experimental data and reasonable values which were derived from a variety of sources in literature. The assumptions behind the values chosen are explained during the development of the model.

The flow through the system is considered to be a homogenous and incompressible flow of ideal gases and the effects of water and CO_2 upon the properties of the exhaust stream are considered to be negligible. The reactants are also assumed to be homogenously distributed throughout the exhaust gas stream. As such, it is possible to model the rate of NO_X conversion throughout the reactor by considering the rate of NO_X conversion within a single channel.

With respect to the flow through the catalyst channels, the axial diffusion effects and thermal gradients are neglected. Therefore, the mass transfer of reactants to and from the active sites is accounted for by mass transfer and reaction considerations alone.

Additionally, the SCR reaction is modeled by considering the mass transfer of NO alone rather than both NO and NH_3. This is reasonable because the difference between the values for the two species is negligible.

The effects of catalyst porosity and tortuosity on diffusion coefficient are accounted by the use of experimentally determined effective diffusion coefficients. To this effect, it is assumed that the plate geometry that was used for the experiments is a sufficient approximation of square channeled catalyst wall structure.

On account of the relatively low concentrations of NO and NH_3 relative to the bulk flow of exhaust, the reactor is assumed to be isothermal and the thermodynamic effects of the reaction are also neglected.

Finally, the reactor is considered to operate under steady state conditions and therefore does not experience fluctuations in exhaust gas flow or species concentration.

2 BACKGROUND

2.1 ENVIRONMENTAL IMPACTS OF SHIPPING AND NO_X EMISSIONS

Statisticians estimate that 90% of world trade is transported by the shipping industry (1), and, with increasing globalization and the expansion of the global economy, the actual tonnage of goods being shipped over the past 60 years has increased dramatically (2). This means that even though low-speed diesel propelled vessels may have low emissions relative to the amount of goods they transport (See Figure 1), they are becoming responsible for an increasingly significant portion of the total global emissions inventory.

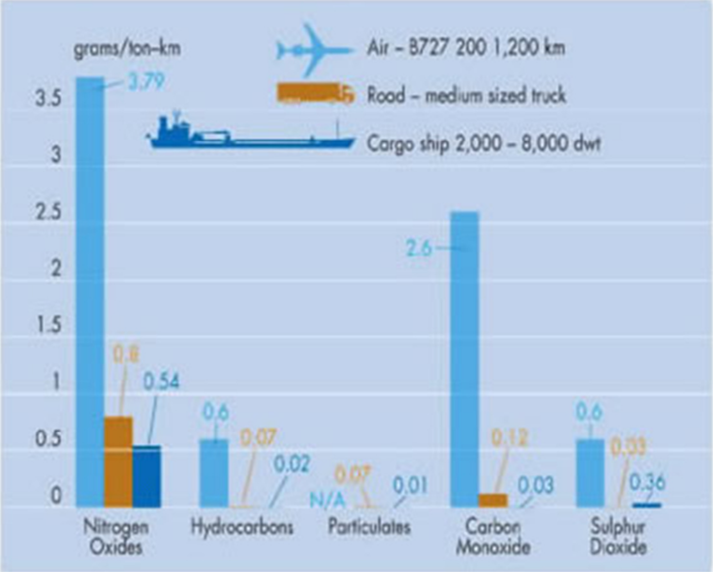

FIGURE 1 - COMPARISON OF TRANSPORTATION MODES' EMISSIONS CONTRIBUTION. (1)

According to Corbett et al. (4), oceangoing ships are responsible for the release of between 5-6.9 million metric tons of NO_X a year which is equivalent to approximately 15% of annual worldwide NO_X emissions.

The effect of NOx emissions is particularly significant in coastal areas near major shipping routes which also tend to have the highest population densities (3). The significance of the impact of NO_X emissions upon these communities is illustrated by the statistic that marine diesel engines may contribute up to 17% of the local NO_X inventory on a typical sunny summer day in San Diego, CA (5).

NO_X emissions are known to have negative impacts on the environment. These include the contribution to the formation of acid rain, over fertilization of lakes and soils, ozone depletion, smog formation, and reduction in air quality by facilitating the formation of small particulates (6). Additionally, prolonged exposure to NO_X is also known to cause adverse health effects including respiratory irritation, lung tissue damage, and possibly premature death. Persons with preexisting heart disease and respiratory diseases, such as emphysema, are considered to be particularly susceptible to the adverse health effects of NO_X emissions (7).

2.2 NO_X GENERATION ABATEMENT FROM MARINE LOW-SPEED DIESEL ENGINES

2.2.1 LOW-SPEED DIESEL ENGINES AND EXHAUST SYSTEMS

The majority of ocean-going merchant ships utilize low-speed diesel engines for main propulsion power. The term low-speed diesel generally refers to compression ignition engines that operate at less than 130 rpm and which utilize a two-stroke cycle rather than a four-stroke cycle (See Figure 2). Two-stroke engines are considered to be more efficient that four-stroke engines because they are able to accomplish the complete thermodynamic cycle in a single revolution as opposed to the two revolutions required by four-stroke engines.

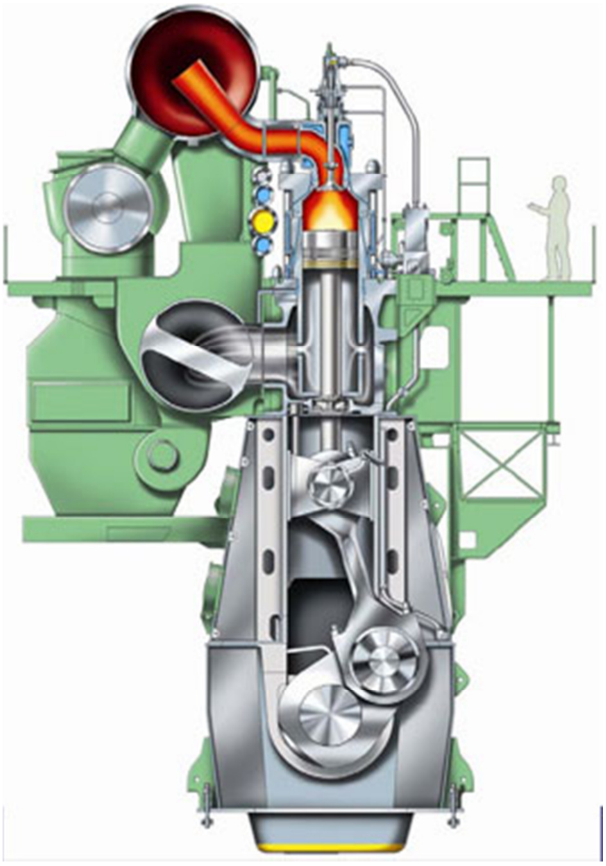

FIGURE 2 - CROSS-SECTION OF A K90MC-C LOW-SPEED DIESEL ENGINE
(COURTESY OF MAN DIESEL)

In terms of modern engine design, low-speed diesel engines are characterized by cylinder diameters (i.e. bore) in the range of 35 cm to 98 cm and length of piston movement (i.e. stroke) in the neighborhood of 2 m. The long engine stroke generates compression pressures of approximately 130 bar and this high pressure results in a correspondingly large increase in the temperature of the compressed intake air just prior to ignition. The high local temperatures that are present in the combustion chamber are very conducive to the formation of NO_X via the Zeldovich NO_X formation mechanism.

Engines are fitted with exhaust gas turbocharger in order to use some of the residual thermal energy in the exhaust gas to increase the flow of intake air to the engine. Because of the mechanical work performed by the turbocharger, the temperature and pressure of exhaust gas downstream of the turbocharger is reduced significantly.

Downstream of the turbocharger, the exhaust system can have many different components. For many years it has been standard to have an exhaust gas economizer (a.k.a. exhaust gas boiler or waste heat boiler) to generate steam from the waste heat of the exhaust gas for use in the auxiliary systems such uses as heating of the fuel system. In recent years it has also become more common to couple the waste heat recovery system with steam driven electrical generation equipment in order to use the exhaust gas to generate a portion of the electrical power required by the ship.

With the recent increase in environmental legislation and a renewed interest in energy efficient operation, several emissions abatement and/or energy recovery systems have been proposed that are designed to be applied to the main engine exhaust system. These systems include salt or freshwater scrubbers that are designed to remove SO_X from the exhaust gas, SCR systems that are designed to remove NO_X, organic Rankine cycle heat recovery systems that are designed to extract even more waste heat from the exhaust gas by using a fluid with a lower operating temperature, as well as exhaust gas turbines for the direct drive of electrical generation equipment.

2.2.2 FUEL DESCRIPTION AND COMBUSTION

Low speed diesel engines typically burn residual fuels with high sulfur contents. The maximum allowable sulfur content as per the ISO 8217 fuel standard is 4.5%. However with implementation of new regulations, there are many areas in which the burning of fuels with much lower sulfur content is or will soon be required.

The combustion process within a low-speed diesel engine is a turbulent non-premixed process. Unlike with spark ignition engines, where fuel and air are premixed prior to entering the combustion chamber, diesel engines operate upon the principle of injecting a small quantity of fuel at extremely high pressures into a charge of air that has been compressed by the upward motion of the piston.

The compression of the air within the combustion chamber prior to injection has the effect of raising both the temperature and the pressure of the charge air. Once the fuel is injected, the temperature within the combustion chamber is high enough that the fuel/air mixture auto ignites in the vicinity of the fuel droplets.

In order to better visualize the combustion process, the atmosphere within the combustion chamber should conceptually be divided into three regions.

The first region, which is inside the flame front, contains a mass of atomized but still unburned fuel droplets. Relative to the rest of the combustion chamber, the ratio of fuel to air within this region is quite high. This ratio is also referred to as the equivalence ratio. Within the inner-flame region, the dominant processes are the heat and mass transfer process which account for the vaporization of the fuel droplets and the kinetic processes account for the dispersion of the fuel droplet spray across the combustion chamber.

The second region comprises the relatively narrow region of the flame front. This region is characterized by a near stoichiometric mixture of fuel and air and by high local temperatures due to the heat release during combustion. The dominant processes in this region are the reaction kinetics and the transfer of oxygen and fuel to and the combustion products away from the flame front.

The third region constitutes the region ahead of the flame front and includes the mass of relatively cool, unburned air. This region is characterized by relatively low equivalence ratios and is dominated by the transfer of oxygen to and combustion the flame front and by the kinetics of a swirling air flow.

Each of the regions described is characterized by very different local characteristics. Additionally, these characteristics are also expected to change with time as a result of the influence of such factors as the rate of combustion, which is itself influenced by the transport of fuel and oxygen to and the combustion products away from the flame front.

Thus, combustion within diesel engines is considered to be a diffusion controlled process, meaning that that the rate of combustion, and therefore heat release, is limited by the ability to transport species to and from the flame front (9).

2.2.3 MECHANISMS OF NO_X FORMATION

Typical concentrations of NO_X in the exhaust of low-speed diesel engines range from between 1,000 and 1,500 parts per million by volume. The three formation mechanisms generally credited with NO_X formation are as follows: the Zeldovich mechanism, which is also known as the thermal mechanism; the Fenimore mechanism, also referred to as the prompt mechanism; and the N_2O mechanism. The following summary of these three main reaction mechanisms is adapted from Turns (9).

The Zeldovich mechanism consists of the following reactions:

$$O + N_2 \Leftrightarrow NO + N \qquad \text{R. 1}$$

$$N + O_2 \Leftrightarrow NO + O \qquad \text{R. 2}$$

And can be extended with the following reaction:

$$N + OH \Leftrightarrow NO + H \qquad \text{R. 3}$$

A common assumption that is used to simplify the Zeldovich mechanism is that O_2 and N_2 have reached their equilibrium values prior the formation of NO. Based upon this assumption, the rate of reaction can be approximated by the following equation (9):

$$\frac{d[NO]}{dt} = 2k_{1,f}[O]_{eq}[N_2]_{eq} \qquad \text{Eq. 1}$$

In which $k_{1,f}$ is determined from the Arrhenius equation:

$$k_{1,f} = 1.8 * 10^{11} e^{\left(\frac{-Ea}{RT}\right)} \qquad \text{Eq. 2}$$

$k_{1,f}$ = Forward rate constant of equation 1
Ea = Activation Energy in kJ/mol
R = Ideal gas constant
T = Temperature in K

Given the large activation energy (319,050 kJ/mol), the Zeldovich mechanism is highly dependent upon temperature. For most applications, the Zeldovich mechanism is considered to be negligible at temperatures below 1,700K – 1,800K (2). Since the Zeldovich mechanism is considered to be relatively slow compared to fuel oxidation, it is generally considered to be of significance in the consideration of high temperature post-flame gases (3).

The N_2O intermediate mechanism consists of the following reactions (9):

$$O + N_2 + M \Leftrightarrow N_2O + M \qquad \text{R. 4}$$

$$H + N_2O \Leftrightarrow NO + NH \qquad \text{R. 5}$$

$$O + N_2O \Leftrightarrow NO + NO \qquad \text{R. 6}$$

The N_2O intermediate mechanism is considered to be important for combustion mechanisms that occur at low temperatures and which have equivalence ratios of less than 0.8. In the reaction R.4 above, M indicates a third body that is necessary for the initiation of the reaction.

The Fenimore, or prompt, mechanism is dependent upon the action of CH radicals that are formed during the combustion of hydrocarbons (4). The Fenimore mechanism has a much shorter time scale than the Zeldovich mechanism and is used to account for NO_X formation at temperatures that would not otherwise support the Zeldovich mechanism.

For reactions which occur at equivalence ratios of less than 1.2, the Fenimore mechanism is described by the following reactions:

$$CH + N_2 \Leftrightarrow HCN + N \qquad \text{R. 7}$$

$$C + N_2 \Leftrightarrow CN + N \qquad \text{R. 8}$$

$$HCN + O \Leftrightarrow NCO + H \qquad \text{R. 9}$$

$$NCO + H \Leftrightarrow NH + CO \qquad \text{R. 10}$$

$$NH + H \Leftrightarrow N + H_2 \qquad \text{R. 11}$$

$$N + OH \Leftrightarrow NO + H \qquad \text{R. 12}$$

The formation of NO_2 can also occur in post-flame gases at conditions that are typical of exhaust systems. Under these circumstances, the formation of NO_2 is described by the following reactions:

$$NO + HO_2 \Leftrightarrow NO_2 + OH \qquad \text{R. 13}$$

$$NO_2 + H \Leftrightarrow NO + OH \qquad \text{R. 14}$$

$$NO_2 + O \Leftrightarrow NO + O_2 \qquad \text{R. 15}$$

And HO_2 is formed by according to:

$$H + O_2 + M \Leftrightarrow HO_2 + M \qquad \text{R. 16}$$

In this mechanism, reactions R. 14 and R. 15 describe the destruction of NO_2 in high temperature regions. The mechanism describes the formation of NO_2 as NO molecules are transported from high temperature regions to areas that are rich in HO_2.

Finally, NO formation is can also be attributed to the oxidation of the nitrogen content of the fuel. This mechanism is generally neglected for fuels that do not contain an appreciable nitrogen content (9). However, in the case of low-speed diesel engines, Goldsworthy suggests that this process must be considered and suggests that up to 10% of the NO_X produced by low speed diesel engines is attributable to the oxidation of the nitrogen content of residual fuels (13).

2.2.4 NO_X FORMATION IN LOW-SPEED DIESEL ENGINES

In comparing the three main mechanisms of NOx generation, there are three properties which help to determine which of the mechanisms is dominant. These are temperature, equivalence ratio, and residence time. However, since the combustion process is non-premixed, all of these properties will vary with respect to time and location in the cylinder. Because of this, it is feasible to expect that different mechanisms of NO_X generation may be dominant in different regions of the combustion chamber (13).

Most authors agree that the majority of NO_X formation during the diesel combustion process is attributable to the Zeldovich mechanism (6) (4) (7) (13) (8), though not at equilibrium concentrations. As such, the Zeldovich mechanism, either in short or extended form, is the mechanism that is most commonly used to model the formation of NO_X in diesel combustion models.

The Zeldovich mechanism is therefore useful in explaining some of the most important and overall characteristic behaviors that are observed during the formation of NO_X in diesel engines. Namely, since NO_X formation is extremely temperature dependent and since the large compression ratios of low-speed diesel engines result in high charge air temperatures, low-speed diesel engines tend to have very high NO_X production rates relative to other types of diesel engines and other combustion processes. Also, as the temperature of the exhaust gas drops during the expansion that accompanies the downward motion of the piston, the Zeldovich mechanisms establishes a cut-off point after which NO_X formation is considered to be frozen (2).

Since NO_X generation is an oxidation process, NO_X production is dependent on the amount of oxygen that is available. The local oxygen content of a region is affected by the efficiency of mixing within the combustion chamber. Several authors attribute the bulk of NO_X formation to the relatively oxygenated regions immediately surround the flame sheet and to diluted post combustion gases. These authors also agree on the relative importance of local mixing processes upon overall NO_X formation (13) (6) .

The majority of authors also agree that the Zeldovich mechanism alone is not sufficient to fully explain NO_X formation.

By considering the local properties in the various regions within the combustion chamber, a number of different mechanisms have been proposed to explain the remaining NO_X production that is not attributable to the Zeldovich mechanism. Particularly attention has been paid do describing the local values of temperature and equivalence ratio since the different production mechanisms are differentiated by different temperature and equivalence ratio profiles.

Verbiezen et al. suggest that NO_X generation initially occurs via the Fenimore mechanism (3) on account of the fact that the equivalence ratio in the fuel cloud is quite high at the start of combustion. The Fenimore mechanism is thought to remain dominant until there has been sufficient diffusion to lower the local equivalence ratio, at which point, the NO_X production shifts to the Zeldovich mechanism.

Arregle et al. assert that the inner flame region is ill suited to NO_X formation because it is a reductive environment, and that the inner flame region actually affects the overall production by supporting reduction mechanisms which consume rather than create NO (6).

Of the sources cited in the discussion above, Goldsworthy is the only author whose work is specifically focused on low-speed diesel engines. Goldsworthy proposes that the following extension mechanism to account for the formation of NO_X in low-speed diesel engines. Goldsworthy's complete mechanism is a combination of the Zeldovich, the N_2O intermediate, and the N_2O extension mechanisms and where M is a third body:

$$N_2O + M \Leftrightarrow N_2 + O + M \qquad \text{R. 17}$$

$$N_2O + O \Leftrightarrow NO + NO \qquad \text{R. 18}$$

$$N_2O + H \rightarrow NH + NO \qquad \text{R. 19}$$

$$N_2O + OH \rightarrow NHO + NO \qquad \text{R. 20}$$

$$NH + OH \rightarrow HNO + H \qquad \text{R. 21}$$

$$NH + O_2 \rightarrow HNO + O \qquad \text{R. 22}$$

$$HNO + M \rightarrow H + NO + M \qquad \text{R. 23}$$

Goldsworthy suggests that at full load the addition of the latter two mechanisms accounts for an additional 15% gain to estimates of NO_X production by the Zeldovich mechanism alone. Figure 3 depicts Goldsworthy's assessment of the relative contributions of the three NOx generation mechanisms to overall rate NO_X production at different temperatures and equivalence ratios. At certain conditions, up to 30% of the NO_X production can be ascribed to the other two mechanisms. It is also interesting to note that at different conditions, different mechanisms have different relative contributions.

Finally, Goldsworthy makes a point to discount the importance of the contributions of the NO_2 and Fenimore mechanisms to the overall NO_X generation relative to the amount that is produced by the other three mechanisms (13).

Krijnsen et al. (6) summarize some of the research regarding factors which affect the production of NO_X in diesel engines. They cite research which shows that increased charge air pressure results in increased NO_X emissions. With regards to charge air cooling, some researchers have found that lowering the temperature of the charge decreases NO_X production while other researcher concluded that lowering charge air temperature can increase NO_X production due to the fact that charge air with a lower temperature has a longer ignition delay which means that more fuel is vaporized and higher peak temperatures exist within the combustion chamber. By the same reasoning, fuels with a longer ignition delay are also found to have higher peak temperature and therefore higher levels of NO_X emissions.

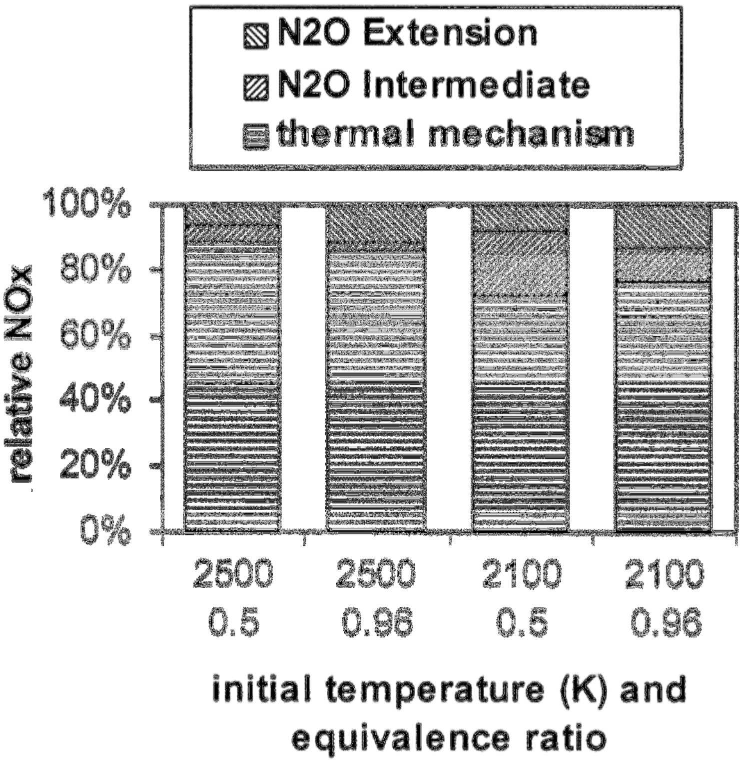

FIGURE 3 - EFFECT OF BURNED GAS CONDITIONS ON RELATIVE CONTRIBUTIONS TO NO_X FROM THE THERMAL, N_2O INTERMEDIATE, AND N_2O EXTENSION MECHANISMS. (13)

2.2.5 NO_X REDUCTION TECHNOLOGY

Several technologies have been developed to limit the emission of NO_X from various power sources including marine diesel engines. Although the majority of these technologies have been developed for applications other than low-speed diesel engines, many of these methods can also be used with low-speed diesel engines, provided that adequate consideration is given to the unique aspects of the application.

NO_X reduction technologies are generally grouped into one of two categories: primary and secondary methods. Primary methods are those methods which reduce NO_X by altering the conditions within the combustion chamber so that the actual production of NO_X is reduced. Examples of primary methods include such approaches as the retarding of fuel injection timing, control and optimization of fuel injection profiles, and the introduction of water into the combustion chamber. Secondary technologies require greater modification to shipboard systems and include after treatment methods such as selective catalytic reduction and exhaust gas scrubbers, which remove NO_X after it has been generated, and exhaust gas recirculation, which lowers NO_X by re-circulating a portion of the exhaust gas back through the combustion chamber. The overall rates of reduction can also be increased by combining more than one of the methods described above.

Given the exponential dependence of the Zeldovich mechanism on temperature, primary methods are designed to reduce NO_X formation by limiting peak temperature in the combustion chamber. This can either be achieved by optimizing the combustion chamber and controlling the rate of heat release so as to avoid local regions with high temperatures, or by altering the timing of fuel injection so that ignition does not coincide with peak cylinder temperatures. Significant reductions in NO_X production can theoretically be achieved with relatively modest reductions in temperature and many of these technologies can be combined to achieve further reductions. The main drawback of this approach, however, is that the overall potential for NO_X reduction is limited which means that the application of these methods alone is not sufficient to satisfy the IMO Tier III requirements. Additionally, the majority of these methods in less than optimal combustion and therefore incur non-negligible penalties in fuel consumption. Estimates put these penalties at approximately 0-3% for 15-20% reduction and up to 10% for 40% NO_X reduction (11).

Another means of reducing combustion temperatures is by introducing fluids with high heat capacities into the stream of reactants in order to reduce the overall temperature of the reaction. Many of these methods rely on introduction of water into the combustion chamber, either by humidification of the intake air (also known as Humid Air Motor), emulsification of water into the fuel, or through the direct injection of water into the cylinder. Some care must be taken with the design of this equipment as uncontrolled moisture (such as from condensation from the intake after the charge air cooler) can have the undesired effect of disrupting the cylinder lubricating oil layer, thereby resulting in rapidly accelerated (and thereby very expensive) wear.

Another possibility which has been adopted from mobile truck applications has been the use of exhaust gas recirculation (EGR). NO_X reduction by EGR is a result of lower combustion temperature due to the high specific heat of CO_2 and H_2O and of decreased NO_X generation due to the decreased oxygen content of the recirculated gas (11).

In contrast to this, exhaust gas treatment methods tend to have much higher installation cost and space requirements, but are also capable of the highest possible reductions. Although scrubber technologies have been shown to have some effect on the reduction of NO_X emissions, their main application and significance is in the reduction of SO_X emissions. However, since both SO_X and maximum NO_X reduction regulations are linked in the ECA areas, the NO_X potential of scrubber technology should not be discounted.

Method	Reduction Possible	Effect on Fuel Consumption	Cost relative to engine price	Operating Costs	Notes
Primary methods: late fuel injection timing, etc.	15% below IMO Tier I	Moderate	Up to 10% for 40% reduction in NO_X	Moderate	Well advanced development
Humid air motor	30-60%	Low	5-30%	Moderate	Water quality requirements if inject before air cooler
Direct water injection	40-50%	Low	10%	3%	Elevated water injection rates can result in excessive smoke and fuel consumption
Water-in-Fuel Emulsions	Up to 20%	Low	5%	5%	· Increased flow rates through fuel injections system · Can reduce smoke generation at low loads
EGR	50-70%				Limitations regarding fuel quality (low sulfur and ash content)
Scrubbers	5-10%		No	Moderate	Primarily designed to reduce SO_X
SCR	90%	None/possible decrease	15-20%	10% (Dependent on reagent price)	· Requires reagent and dosing system · Sensitive to fuel sulfur content · Temperature operating window is crucial · Installed before Turbocharger on 2-Stroke engines · Engine may be optimized for lower fuel oil consumption

TABLE 1 - SUMMARY OF THE CHARACTERISTICS OF VARIOUS NO_X REDUCTION TECHNOLOGIES.

By far the technology with the greatest potential for reducing NO_X emission is selective catalytic reduction, which is the subject of this thesis. SCR has been well established in shoreside applications and is capable of NO_X reductions up to 99%. The disadvantages of the system are the large capital investment, the large space requirement for the installation, and the sensitivity of the system of operating temperature and fuel sulfur content.

The following table summarizes the various NO_X reduction methods available, the theoretical conversion that is achievable, and the major advantages and disadvantages of each (11).

2.2.6 REGULATORY REQUIREMENTS

According to MARPOL Annex VI, the maximum emissions rate of NO_X for vessels built after January 1, 2000 has been set at 17 g/kW-hr for engines that operate at less than 130 rpm, which is the effective range for low-speed diesel engines. This is the so-called IMO Tier I standard. Effective January 1, 2011 the allowable emissions for low-speed engines are further reduced to 14.4 g/kW-hr for newly built vessels. These are the IMO Tier II standards. Finally, effective January 1, 2016, IMO Tier III standards come into force which limit the allowable NO_X emissions from low-speed diesel engines to 3.4 g/kW-hr for vessels which are operating within specially defined emissions control areas (ECA). Vessels operating within these ECA areas are further subject to regulations which limit the sulfur content of the fuel that they are allowed to burn within the geographical limits of the ECA. As of July 1, 2010, these limits are set at a maximum sulfur content of 1.0% by mass and will be further reduced to 0.10% by mass on January 1, 2015.

Currently, only the North Sea and the Baltic Sea have been designated as emissions control areas. Also, there are several additional ECAs under consideration, one of the most significant of which is the North American ECA. The North American ECA is scheduled to come into effect in 2015 and will include the waters off the coasts of the United States, Canada, and Mexico to a distance of 200 nm (11).

The practical result of these regulations is that as of 2016, any newly constructed vessel wishing to be able to call on a port within an ECA area will need to be fitted with a means of reducing NO_X emissions by almost 80% from current standards.

In addition to the global regulations adopted by the IMO, there are also several localities which have adopted their own and even more stringent regulations including the Rhine River and Bodensee, as well as the NO_X differentiated tonnage tax system and the NO_X emissions taxes in Norway and the differentiated fairway and harbor fee system in Sweden (12).

2.3 SELECTIVE CATALYTIC REDUCTION

The basic operating principle of a selective catalytic reduction unit is the reduction of the NO_X content of exhaust gases by ammonia (NH_3) as it passes over a catalytic material. Depending upon the dosage of ammonia, conversion efficiencies of 99% can reasonably be achieved and the products of this reaction are simply N_2 and H_2O.

The catalyst serves to enable a set of reactions between NH_3 and NO that otherwise would not spontaneously occur. The ammonia can either be injected into the exhaust gas in gaseous form or as part of an aqueous solution of Urea in which the droplets of urea solution are first evaporated by the heat of the exhaust gas and the urea is then decomposed into NH_3 and CO_2.

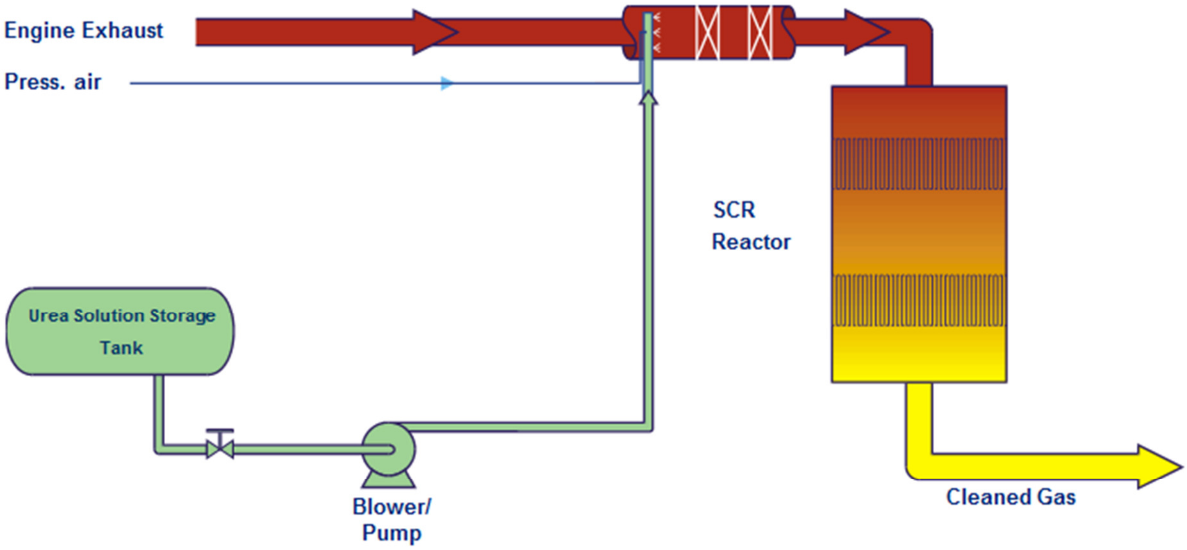

FIGURE 4 - SCHEMATIC OF A TYPICAL SCR SYSTEM. (21)
(DIAGRAM COURTESY OF HALDOR TOPSØE.)

A schematic of a simple SCR system is shown in Figure 4. The system includes the SCR reactor, which contains the catalyst elements and a Urea dosing system, including a storage tank, supply pump, injection nozzles, and mixing elements. Compressed air is used for nozzle cooling and cleaning air.

Not shown is the control system which is used to control the dosage of urea to the reactor to ensure adequate operation and minimum slip.

2.3.1 CHEMICAL REACTIONS

The process of selective catalytic reduction by urea can be broken down into two basic subprocesses. First, urea, which is contained in the injected solution, must be broken down into ammonia and second, the ammonia and NO_X must react to form N_2 and H_2O.

2.3.2 DECOMPOSITION OF UREA

The first step in the decomposition of the urea solution is the evaporation of the water molecules. The heat for of vaporization is provided by the high temperature exhaust gas into which the urea solution droplets are entrained.

$$(NH_2)_2CO(aq) \rightarrow (NH_2)_2CO(l) + H_2O(g) \qquad \text{R. 24}$$

The liquid urea is then further heated and vaporized into gaseous form.

$$(NH_2)_2CO(l) \rightarrow (NH_2)_2CO(g) \qquad \text{R. 25}$$

The rate of the vaporization reaction is given by the following equation in which the vaporization energy (h_{vap}) is 87.4 kJ/mol (12).

$$k_{urea,vap} = (1.0 * 10^{12}) * e^{\left(\frac{h_{vap}}{R*T}\right)} \qquad \text{Eq. 3}$$

The vaporized urea molecules are then broken down by one of two possible mechanisms: thermolysis or hydrolysis. The thermolytic reaction is involves the decomposition of a urea molecule into ammonia and isocyanic acid according to the following reaction:

$$(NH_2)_2CO(g) \rightarrow HNCO + NH_3 \qquad \text{R. 26}$$

The hydrolytic reaction the uses water to further decompose the isocyanic molecule into ammonia and CO_2.

$$HNCO + H_2O \rightarrow NH_3 + CO_2 \qquad \text{R. 27}$$

The hydrolytic reaction is kinetically favored at temperatures around 200°C, however at 400°C, which is near to the temperature of the exhaust gas, the reaction rates of the thermolytic and hydrolytic mechanisms are about equal (13).

2.3.3 SELECTIVE CATALYTIC REDUCTION

The two main reaction mechanisms by which NO can be reduced are the main SCR reaction:

$$4NH_3 + 4NO + O_2 \rightarrow 4N_2 + 6H_2O \qquad \text{R. 28}$$

And the fast SCR reaction:

$$4NH_3 + 2NO + 2NO_2 \rightarrow 4N_2 + 6H_2O \qquad \text{R. 29}$$

Although the fast SCR reaction is kinetically favored over the main SCR reaction, most of the NOx reduction is accomplished via the main SCR reaction on account of the fact that diesel exhaust typically only contain 10% NO_2 versus 90% NO (13) (10). Therefore, the stoichiometric ratio between NO and NH_3 in the SCR process is approximately 1:1.

2.3.4 OXIDATION OF SO_2

The most significant side reaction that occurs along with the selective catalytic reduction of NO is the simultaneous oxidation of SO_2 to SO_3 by the following reaction:

$$SO_2 + \frac{1}{2}O_2 \rightarrow SO_3 \qquad \text{R. 30}$$

SO_2 is present in the exhaust gas as a result of the combustion of such sulfur containing fuels such as the heavy fuel oils that are commonly burned in low-speed diesel engines. Approximately 3-8% of the SO_2 that is formed during combustion is then further converted to SO_3 in the combustion chamber.

The SO_3 content in the exhaust gas is already undesirable because it reacts with the water vapor in the exhaust stream to form sulfuric acid (H_2SO_4). Depending on the concentration of H_2SO_4 in the exhaust gas, the gaseous sulfuric acid can condense onto various components of the exhaust system and result in the corrosion of components.

This situation is further complicated by the fact that the catalysts which are commonly used in SCR also promote the oxidation of SO_2 to SO_3 and the fact that the greater the concentration of H_2SO_4 in the exhaust gas, the lower the dew point temperature at which the acid will condense.

Also, SO_3 can react with NH_3 in the exhaust gas stream to form ammonium sulfate according to the following reactions:

$$NH_3 + SO_3 + H_2O \rightarrow (NH_4)HSO_4 \qquad \text{R. 31}$$

$$2NH_3 + SO_3 + H_2O \rightarrow (NH_4)_2SO_4 \qquad \text{R. 32}$$

These compounds are undesirable because the can condense at temperatures below 300°C, and can then either impede the function of the catalyst or result in the corrosion of downstream components of the exhaust system (16).

2.3.5 CATALYST FUNCTION AND DESCRIPTION

The purpose of a catalyst is to promote a reaction that would otherwise not be likely to occur without the presence of the catalyst. While catalytic materials are used in a wide variety of modern industrial processes, the catalysts that are used for a particular process must be tailored to meet the needs of that specific application. To do so, the catalyst must not only support the relevant chemical reactions, but it must also physically be constructed to meet the needs of the environment.

Typically, catalytic materials will be comprised of active sites, such as iron, chromium, or vanadium, which actively promote the reactions, and of an appropriate support material, such as TiO_2, Al_2O_3, SiO_2, and zeolites. Although there are many materials which have been shown to be active in promoting the SCR reaction, the materials that aremost commonly used for SCR applications are V_2O_5 active sites on a TiO_2 support.

In titania-vanadia catalysts, titianium oxide (TiO_2) functions as a support material for the active components (active sites) of these catalysts. TiO_2 is a suitable carrier because it is only weakly and reversibly sulfated and because it increases the activity of the vanadium actives sites more so than other support materials.

Vanadium (as V_2O_5) is a good promoter of the SCR reaction, but also has the undesirable effect of promoting the oxidation of SO_2 to SO_3. As such, and especially in high sulfur applications, the vanadium content of the catalyst is usually limited to below 1% (by mass). Additionally, WO_3 and MoO_3 are often added to in concentrations around 6% and 10% (by mass) respectively to increase the thermal stability and activity of the catalyst as a whole.

The physical configuration of the catalyst likewise depends upon the application. For flue gas treatment, some of the relevant concerns include the large volumetric flow rates, the tendency for relatively high particulate content, and the restrictions with regard to allowable pressure drop.

Because of these restrictions, monolithic catalysts are the most common type of structure used for flue gas treatment applications. Monolithic catalysts are blocks of catalytic material that contain channels with either a honeycomb or a rectangular geometry. One of the main advantages of monolith catalysts is the low pressure drops that can be achieved versus other catalyst configurations. Another important consideration in the selection and sizing of a catalyst is the expected and/or required lifespan. Although catalyst deactivation will be discussed in greater detail in a subsequent section, one of the major sources of catalyst deactivation is the deposition of and blocking of pores by the particulate matter that is entrained in the exhaust gas. As such, one of the critical factors affecting the sizing of the channel is the minimizing of particle deposition by ensuring that sufficiently large channels are chosen in the case of highly particulate loaded exhaust gases.

Finally, in order to allow for ease of manufacture and handling, the monolithic catalyst materials are then often manufactured in standardized sizes, and packaged as elements which can be assembled to form layers within the catalytic reactors (See Figure 5).

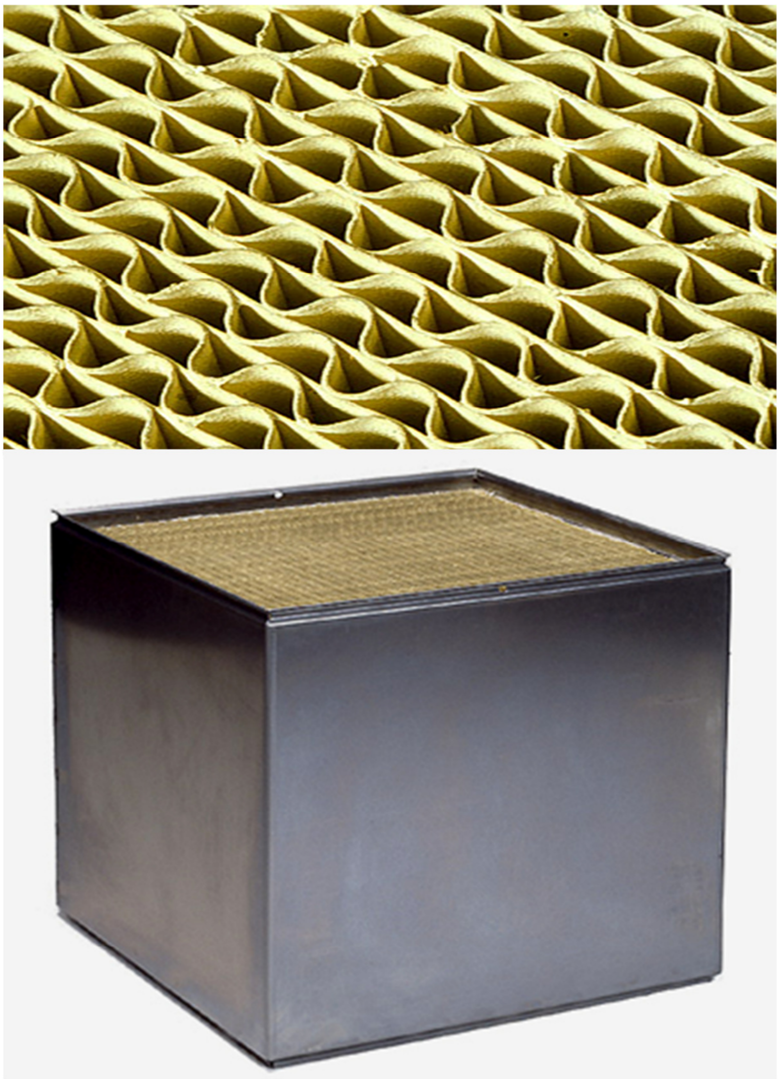

FIGURE 5 - EXAMPLE OF TYPICAL HONEYCOMB TYPE CATALYST. (27)
(PICTURE COURTESY OF HALDOR TOPSØE.)

2.3.6 Mechanisms of Catalysis

A number of different mechanism have been proposed to explain the mechanism by which NO and NH_3 react within the context of a titania-vanadia catalyst, however there is still disagreement over the precise nature of the mechanism, especially with regards to the nature of the active sites to which the various species adsorb.

Topsoe et al. have proposed the following semi-empirical mechanism which suggests that NH_3 is first adsorbed onto an adsorption site and then is activated at a nearby reaction site before reacting with NO. In the mechanism below M represents an adsorption site and S represents the reactive site upon which NH_3 is then activated.

$$NH_3 + M \Leftrightarrow NH_3{}^{-}M \qquad \text{R. 33}$$

$$NH_3{}^{-}M + S \Leftrightarrow NH_3{}^{-}S + M \qquad \text{R. 34}$$

$$NO + NH_3{}^{-}S \Leftrightarrow Products + S \qquad \text{R. 35}$$

In order to determine the precise nature of the S and M sites, Topsoe et al. (24) performed further investigations and they proposed the following mechanism (See Figure 6).

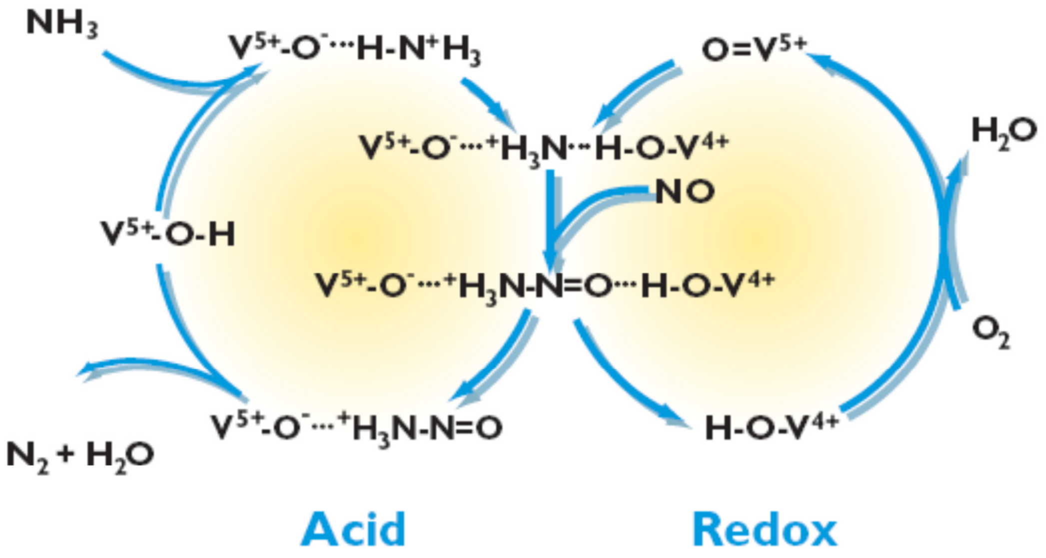

FIGURE 6 - CATALYTIC CYCLE FOR THE SCR REACTION OVER VANADIA/TITANIA. (23)

In this mechanism, the VOH site is found to be the adsorption site and V=O is the activation site. The mechanism is summarized as follows: once NH_3 has been activated, it reacts with NO to produce N_2 and H_2O. The active site is released as V^{4+}-OH and is replenished by O_2 to return to its original state as V=O, in the process producing H_2O (14).

2.3.7 REACTION KINETICS

A generalized expression for the rate of conversion of NO according to the main SCR reaction is as follows:

$$r_{NO} = k c_{NO}^{\alpha} c_{NH_3}^{\beta} c_{O_2}^{\gamma} c_{H_2O}^{\delta} \qquad \text{Eq. 4}$$

In the equation above, r is the rate of reaction, k is the rate constant as derived from the Arrhenius equation, c is the concentration of the respective species, and the Greek letters signify the respective orders of reaction for each of the species (25).

From experimental data, and for the purposes of engineering calculations, the rate the main SCR reaction is found to be independent of the concentrations of NH_3, O_2, and H_2O. The expression is therefore simplified to:

$$r_{NO} = kc_{NO} \qquad \text{Eq. 5}$$

Where the rate constant k is given the Arrhenius equation:

$$k = Ae^{\frac{-E_a}{RT}} \qquad \text{Eq. 6}$$

The expression above is sometimes extended to account for the adsorption of ammonia:

$$r_{NO} = kc_{NO}\frac{K_{NH_3}c_{NH_3}}{1 + K_{NH_3}c_{NH_3}} \qquad \text{Eq. 7}$$

Where K is the adsorption equilibrium constant and is given by:

$$K_{NH_3} = K_{NH_3,s}e^{\frac{-H_{ads,NH3}}{RT}} \qquad \text{Eq. 8}$$

In the equation above, $K_{NH_3,s}$ is the adsorption equilibrium constant at the channel surface and $H_{ads,NH3}$ is the enthalpy of adsorption and the values of which are specific to the type of catalyst that is being used.

The kinetics expressions described in this section are limited because they only describe the rate of reaction. The expressions cannot adequately describe the rate of NO conversion in a monolithic catalyst because they do not account for the effects of the structure of the catalyst, nor do they take into account the bulk fluid motion. Therefore, in order to be able to determine the rate of NO destruction, the rate expression must be extended in order to account for these influences.

2.3.8 INFLUENCE OF CATALYST MICROSTRUCTURE

On a microscopic level, the surface of catalyst is not smooth. Rather, the surfaces of the catalyst are porous so as to maximize the surface area, and therefore the number of active sites, that are available per unit volume of catalyst.

Depending on the method by which the catalyst is produced, catalyst pores will have different geometries with different sizes and different size distributions. Large pores, which are known as macropores, tend to have pore diameters greater than 50 nm. Medium sized pores are known as mesopores have pore diameters between 2nm and 50 nm. And finally, micropores and ultramicropores have pore diameters of less than 2nm and less than 0.7 nm respectively.

The differences in catalyst pore geometry are illustrated in Figure 7, in which the pore size distribution of three different SCR catalysts is compared.

Of the catalysts compared in Figure 7, two of the catalysts have relatively narrow distributions of pore sizes which means that most of the pores are about the same size. In contrast to this, the third catalyst has three distinct peaks in the pore size curve. This type of curve is typical of catalysts that employ a branched pore structures, with small pores branching off of larger ones. The advantage of this configuration is increased resistance to deactivation on account of the clogging of pores by soot deposition.

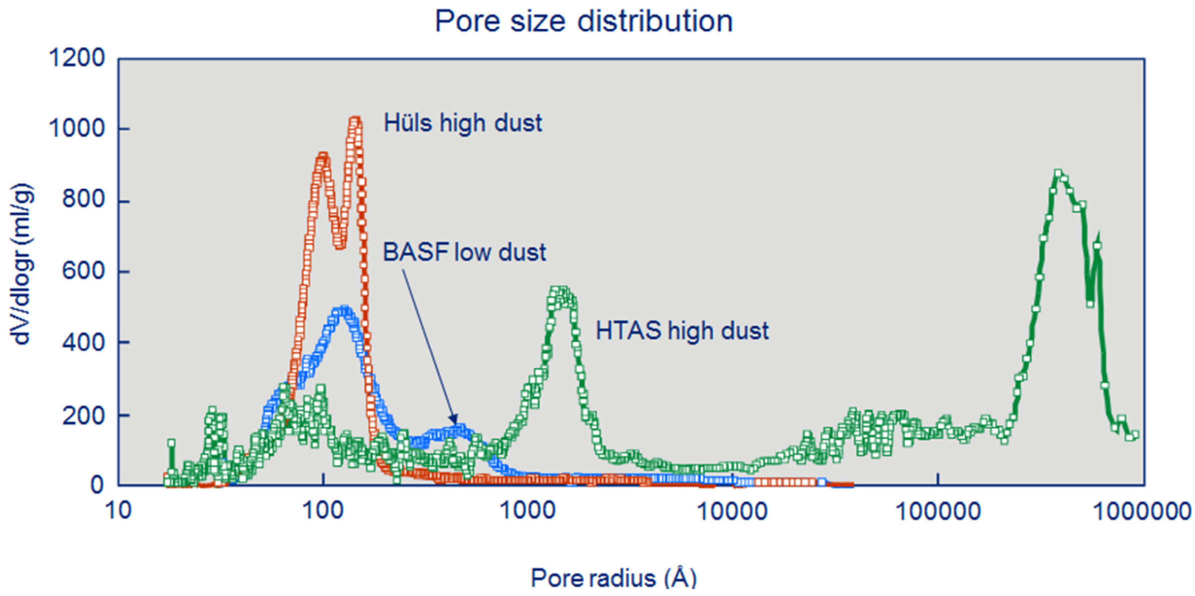

FIGURE 7 - EXAMPLES OF CATALYST PORE PROPERTIES. (20)
(FIGURE COURTESY OF HALDOR TOPSØE.)

With regards to determining the rate of NO_X conversion, the pore size and the relative fraction of catalytic material to void space (also known as void fraction) are important because they present an effective resistance to the transfer of species to and from the active sites within the pores. The magnitude of this effect is accounted for by an effectiveness term which is factored into the overall mass transfer coefficient effectiveness values in the range of 10-20% are not uncommon (26). As such, the geometry of the pore structure of the catalyst has a significant effect on the overall NO_X conversion rate.

2.3.9 CATALYST DEACTIVATION

In selecting a catalyst for a particular application, one of the most important behaviors that must be accounted for is the loss of catalyst activity over the expected operating cycle of the system.

The deactivation of a given activist is the result of the combination of a number of different factors, some of which are inherent to the material and structure of the catalyst, while others are a result of the operating conditions and characteristics of the exhaust gas.

For titania-vanadia catalysts, the loss of catalytic activity can be the result of many different factors, including poisoning of the catalyst active sites by alkaline metals such as sodium and potassium. It is possible for these elements to be present in the exhaust gas as a result of seawater contamination of the fuel, or as natural constituents of the fuel itself. Another significant poison of titania-vanadia catalysts is arsenic. These elements affect the overall activity of the catalyst because they irreversible chemisorb to active sites, thereby decreasing the total number of active sites that are available for promoting the catalytic reaction.

Another important factor which decreases the overall effectiveness of a catalyst is catalyst fouling. Catalyst fouling can occur in the form of particulate deposition, by the coating of catalyst surface by unwanted compounds, and by the plugging of catalyst pores by particulate.

The deposition of ammonium sulfates (NH_4SO_4) on catalyst surfaces is an important example of catalyst deactivation due to the coating of the catalyst surface by unwanted compounds. Deposition of ammonia sulfate occurs when the operating temperature of the catalyst drops below the dew point of the compound which is typically considered to occur around 300°C. As such, titania-vanadia catalyst should not be operated at low temperatures in the presence of exhaust gases that contain high concentration of sulfur containing fuels. This being said, the effects of ammonium sulfate deposition can be counteracted by operating the system at elevated temperatures for a short period of time in which case the ammonium sulfate is evaporated from the surface of the catalyst (23).

The deactivation of a catalyst by particulate deposition is greatly affected by the particulate content of the exhaust gas passing through the catalyst channels. Fu et al. note that the effects of particulate deposition are compensated for by the selection of channel diameter and the flow rate of the exhaust through the channel. For application with high particulate loading, larger channel openings are generally employed and the number of channels is chosen so as to limit the flow rate through the individual channels. The flow rate is therefore selected so as to be high enough to help avoid deposition, but low enough so as not to cause the erosion of the catalyst material. Typical flow rates for SCR applications range between the values of 5-7 m/s. Another important to avoidance of foulant deposition is the proper control of exhaust flow through the catalyst channels. This is due to the fact that a local misdistribution in flow can result in reduced local velocities which, in turn, may lead to increased local foulant deposition. Fu et al. recommend the configuration of catalyst units to have downward flow so as to limit foulant deposition (27).

The final type of catalyst deactivation is the result of the thermal degradation of the catalyst material. This can occur either through sintering, which is an actual change in the catalyst structure, or through the agglomeration of catalyst active sites in larger and relatively less effective sites (25). In the case of titania-vanadia catalysts, the titanium oxide support structure is susceptible to thermal deactivation due to the degradation of the anatase form of titanium to the rutile form. The overall susceptibility of a catalyst to thermal effects is often affected by the thermal conditions to which the catalyst was exposed to during its manufacture. Catalysts which were manufactured at high temperature conditions are therefore less susceptible to thermal degradation than those which were manufactured at lower temperatures.

2.3.10 OVERALL MASS TRANSFER AND BULK FLUID MOTION

From the discussion above, it is evident that the overall SCR process is highly affected by the effectiveness of the transport processes that bring reactants to and carry the products away from the active sites where the reactions takes places.

In order to understand the transfer process as a whole, it is therefore convenient to break the process up into discrete steps which describe the individual mass transfer steps.

First, bulk fluid motion within the catalyst channel is responsible for convecting NH_3 and NO to the surface of the channel. Once at the surface, the species diffuse from the surface into the macropores and then from the macropores to the micropores. Once in the pores, HN_3 must adsorb to the catalyst active sites at which point it will react with weakly adsorbed NO to form N_2 and H_2O. The products must then desorb and be transported from the micropores to the macropores, and then out into the bulk of the exhaust stream.

This process is summarized in Figure 8.

From the discussion above, it is evident that the rate at which NO_X is removed from the exhaust gas is highly affected by the mass transfer processes which are responsible for the transport of reactants and products to and from the catalyst active sites that are located in the pore structure.

The computational model which is described in subsequent sections is a lumped parameter model which accounts for the effects of mass transfer and reaction rate via the use of an overall parameter which incorporates both the mass transfer and the rate of the of the SCR reaction.

In previous sections, the specifics of monolith geometry have been discussed and identified. Particularly significant was the distinction between the large scale geometry of the catalyst channel and the smaller scale geometry of the catalyst pore structure, including the macropores, mesopores, and micropores.

In order to adequately describe the transport of species through the catalyst as a whole, it is therefore necessary to consider the dominant processes that are responsible for the transport of species through each of the individual regions. The different regions and their respective transport processes are summarized in Figure 8.

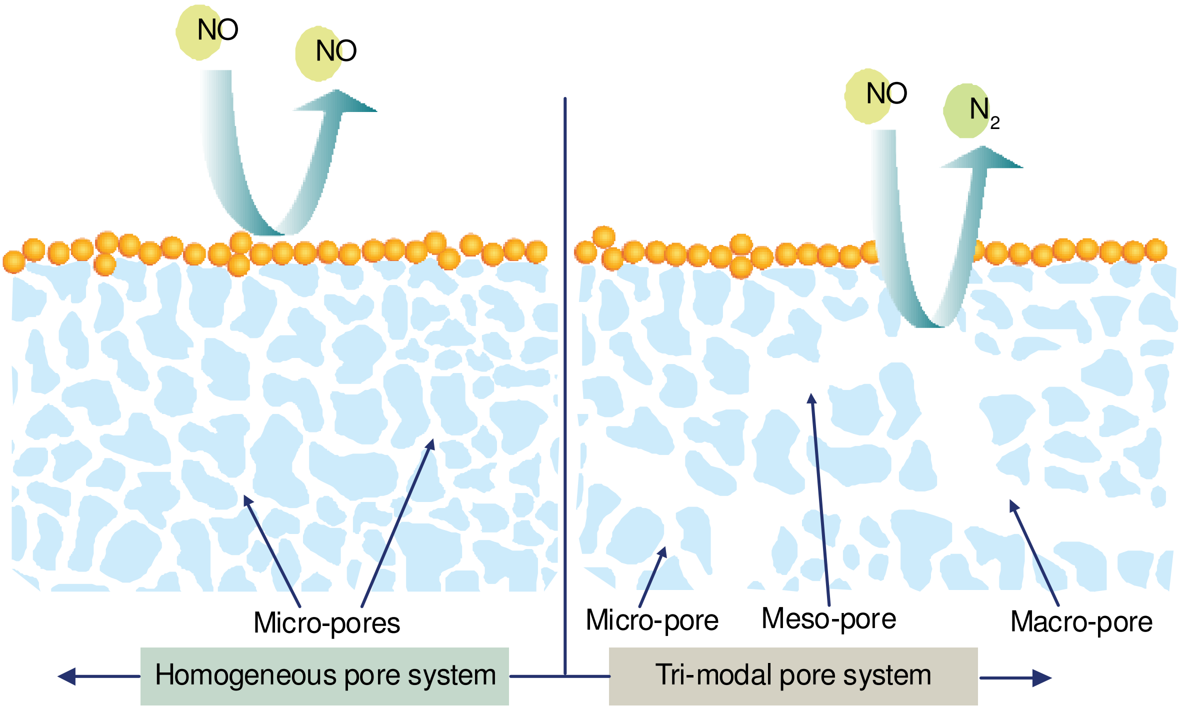

FIGURE 8 - TRANSPORT OF SPECIES WITHIN CATALYSTS OF DIFFERENT STRUCTURE. (DIAGRAM COURTESY OF HALDOR TOPSØ.) (20)

The following discussion is a summary of the treatment of the topic in Mill's Heat and Mass Transfer (26).

2.3.11 CONVECTIVE MASS TRANSFER

The dominant transport scheme within the SCR reactor as a whole is the bulk mass flow of exhaust gas through the reactor. Based upon the calculations that are presented in subsequent sections of the report, the hourly mass flow rate of exhaust of exhaust was calculated to be approximately 440,000 kg/hr. Given the number of catalyst channels that were determined for the design, this was equivalent to a volumetric flow rate of approximately .15 liters of exhaust per second per channel. As such, the dominant transport scheme within the catalyst channel is the bulk fluid motion of the exhaust gas.

Therefore, the transport of NO and NH_3 to from the bulk fluid to the catalyst wall is the result of convective mass transfer. The transport of a given species (species 1) from the bulk flow to the catalyst wall is described the following equation:

$$j_1 = k_{m\,1}(m_{1,s} - m_{1,b}) \qquad \text{Eq. 9}$$

In whichj_1 is the mass flux of a given species in kg/m^2-sec, $k_{m\,1}$ is the mass transfer coefficient of that species likewise in kg/m^2-sec, and Δm_1 is the difference between the mass fractions of the selected species in the bulk fluid and at the wall.

The format of this equation is identical to that of the equation that describes convective heat transfer. This similarity is exploited via the use of similar dimensionless groups in order to extend the solution of convective heat transfer to the case of convective mass transfer.

The mass transfer coefficient is determined from the Sherwood number, which is analogous to the Nusselt number in convective heat transfer.

The Sherwood number is given by the following relation:

$$Sh = \frac{k_{m\,1} d_h}{\sigma D_{12}} \qquad \text{Eq. 10}$$

In which d_h is the hydraulic diameter of the channel, σ is the exhaust gas density, and D_{12} is the diffusion binary diffusion coefficient in the mixture.

The diffusion coefficient can either be determined from experimental data or it can be calculated from either an empirical correlation or by a method such as the Chapman-Enskog theory (28).

Although the exhaust gas is technically a multi-component gas, it is feasible to approximate the diffusion coefficients of NO and NH_3 using binary diffusion coefficients because the concentrations of NO and NH_3 relative to the bulk of the exhaust gas are very small. Additionally, since the relative difference between the diffusion coefficients of NO and NH_3 is very small, it is common practice to use the diffusion coefficient of NO to approximate the values for both (29).

A commonly used expression for Sherwood number in monolithic catalyst elements is derived from the solution to the Graetz problem, which is an empirical expression for Nusselt number in square channels (29) (30).

In which:

$$Sh = 2.977 + 8.827(1000 * z^{*})^{-0.545} * exp(-48.2 * z^{*}) \qquad \text{Eq. 11}$$

And:

$$z^{*} = \frac{LD_{12}}{d_h v} \qquad \text{Eq. 12}$$

Where z^{*} is a dimensionless mass transfer length, L is the length of the channel, and v is the velocity of flow through the channel.

2.3.12 INTRAPOROUS MASS TRANSFER

Once the reacting species have reached the wall of the catalyst and entered the pores, the mass transfer scheme ceases to be convective. The transport of species within the pores is then function of the geometry and distribution of pore volumes (See Figure 8.). Since the mass transfer scheme is now diffusion based, the effect of these factors is accounted for by an effective diffusion coefficient which takes into account pore geometry upon the binary diffusion coefficient and also factors in the effect of Knudsen diffusion.

Therefore, the expression for effective diffusion coefficient is as follows:

$$\frac{1}{D_{1,eff}} = \frac{1}{D_{12,eff}} + \frac{1}{D_{K1,eff}} \qquad \text{Eq. 13}$$

In which $D_{12,eff}$ and $D_{K1,eff}$ are the effective binary diffusion and Knudsen diffusion coefficients, respectively.

This are obtained from the following expressions:

$$D_{12,eff} = \frac{\varepsilon_v}{\tau} D_{12} \qquad \text{Eq. 14}$$

And:

$$D_{K1,eff} = \frac{\varepsilon_v}{\tau} D_{K1} \qquad \text{Eq. 15}$$

In which ε_v is the void fraction of the catalyst, τ is the pore tortuosity, and D_{12} and D_{K1} are the binary diffusion and Knudsen diffusion coefficients respectively.

The Knudsen diffusion coefficient, which describes the diffusion of molecules due to their collision with the walls of the pore rather than with each other, is described by the equations for free molecule flow (26).

The Knudsen diffusion coefficient is determined from the following equations:

$$D_{K1} = \frac{2}{3} r_e \bar{v}_1 \qquad \text{Eq. 16}$$

Where r_e is the effective pore radius and $\bar{v}_1$is the average molecular speed of species 1 as determined by the following equation:

$$\bar{v}_1 = \left(\frac{8RT}{\pi M_1}\right)^{1/2} \qquad \text{Eq. 17}$$

In which M_1 is the molecular weight of the given species and R is the ideal gas constant.

Once the effective diffusion coefficient is known it can be incorporated into a dimensionless group that is known as the Thiele modulus.

The Thiele modulus is obtained from the following:

$$\Lambda = \frac{t_w}{2} \sqrt{\frac{k_{SCR} \rho_{cat}}{D_{1,eff}}} \qquad \text{Eq. 18}$$

Where t_w is the wall thickness, and k_{SCR} is the rate coefficient for the SCR reaction, which has previously been determined and which takes into account the effects of NH3 adsorption on the rate that is determined from the Arrhenius equation.

The Thiele modulus is used to determine a so-called effectiveness factor which is used to correct the reaction rate coefficient for the effects of intraporous mass transfer.

In cases where the Thiele modulus is large, the effectiveness is approximated by:

$$\eta = \frac{1}{\Lambda} \qquad \text{Eq. 19}$$

In the lumped parameter model, the cumulative effects of the individual mass transfer processes, including the actual rate of the SCR reaction, are incorporated into an overall mass transfer coefficient which replaces the usual mass transfer coefficient in a convective mass transfer problem.

The overall mass transfer coefficient is given by the following equation:

$$\frac{1}{k_{1m}^{oa}} = \frac{1}{k_{SCR}\eta} + \frac{1}{k_{1m}} \qquad \text{Eq. 20}$$

On the basis of the analogy for heat and mass transfer, the reduction of NO_X from the exhaust stream is determined by the following equation which is analogous to the governing equation convective heat transfer in a single stream heat exchanger:

$$\frac{\dot{m}_{in} - \dot{m}_{out}}{\dot{m}_{in}} = 1 - e^{\frac{-k_{1m}^{oa}\mathcal{P}L}{\dot{m}}} \qquad \text{Eq. 21}$$

In which $\mathcal{P}$ and L are the perimeter and length of the channel respectively.

2.3.13 CATALYST SELECTION

Ultimately, there are many different factors which affect the overall ability of a particular catalyst to remove NO from the exhaust stream. Some of these factors, such as soot loading and sensitivity to SO_X conversion, are specific to the application and are accounted for by the dimensioning and selection of materials. Other factors, such as the pore structure and activity, are inherent to the materials themselves and although there are mathematical correlations which have been derived to describe the effect of many of these factors upon the overall conversion rate, these factors are best accounted for by the use of experimentally derived data.

Therefore, the proper selection of a catalyst and the associated catalyst structure/geometry relies on the careful assessment of the expected operating conditions and service requirements, as well as the particular characteristics of the selected catalyst.

2.3.14 SCR FOR MARINE APPLICATIONS

Considerable experience has been developed with the application of SCR to industrial and mobile truck applications. This being said, there have been relatively few instances in which SCR systems have been installed on marine vessels, and even fewer of these have been for propulsion plants with low-speed diesel engines. The main reason for this is that until recently, there was not a regulatory impulse to justify the added cost and expenditure of installing an SCR unit.

The application of SCR to marine vessels with two-stroke diesel engines entails a set of problems and operating criteria which is quite unique to this particular application. Nevertheless, the experience that has been developed in other fields is invaluable because the shipboard environment is a combination of the attributes of the other environments. So, for example, while shipboard systems are similar to large industrial SCR units with regards to the flowrates that they experience, they are, at the same time, also similar to truck applications in that they are likewise constrained by size and storage capacity limitations.

When deciding upon and specifying an SCR unit, there are a number of considerations and limitations that must be taken into account. Loosely grouped, these considerations and limitations fall into one of four categories: regulatory requirements, the basic conditions at which the system is expected to operate, the overall integration of the SCR unit into shipboard systems, and further operational considerations such as maintenance and reliability.

The importance of regulatory considerations is twofold. First and foremost, regulations such as MARPOL Annex VI, are the justification for and reason why an SCR unit would be installed on a ship in the first place. This, in itself, is an important consideration because the regulatory environment can be quite complex, with local, regional, national, and international governments all having the right to decide the manner of regulations in their own particular jurisdictions. As such, even though a certain set of regulations may have been adopted internationally, there is nothing to guarantee that local authorities will not adopt even more stringent albeit local regulations. It is therefore important to have not only a sense of the regulations that have already been enacted, but to also understand the trends of forthcoming regulation and how they might be applied by various localities.

Secondly, regulations establish the limits of the permissible performance for an SCR unit. This is done by specifying the maximum allowable emission of NO_X from an engine and also the conditions under which it may be emitted. The significance of this point is not only in the limits that are set, but in the effect that the wording of the regulations can have upon the feasibility of the application of a particular technology. For example, one of the known limits of SCR is its performance when burning high sulfur fuels. Since high sulfur fuels are less expensive than low sulfur fuels, it would not normally be desirable to install an SCR system if it meant that the vessel could only burn low sulfur fuels when operating the system. However, since current regulations have linked the areas requiring the highest levels of NO_X emissions reduction to areas which also have regulations limiting the maximum allowable sulfur content of the fuel being burned (i.e. ECA areas), the application of SCR units once again becomes feasible. In this case, the regulations have served to support the application of SCR, but just as easily, a technology can be made infeasible by the careless wording of a particular rule.

The basic conditions at which a proposed system is expected to operate dictate whether the application of SCR is feasible and have significant effect on the selection of the design details. When considering at two-stroke application, the sensitive conditions which must be considered include the operating temperature range, the mass flow rate of the exhaust, and the fuel sulfur content.

The success of catalytic processes is extremely dependent upon the temperature at which it is carried out. For titania-vanadia catalysts, this optimum temperature window is typically between 300°C and 400°C. This is an important consideration for two-stroke applications because the exhaust temperature at the outlet of the turbocharger for a typical two-stroke engine is only about 250°C. As such, the SCR unit can only be placed before between the exhaust manifold and the turbocharger where typical exhaust temperatures are in the range of 350°C to 400°C. This limitation poses its own set of challenges since the most convenient location for the reactor is be to locate it near to the engine. Unfortunately, the space density of equipment in this area of the vessel tends to be very high according to current standard practices of machinery arrangement. This is a marked difference from the application of SCR to four-stroke marine diesel engines, since they tend to have turbocharger outlet temperatures in the range of 350°C and can therefore accommodate an SCR unit after the turbocharger and in the stack casing.

Another important limitation on SCR performance is the sulfur dioxide content of the exhaust gas. As we have discussed previously, the SO_2 content of the exhaust gas is a direct result of the sulfur content of the fuel being burned and the current practice within the marine industry is to burn residual fuels with a sulfur content of up to 4.5%. The SO_2 itself does not affect the ability of an SCR unit to reduce NO_X per se. Rather, the difficulty lies in the fact that the vanadium active sites in the catalyst also promote the oxidation of SO_2 to SO_3, which then either reacts with H_2O to form sulfuric acid or with HN_3 to form $(NH_4)HSO_4$ or $(NH_4)_2SO_4$. These compounds can lead to either the corrosion or fouling of downstream components in the exhaust system and their generation must be minimized. This is accomplished partly by the selection of catalyst materials with reduced vanadium content. The effect of decreased vanadium content on NO_X reduction and SO_2 oxidation is shown in Figure 9, in which it can be seen that although the catalyst with a lower vanadium content is also less effective at reducing NO_X concentration, the relative loss of effectiveness is much less than the corresponding reduction in SO_2 oxidation.

However, as was discussed discussed above, the required operation of SCR units will currently only be required in area which also have requirements for the operation on low sulfur fuels, thus the effect of the SO_2 conversion will be much less than if the units were being operated with fuels with maximum sulfur content.

The integration of the SCR system with the remainder of the shipboard systems requires that the SCR system does not have any negative effects upon the operation of other equipment and that the system can be successfully integrated into the machinery arrangement of the vessel.

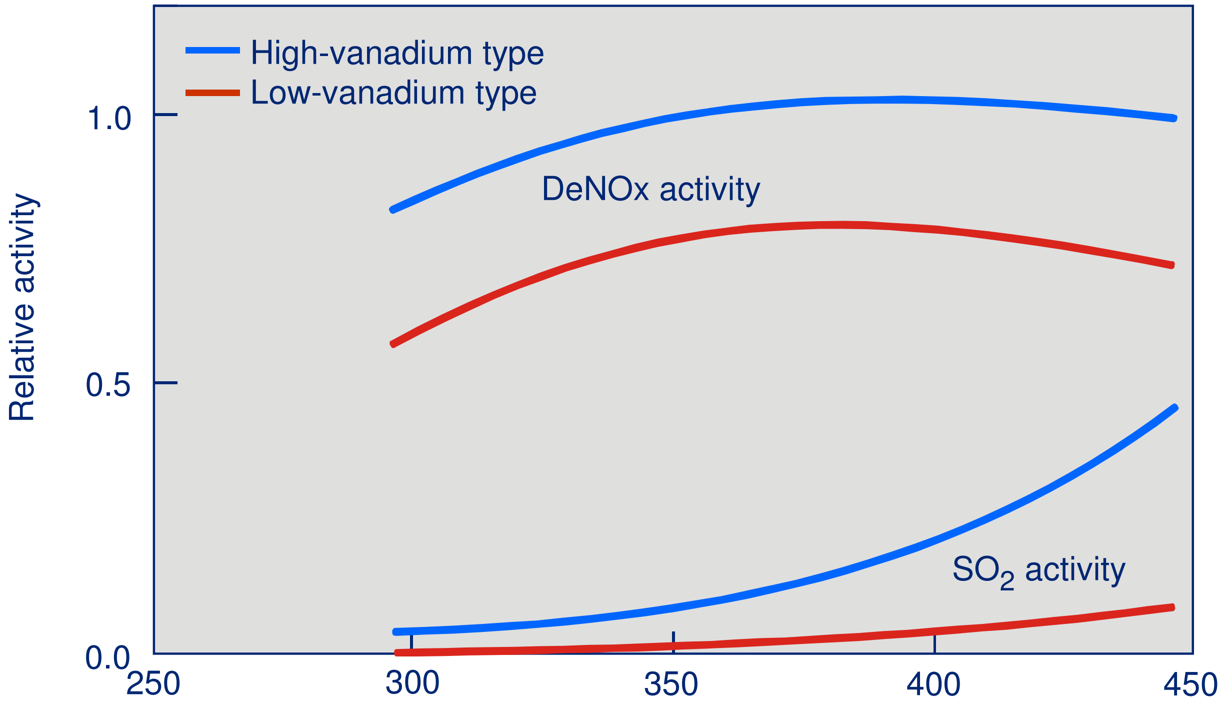

FIGURE 9 – EFFECT OF VANADIA CONTENT ON NO_X REDUCTION AND SO_2 OXIDATION. (23)
(FIGURE COURTESY OF HALDOR TOPSØE.)

One of the most significant challenges of the SCR system is the relatively large footprint of the unit. This topic will be investigated in greater detail in the modeling portion of this paper. However, sufficed to say, the footprint is relatively large and the equipment is best installed near to the main engine. This deck space is typically accounted for in typical machinery arrangements. The aim of this paper is therefore to size a typical SCR unit for a large bore containership engine in order to determine the feasibility of installing such a piece of equipment in the engine in the engine room of such a vessel. Regardless, the placement of the SCR unit is likely to be a challenge. In this respect, the best approach will be not to attempt to “fit” the SCR unit into a typical engine room arrangement, but rather to take a proactive approach and to design a machinery arrangement that is built around the main engine *and* SCR unit installations.

Secondly, the SCR system will also have to integrate seamlessly with the remainder of the ship’s systems. This means that the unit will not only have to integrate with other systems such as the engine and machinery control systems, but that it should not have negative effects on the operations of other equipment, including the exhaust gas boiler. Additionally, if other exhaust gas treatment or waste heat recovery systems are installed, the SCR unit will have to function without negatively impacting the function of those systems.

Figure 10 presents the schematic of a proposed SCR unit for a low-speed diesel marine application, and includes the arrangement of the unit relative to the engine exhaust system as well as auxiliary systems such as the urea dosing system and the SCR control system.

One of the interesting things to note in the diagram is the inclusion of a bypass around the SCR system. This arrangement is important because it allows the operation of the main engine without the SCR system in operation. This feature is necessary during the start-up of the SCR unit because the thermal load of a cold SCR reactor can cool the exhaust gas at the outlet of the unit to the point where it will cause the turbocharger to trip. Therefore, in order to ensure reliable operation of the engine, a bypass is included around the SCR system to allow for the unit to be warmed up prior to putting it into service.

This effect that the SCR reactor can have upon the operation of the engine highlights the importance of operational criteria in considering the addition of an SCR unit to a vessel design. For one, the installation of the SCR system must be part of an overall reliable design. In this respect, the unit must be designed so as to limit the effects of that a malfunction might have on the overall operational integrity of the vessel. In other words, the system should be designed so to minimize the chances of a loss of propulsion should an abnormal condition occur.

Additionally, the unit must be able to function on a timescale that is in line with typical vessel maintenance schedules. Since most vessels operate on a 5 year maintenance schedule for major items, i.e. 5 year dry-docking schedule, the system needs to be designed so as to be to operate within acceptable constraints during the interval between major repair periods. Since catalyst deactivation is expected, the system needs to be oversized in order to meet minimum operating requirements at the end of the 5 year overhaul cycle.

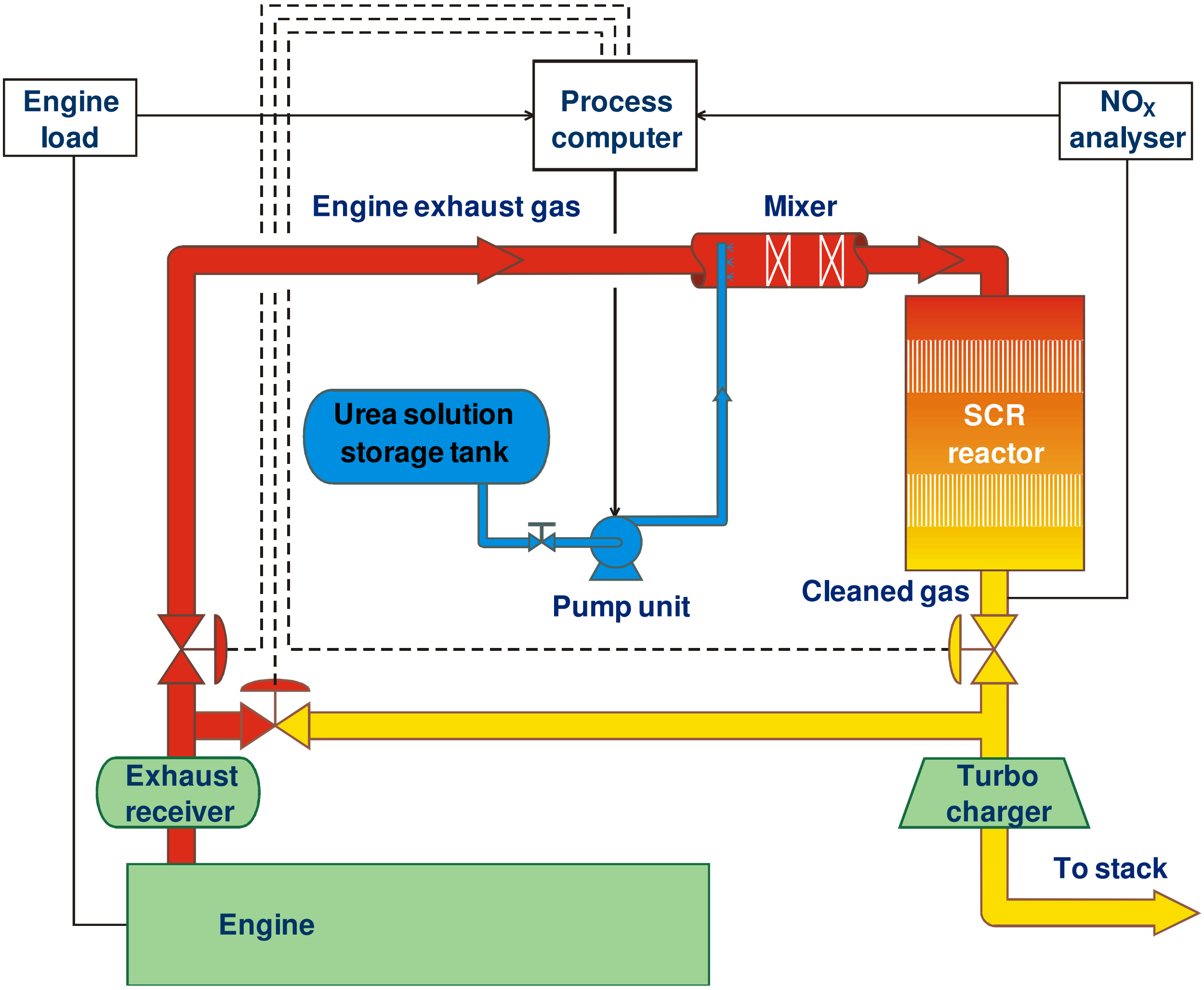

FIGURE 10 - SCHEMATIC OF A PROPOSED LAYOUT FOR AN SCR UNIT FOR A MARINE LOW-SPEED DIESEL APPLICATION. (27)
(DIAGRAM COURTESY OF HALDOR TOPSØE.)

FIGURE 11 - INSTALLATION OF HONEYCOMB CATALYST BLOCKS. (27)
(PICTURES COURTESY OF HALDOR TOPSØE.)

3 MODEL

3.1 PROGRAM DESCRIPTION

The previous sections have included a discussion regarding the general theory behind and aspects pertaining to the application of selective catalytic reduction to low speed marine diesel propulsion engines. In the course of this discussion, a number of important design criteria have been identified and discussed. These criteria include, but are not limited to, such considerations as the dependence of catalyst activity upon temperature, the effects of particulate loading on catalyst lifespan and catalyst geometry, and the practical limits of the velocity of flow through the a given catalyst channel.

In this section, the factors and constraints identified above are incorporated into a computational program which is developed as a tool for determining the minimum required size of an SCR unit for a marine low speed diesel application. The program is formulated so to as to give the user the maximum flexibility with respect to the types of low speed diesel installations that the specified SCR units can be applied to.

The object of the investigation is to determine the size and relevant operating parameters of a conservatively sized unit that would still meet the minimum reduction requirements so as to bring the engine into compliance with IMO Tier III standards. In the interest of evaluating whether SCR is feasible for engines with large exhaust flow rates, the calculations are based upon a large 11 cylinder, 90 cm bore containership engine that is rated at 52000 kW at full load. Although this is not the largest engine that is available on the market, this particular engine size was chosen because of the availability of published emissions data for this engine, including NO_X emissions measurements at different loads.

For the purposes of this project, the calculations are executed using a combination of empirical data and representative data that from various sources in literature. However, in order to allow for maximum flexibility in using the program to size SCR units for a variety of low speed diesel engine types, all values have been defined as variables so that if the user has more specific data available, the calculations can be performed so as to reflect the specific conditions for that particular application.

The program is designed to be a non-specific sizing tool. As such, input values were chosen so as to be readily available from such sources as engine selection project guides, catalyst data sheets, and specification sheets from urea solution manufacturers. A summary of the inputs in included in Appendix D.

3.1.1 GOVERNING EQUATIONS:

The SCR reactor is described using a lumped parameter model in which the effects of reaction rate, intraporous mass transfer, and intra-channel mass transfer are accounted for by the use of a single overall mass transfer coefficient.

Tronconi et al. compared the adequacy of a single dimensional lumped parameter model such as this relative to a more rigorous two dimensional model and found that the lumped parameter models was a very good approximation for calculations relating to catalyst with square channel geometry, with the added benefit of having a significantly smaller computational time than a corresponding two dimensional models (31).

The model assumes that the SCR reactor is isothermal and that the flow exhaust gas is evenly distributed between the various channels in the reactor. This assumption makes it possible neglect heat transfer considerations and to model the behavior of the entire reactor by considering the behavior of a single channel (30).

The governing equation which describes the rate of removal of NO_X from exhaust gas in a single channel is as follows:

$$\varepsilon = 1 - e^{\frac{-k_m^{oa}\mathcal{P}L}{\dot{m}_{exh,ch}}} \qquad \text{Eq. 22}$$

In which $\mathcal{P}$ is the perimeter of the channel, L is the length of the channel, $\dot{m}_{exh,ch}$ is the mass flow of exhaust through a single channel, k_m^{oa} is the overall mass transfer coefficient, and ε is the required effectiveness of reduction.

The dimensions effectiveness of NO_X reduction is obtained from the following equation where $\dot{m}$ is the mass flow NOx:

$$\varepsilon = \frac{\dot{m}_{NOx\ in} - \dot{m}_{NOx\ out}}{\dot{m}_{NOx\ in}} \qquad \text{Eq. 23}$$

For the purposes of the program, two values of different effectiveness values are evaluated and then compared. The first effectiveness value is based upon Marpol Annex VI regulations. The NOx emissions rate from an engine is assumed to be maximum which is specified according to the Tier I regulations, i.e. 17 g/kW-hr and the maximum allowable emissions rate according to Tier III regulations is 3.4 g/kW-hr and this value is used to determine the minimum effectiveness of NO_X removal, i.e. 80%.

The second effectiveness factor is based upon experimental data from an 11 K90 MC-C engine which included measurements of NO_X emissions. The source and correction of this will be discussed in greater detail in subsequent section, but it is nevertheless interesting because the engine tested emitted a significantly higher concentration of

NOx. Consequently, an effectiveness of approximately 90% is required to meet the Tier III standards.

In equation XXX above, $\dot{m}_{exhaust,ch}$ is the mass flow of exhaust per channel. This value is obtained from the calculation of exhaust gas flow rate and from the number of required number of channels that were calculated.

The lumped mass transfer coefficient is represented by k_m^{oa} and is obtained from:

$$\frac{1}{k_m^{oa}} = \frac{1}{k_{SCR} * \eta * \rho_{exh}} + \frac{1}{k_m} \qquad \text{Eq. 24}$$

In which k_m is the mass transfer coefficient as obtained from the Sherwood number, ρ_{exh} is exhaust gas density, k_{SCR} is the intrinsic rate of reaction for the SCR eraction, and η is the effectiveness factor which describes inter and intraporous mass transfer.

The value of k_{SCR} is obtained from experimental data that determined by (32) for a sample of Haldor Topsoe catalyst.

The terms $\mathcal{P}$ and L refer to the perimeter of the catalyst channel and the required length of the catalyst respectively. The value of L is the quantity that is being solved for with the program.

3.1.2 PROGRAMMING CONCEPT

The SCR reactor is sized upon the basis of a number of different considerations and ultimately, the length of the reactor, as per equation Eq. 22, is only determined after all of these other factors have been taken into consideration.

Once the required data has been calculated and assembled, the sizing of the reactor can proceed according to the following considerations:

In order to avoid particle deposition and, at the same time, erosion of the monolith, a flow velocity of between 5-7 m/s is chosen (33) as a guide value. Based upon the assumption of laminar flow through the channel (30), a Reynolds number of 2000 is used to establish a maximum flow velocity through the channel (34).

Once the velocity of flow is known, the total required channel surface area is determined on the basis of the mass flow rate, the surface area of a single channel. From this, the number of catalyst blocks per layer and the cross sectional area of the reactor can be determined.

Once the cross sectional area of the reactor has been determined, the length of the reactor is now obtained on the basis of the governing equation.

The effective diffusion coefficient of NO through the catalyst and the intrinsic rate constant for the SCR reaction are calculated and corrected on the basis of experimentally determined values from literature (31).

Once these values have been obtained and corrected for the conditions within the reactor, various values including the Thiele modulus, effectiveness, Sherwood number, and mass transfer coefficient are determined so as to allow the calculation of the required length and the length is corrected for the effects of catalyst deactivation.

Finally, the pressure drop across the length of catalyst is obtained so as to ensure that the design is within the previously discussed pressure drop constraints.

3.2 MODEL ASSUMPTIONS

The base assumptions of the model are that a urea based SCR system is to be sized for a PANAMAX containership. The general layout of the system is illustrated in Figure 10.

The urea based system is selected because of the relative ease of handling of urea water solutions compared to other ammonia delivery options. The alternative is an ammonia delivery system which is not as convenient because it requires a compressed gas delivery system and special handling due to the its flammable nature (34).

The urea water solution was chosen to contain 40% urea by weight which is a standard and readily available urea solution concentration and which is a commonly employed for SCR applications.

The catalytic reactor is assumed to contain of several layers of modular monolithic catalyst elements, with each individual element being the same size as the other elements. This reflects the fact that catalyst manufacturers typically offer a limited range of catalyst element sizes and the fact that eventually the catalysts elements will have to be replaced due to deactivation and that this is best accomplished via the use of modular and relatively easy to handle element sizes.

The catalyst monolith is assumed to contain channels with a square cross-sectional area which is one of the more common, though by no means only, catalyst configuration available. The assumption of a square cross sectional area is a limiting assumption for the model because the expression for determining Sherwood number is limited in its applicability to square channels alone.

The channel width is chosen on the basis of a recommendation from a technical paper by Haldor Topsoe (35)regarding SCR systems for marine two stroke engines. For diesel exhaust gas applications, the paper recommends a hydraulic diameter of 5mm.

The SCR catalyst is assumed to lose 5% of its activity per 10,000 hours operation. This is a representative value of the typical deactivation rates that are found in industry and the catalyst size is also calculated taking into account catalyst deactivation Ref.

Since the vessel is expected to operate on a 5 year drydock and major repair cycle, the catalyst was also expected to maintain satisfactory reduction of NOx for a least five continuous years of operation, based upon the expected yearly service requirements of the vessel, i.e. days in service per year.

4 MODEL DESCRIPTION

The model was developed and executed using MATLAB R2010b. The model is based upon a series of individual modules which are used to calculate the properties of different elements of the system. The relevant outputs each of the individual models are assembled into the final model which determines the actual size of the reactor that is required. A stand alone is used to calculate the required consumption of urea for system.

A copy of the MATLAB scripts is included in Appendix B. A summary of the module input parameters is contained in Appendix A and Appendix C contains the module output files.

4.1 MODULE 1: CALCULATION OF EXHAUST GAS FLOW RATE

The purpose of Module 1 is to determine the mass flow rate of exhaust for a given engine design. The model is executed using a combination of readily available project data from the engine manufacturer (28) (29) and of engine specific data from previous work (39). By use of feasible assumptions, the model is designed to be applicable even when the engine specific data referenced above is not available.

The exhaust gas module was executed for four load conditions: 25%, 50%, 75%, and 100%. However, only the outputs from 100% load case were passed to the continuing modules as this is the applicable load case for sizing the catalytic reactor.

The engine is considered as an open system and the mass flow of engine exhaust is calculated based upon the principle of conservation of mass.

The working fluids that enter into the combustion chamber are fuel, air, and cylinder lubricating oil. Under normal operating conditions, all of the fluids that enter into the combustion chamber are exhausted as part of the exhaust gas stream. The only exception is the minute quantity of cylinder lubricating oil which is collected from the stuffing box drains. However, relative to the mass flow of air into the combustion chamber, it is feasible to assume that all of the cylinder lubricating oil that is injected into the combustion chamber is burned and exhausted along with the rest of the exhaust gas flow.

The mass flow air through the engine is obtained from volume of the cylinder using ideal gas equation.

The volume of the cylinder is determined from the stroke and bore of the cylinder. The compression volume is obtained by subtracting the height of the intake ports from the nominal stroke since compression of the intake air above the scavenge air pressure only occurs once the scavenge air ports have been closed.

$$V_{comp} = \frac{\pi D^2}{4}(S - h_{port}) \qquad \text{Eq. 25}$$

Where:

V_{comp} = Volume of cylinder in m^3/cyl
D = Cylinder bore in m
S = Stroke in m
h_{port} =Height of scavenge air ports in m

The mass of combustion air in the cylinder is determined from the ideal gas equation and using the temperature and pressure of the scavenge air. The temperature and pressure of the scavenge air will be different at different load conditions and with different ambient and sea water temperatures, but for full load feasible values are approximately 35°C and 3.5 bar.

$$m_{air,c} = \frac{PV_{comp}MW_{air}}{RT * 1000} \qquad \text{Eq. 26}$$

Where:

$m_{air,c}$ =Mass of air in kg/cyl
P = Scavenge air pressure in Pa
MW_{air} = Molecular weight of air in g/mol
R = Ideal gas constant in m^3 Pa/mol K
T =Temperature of scavenge air in K

The mass combustion air is next corrected for the amount of scavenging air that passes through the cylinder. Although the terms intake and scavenge air are often used interchangeably, the purpose of the scavenge air is to remove the maximum amount spent exhaust gas from the combustion chamber prior to the start of the next compression stroke.

If the combustion excess air and total excess air are known, the mass of the air in the cylinder is corrected by the ratio of the two values.

$$m_{air,i} = \frac{EA_{total}}{EA_{comb}} * m_{air,c} \qquad \text{Eq. 27}$$

Where:

$m_{air,i}$ = Mass of intake air in kg/cyl
EA_{total} = Excess air total including scavenge air
EA_{comb} = Excess air for combustion

For an engine that is not coupled to controllable pitch propeller or shaft generator, engine rpm varies with load. Although not strictly linear, the dependence between load and rpm can be approximated as a linear relationship. Therefore, for a given load, the mass flow through the engine is obtained from:

$$\dot{m}_{air} = \frac{m_{air,i} rpm}{60 \frac{sec}{min}} * Load \qquad \text{Eq. 28}$$

Where:

$\dot{m}_{air}$ = Mass flow air in kg/sec-cyl
$Load$ = % Load as fraction
rpm = Revolutions per minute at full load

Fuel and cylinder lubricating oil consumption are specified in terms of brake specific consumption. The values are given in g/kW-hr. Since we have calculated the mass flow of air though an individual cylinder, the fuel and cylinder lube oil flows much likewise be corrected to reflect the flow through a single cylinder.

$$\dot{m}_{fuel} = \frac{SFOC * Load * KW}{N * 3600 * 1000} \qquad \text{Eq. 29}$$

$$\dot{m}_{CLO} = \frac{SLOC * Load * KW}{N * 3600 * 1000} \qquad \text{Eq. 30}$$

Where:

$\dot{m}_{fuel}$ = Mass flow fuel in kg/sec-cyl
$\dot{m}_{CLO}$ = Mass flow cylinder lubricating oil in kg/sec-cyl
$SFOC$ = Specific fuel oil consumption in g/kW-hr
$SLOC$ = Specific lube oil consumption in g/kW-hr
KW = Rated power of the engine at full load, in kW/hr
N = Number of cylinders

Once the mass flow of air, fuel, and cylinder lube oil into a given cylinder are known, the mass flow of exhaust gas from each cylinder can be determined.

$$\dot{m}_{exh,c} = \dot{m}_{air} + \dot{m}_{fuel} + \dot{m}_{CLO} \qquad \text{Eq. 31}$$

Where:

$\dot{m}_{exh,c}$ = Mass flow of exhaust in kg/sec-cyl

And the mass flow of exhaust from the entire engine is:

$$\dot{m}_{exh} = N\dot{m}_{exh\ cyl} \qquad \text{Eq. 32}$$

Where:

$\dot{m}_{exh,c}$ = Mass flow exhaust in kg/sec

If the exhaust temperature and pressure are known, then the volumetric flow rate of exhaust gas can likewise be determined. It should be noted since the SCR unit is located before the exhaust gas turbocharger, the exhaust temperature and pressure are those of the exhaust manifold rather than those of the exhaust system after the turbocharger.

$$\dot{V}_{exh} = \frac{\dot{m}_{exh}RT}{P}\frac{1000}{MW_{exh}} \qquad \text{Eq. 33}$$

Where:

$\dot{V}_{exh}$ = Volumetric flow of exhaust in m^3/hr
T = Temperature of exhaust gas in K
P = Pressure of exhaust gas in Pa
MW_{exh} = Molecular weight of exhaust in g/mol

The molecular weight of exhaust gas is obtained from previous work. The exhaust gas composition was determined for a heavy fuel oil with a sulfur content of 4.5% by mass, which is the maximum sulfur content currently allowable under MARPOL Annex VI regulations. This corresponds to a molecular formula of $C_1H_{1.53}S_{0.02}$. The excess combustion air was 2.37, which corresponds to an equivalence ratio of 0.4224. And finally, pursuant to ISO standards, the relative humidity of the intake air was assumed to be 56%.

The molecular weight of the exhaust was determined to be 30.03 g/kW-hr. However, since the exhaust gas stream is actually a mixture of scavenging air and exhaust gas, the final molecular weight of the exhaust gas must be corrected as follows:

$$MW_{exh} = \frac{MW_{exh,c} * EA_{comb} + MW_{air}(EA_{total} - EA_{comb})}{EA_{total}} \qquad \text{Eq. 34}$$

Where:

$MW_{exh,c}$ = Calculated molecular weight of undiluted exhaust gas in g/mol
MW_{air} = Molecular weight of air in g/mol

4.2 MODULE 2:

The purpose of module 2 is to calculate the density and viscosity of the exhaust gas.

The density of the exhaust gas is determined from the ideal gas equation:

$$\rho_{exh} = \frac{P_{exh,a}}{RT}\frac{MW_{exh}}{1000} \qquad \text{Eq. 35}$$

Where:

ρ_{exh} = Density of exhaust in kg/m^3
$P_{exh,a}$ = Average exhaust pressure in Pa

The average exhaust pressure in the system takes into account the pressure drop across the SCR reactor. For initial calculations this can be taken as 1000 Pa, which is equivalent to 100 mmH$_2$Og.

$$P_{exh\,,a} = P_{exh} + \frac{\Delta P_{avg}}{2} \qquad \text{Eq. 36}$$

The dynamic viscosity is approximated by the dynamic viscosity of air at the exhaust gas temperature. Once the dynamic viscosity is known, the kinematic viscosity can be determined.

$$\upsilon_{exh} = \frac{\mu_{exh}}{\rho_{exh}} \qquad \text{Eq. 37}$$

Where:

υ_{exh} = Kinematic viscosity of exhaust in m^2/sec
μ_{exh} = Dynamic viscosity of exhaust in kg/m-sec

4.3 MODULE 3:

The purpose of Module 3 is to determine the required reduction of NO$_X$ across the SCR reactor. Since the aim of this paper is to size a unit which will be compliant with IMO Tier III standards, the maximum allowable emission of NO$_X$ is be 3.4 g/kW-hr.

IMO Tier I standards specify that the maximum emission of NO$_X$ for any engine built after 2000 is 17g/kW-hr. Since this standard has already been attained without the use of secondary NO$_X$ reduction methods, this value is taken as a starting point for determining the current NO$_X$ emissions.

This module also evaluates the diffusion NOx emissions rates from Miller at al. and corrects them for correct mass flow rate for a K 90 engine.

The mass flow of NO$_X$ from a Tier I compliant engine is given by:

$$\dot{m}_{NOx\,Tier\,I} = \frac{NOx_{Tier\,I}KW * Load}{3600 * 1000} \qquad \text{Eq. 38}$$

Where:

$\dot{m}_{NOx\ Tier\ I}$ = Mass flow of NOx in kg/sec
$NOx_{Tier\ I}$ = Specific emission rate of NO_X in g/kW hr

The maximum allowable NO_X flow from a Tier III compliant engine is then obtained by:

$$\dot{m}_{NOx\ Tier\ III} = \frac{NOx_{TierIII}KW * Load}{3600 * 1000} \qquad \text{Eq. 39}$$

Where:

$\dot{m}_{NOx\ Tier\ III}$ = Mass flow of NO_X in kg/sec
$NOx_{TierIII}$ = Specific emission rate of NO_X in g/kW-hr

The required effectiveness of the SCR unit then obtained by the following:

Eq. 40

Where:

ϵ = Effectiveness of mass exchanger

The NOx emissions data from Miller at al. includes a value for the grams of NOx emitted per hour. In order to determine the actual emissions from the engine that was tested, this values is scaled up relative to the calculated volumetric flow rate of exhaust that has been determined from Module 1 and which has been scaled for the temperature and pressure conditions that correspond to the sampling point used by Miller et al.

The volumetric flow rate at the experimental conditions is determined as follows:

$$V_{calc,corr} = \frac{\dot{M}_{exh}RT}{P} \qquad \text{Eq. 41}$$

Where:

$V_{calc,corr}$ = Corrected volumetric flow rate from Module 1 in m^3/s
$\dot{M}_{exh}$ = Molar flow of exhaust as determined in module 1 in mol/sec

The correct value of gram of NOx emitted per hr is follows:

$$\dot{m}_{UCI,corr} = \frac{\dot{m}_{NOx,UCI} * \dot{V}_{calc,corr}}{\dot{V}_{exh,UCI}} \qquad \text{Eq. 42}$$

Where:

$\dot{m}_{UCI,corr}$ = Actual emission of NO_X from engine in g/hr
$\dot{m}_{NOx,UCI}$ = Measured emission of NO_X from Miller et al. in g/hr
$\dot{V}_{exh,UCI}$ = Volumetric flow rate of exhaust gas as reported by Miller et al. in m^3/sec

The specific NOx emissions rate is then calculated:

$$NOx_{UCI} = \frac{\dot{m}_{UCI,corr}}{KW * Load} \qquad \text{Eq. 43}$$

In which:

NOx_{UCI} = Specific NOx emission rate based on UCI data in g/kW-hr

And the mass flow of NOx is obtained as follows:

$$\dot{m}_{NOx\ UCI} = \frac{NOx_{TierUCI} KW * Load}{3600 * 1000} \qquad \text{Eq. 44}$$

Where:

$\dot{m}_{NOx\ UCI}$ = Mass flow of NOx in kg/sec

The required effectiveness based up on the measurements of Miller et al. is obtained from the following:

$$\varepsilon = \frac{\dot{m}_{NOx\ UCI} - \dot{m}_{NOx\ Tier\ III}}{\dot{m}_{NOx\ Tier\ I}} \qquad \text{Eq. 45}$$

4.4 MODULE 4: UREA CONSUMPTION AND STORAGE REQUIREMENTS

The purpose of module 5 is to estimate the urea consumption requirements for the installation using the method from (40).

The solution is assumed to be 40% Urea by mass.

The consumption of NH3 for a particular condition is obtained from the following:

$$\dot{m}_{NH3} = \dot{m}_{exh,hr} * \left(\frac{ppm_{mass,Tier\ I}}{1 * 10^6}\right) * \left(\frac{MW_{NH3}}{MW_{NO}}\right) * R_{NO-NH3} \qquad \text{Eq. 46}$$

Where:

$\dot{m}_{NH3}$ = Mass flow rate of NH_3 in kg/hr
$ppm_{mass,Tier\ I}$ = Concentration of NO in parts per million by mass
MW_{NH3} = Molecular weight of ammonia in g/mol
MW_{NO} = Molecular weight of NO in g/mol
R_{NO-NH3} = Ratio of NH_3 to NO

The dosing ratio of NH3 to NO takes into account the required reduction and the allowable slip of ammonia from outlet of the SCR unit. Slip is that ammonia which has not been reacted in the SCR unit and passes out of the unit unreacted.

$$R_{NO-NH3} = \left(\varepsilon + \frac{Slip * \left(\frac{MW_{exh}}{MW_{NO}}\right)}{ppm_{mass,TierI}}\right) \qquad \text{Eq. 47}$$

In which:

ε = Effectivness
$Slip$ = Maximum allowable NOx at reactor outlet in ppm by vol

Once the required mass flow rate of NH_3 is known, the mass flow rate of urea solution can be determined:

$$\dot{m}_{Urea} = \frac{\dot{m}_{NH3}}{urea} \frac{MW_{urea}}{MW_{NO}} \frac{100}{2} \qquad \text{Eq. 48}$$

Where:

$\dot{m}_{Urea}$ = Mass flow of urea in kg/hr
MW_{urea} = Molecular weight of Urea in g/mol
$urea$ = Percent of urea in solution by weight

And the specific gravity of the urea water solution is used to determine the volumetric flow rate of Urea water solution.

$$\dot{V}_{Urea} = \frac{\dot{m}_{Urea}}{SG_{urea} * 1000} \qquad \text{Eq. 49}$$

Where:

$\dot{V}_{Urea}$ = Volumetric flow rate of urea solution in m^3/hr
SG_{urea} = Specific gravity of urea

4.5 MODULE 5: DIFFUSION COEFFICIENTS

The purpose of module 5 is to estimate the diffusion coefficients of NO and NH_3 in the exhaust gas using the Chapman and Enskog solution of the Boltzmann equation. From [Reid], the binary diffusion coefficients of gases A and B are given by:

$$D_{AB\ cm} = \frac{0.00266T^{3/2}}{PM_{AB}^{1/2}\sigma_{AB}^2\Omega_D} \qquad \text{Eq. 50}$$

Where:

D_{AB} = Diffusion coefficient in cm^2/sec
T = Temperature in K
P = Pressure in bar
M_{AB} = Molecular weight in g/mol
σ_{AB} = Characteristic length in Å
Ω_D = Diffusion collision integral, dimensionless

The diffusion collision integral is obtained from the following equation:

$$\Omega_D = \frac{A}{(T^*)^B} + \frac{C}{\exp(DT^*)} + \frac{E}{\exp(FT^*)} + \frac{G}{exp(HT^*)} \qquad \text{Eq. 51}$$

Where:

$$T^* = \frac{k_B T}{\epsilon_{AB}} \qquad \text{Eq. 52}$$

Where:

ϵ_{AB} = Characteristic energy parameter
k_B = Boltzman constant

The values for the diffusion collision integral coefficients are summarized by the following table:

Coefficient	Value
A	0.19300
B	0.15610
C	0.19300
D	0.47635
E	1.03587
F	1.52996
G	1.76474
H	3.89411

The values ϵ and σ for pure substances are obtained from tabulated property data in (40). Air is considered a pure substance.

The interaction values for MW_{AB}, ϵ_{AB}, and σ_{AB} are obtained from the pure substance values according to the following relations:

$$\epsilon_{AB} = (\epsilon_A \epsilon_B)^{1/2} \qquad \text{Eq. 53}$$

$$\sigma_{AB} = \frac{\sigma_A + \sigma_B}{2} \qquad \text{Eq. 54}$$

$$MW_{AB} = \frac{2}{\frac{1}{MW_A} + \frac{1}{MW_B}} \qquad \text{Eq. 55}$$

Finally, the diffusion coefficient is converted to m^2/sec in order to maintain consistency with the system of units employed in the rest of the calculations.

$$D_{AB} = \frac{D_{AB\ cm}}{10000} \qquad \text{Eq. 56}$$

Where:

D_{AB} = Diffusion coefficient in m^2/sec

4.6 MODULE 6: CATALYST PROPERTIES

The purpose of Module 6 is to characterize the configuration and physical properties of the catalyst based upon reasonable assumptions. The module is designed so that different configurations of the catalyst can be specified for investigation in the SCR module.

The catalyst is assumed to be an extruded monolith with square channels, which is a design configuration that is typical of many, but not all catalyst manufacturers.

For ease of production and installation, the catalyst is assumed to be available in standard-size blocks, or elements, which are of a size so as to allow ease of handling.

The primary dimension of the catalyst is the width of the channel. Although it is most convenient to specify the width of the channel in millimeters, meters are used in these calculations in order maintain consistency with the rest of the program.

If the width of the channel is known, it is then possible to determine the area, perimeter, and hydraulic diameter of the channel.

$$A_{ch} = w_{ch}^2 \qquad \text{Eq. 57}$$

$$\mathcal{P}_{ch} = 4w_{ch} \qquad \text{Eq. 58}$$

Where:

A_{ch} = Channel area in m^2
w_{ch} = Channel width in m
$\mathcal{P}_{ch}$ = Perimeter of channel in m

Since the channel is square in cross section, the hydraulic diameter is simply the width of the channel:

$$d_h = \frac{4A_{ch}}{\mathcal{P}_{ch}} = w_{ch} \qquad \text{Eq. 59}$$

Where:

d_h = Hydraulic diameter of channel in m

The surface area of the inner wall of a single channel is given by:

$$A_{surf,ch} = 4\mathcal{P}_{ch} H_{block} \qquad \text{Eq. 60}$$

The size of a rectangular catalyst element is specified by the number of channels along the length and width of the catalyst element.

$$n_{ch} = n_{ch,x} * n_{ch,y} \qquad \text{Eq. 61}$$

Where:

n_{ch} = Total number of channels in a single element
$n_{ch,x}$ = Number of channels along the length of an element
$n_{ch\,y}$ = Number of channels along the width of an element

Assuming a feasible wall thickness of 0.8 mm [], the cross sectional area of an element is determined:

$$W_x = n_{ch,x}(t_w + w_{ch)} + t_w \qquad \text{Eq. 62}$$

$$W_y = n_{ch,y}(t_w + w_{ch)} + t_w \qquad \text{Eq. 63}$$

$$A_{element} = W_x * W_y \qquad \text{Eq. 64}$$

Where:

W_x = Width of element in m
W_y = Length of element in m
t_w = Wall thickness in m
$A_{element}$ = Cross sectional area of element in m^2

A feasible height for the catalyst element is assumed. This is the same as the length of the channel for the purposes of the mass transfer model. Once the height of the catalyst element is known, then the nominal volume of a catalyst block can be determined.

$$V_{element} = A_{element} * H_{block} \qquad \text{Eq. 65}$$

Where:

$V_{element}$ = Volume of catalyst element in m^3
H_{block} = Height of catalyst element in m

The volume of the active catalyst within the catalyst element is given by:

$$V_{cat} = \left(A_{element} - (n_{ch} * A_{ch})\right) * H_{block} \qquad \text{Eq. 66}$$

Where:

V_{cat} = Volume of active catalyst material

The volume of catalytic material per channel is:

$$V_{cat,ch} = \frac{V_{cat}}{n_{ch}} \qquad \text{Eq. 67}$$

The total surface area of a catalyst element is given by:

$$A_{surf,block} = A_{surf,ch} * n_{ch} \qquad \text{Eq. 68}$$

4.7 MODULE 7: SCR REACTOR

The purpose of Module 7 is to determine the required size of the catalytic reactor. The method employed in Module 7 is based upon the analogy between heat and mass transfer and is analogous to the solution of a single stream heat exchanger.

The catalytic reactor is designed to operate in the laminar flow regime. Recognizing that the transition between laminar and turbulent flow occurs around Reynolds numbers of 2800, the maximum velocity through the channels is solved as follows:

$$v_{max} = \frac{Re_{max} v_{exh}}{d_h} \qquad \text{Eq. 69}$$

Where:

v_{max} = Maximum velocity in m/s
Re_{max} = Reynolds number

Based upon the velocity and the volumetric flow rate, the total required cross-sectional area of the channels is determined:

$$A_{ch,req} = \frac{\dot{V}_{exh}}{v_{max}} \qquad \text{Eq. 70}$$

Where:

$A_{ch,req}$ = Minimum number of channels

Based upon the geometry derived in Module 6, the minimum number of catalyst blocks in a single layer of catalyst is determined.

$$n_{ch,req} = \frac{A_{ch,req}}{A_{ch}} \qquad \text{Eq. 71}$$

$$n_{el} = \frac{n_{ch,req}}{n_{ch}} \qquad \text{Eq. 72}$$

Where:

$n_{ch,req}$ = Minimum number of channels required
n_{el} = Minimum number of catalyst blocks

And minimum cross-sectional area of the reactor is determined:

$$A_{SCR} = n_{el} * A_{element} \qquad \text{Eq. 73}$$

Where:

A_{SCR} = Minimum cross sectional area of reactor in m^2

The validity of the design is checked by determining the pressure drop across a layer of catalyst with a channel height of one meter. The maximum allowable pressure drop across the reactor is determined from the design of the turbocharger pressure curves. It should be noted that the turbocharger must be designed to account for the added backpressure of the SCR reactor. As a guideline, the maximum pressure drop across the reactor should not exceed 100mmWC, which is equivalent to 980 Pa.

From Tronconi (41), the pressure drop across the catalyst is obtained from:

$$\Delta P = \frac{2 f_m \rho_{exh} v_{max}^2}{d_h} L + n \frac{\rho_{exh} v_{max}^2}{2} \qquad \text{Eq. 74}$$

Where:

ΔP = Pressure drop in Pa
L = Length of catalyst in m
n = Expansion term
f_m = Friction factor, dimensionless

And:

$$f_m = \frac{14.227}{Re} \qquad \text{Eq. 75}$$

Where:

Re = Reynolds number, dimensionless

The expansion term is used to account for entrance and exit losses in large scale monoliths. A typical value for the expansion term is n = 1.5. (41)

If the pressure losses obtained are feasible, then the design process is continued. Otherwise, the cross-sectional area and/or hydraulic diameter must be altered in order to reduce the design pressure drop across the reactor.

In order to determine length of channel required to achieve the desired NO_X reduction, it is necessary to evaluate the overall mass transfer conductance. The overall mass transfer conductance accounts for all of the mass transfer processes within the system, including the external mass transfer from the exhaust stream to the catalyst wall, the internal mass transfer from the catalyst surface to the active sites within the catalyst pores, and for the rate of the catalytic reaction.

The effect of internal mass transfer upon the rate of NO_X removal is accounted a term which describes effectiveness of intraporous mass transfer. The effectiveness is related to the Thiele modulus and the values which are used to determine the Thiele modulus are obtained from experimental data (33).

According to Tronconi (41), the relation between effectiveness and Thiele modulus is given by the following relations:

$$\Lambda = \frac{t_w}{2}\sqrt{\frac{D_{eff,NO\ corr}\rho_{cat}}{k_{NO,int}}} \qquad \text{Eq. 76}$$

$$\eta = \frac{1}{\Lambda} \qquad \text{Eq. 77}$$

Where:

η = Effectiveness, dimensionless
Λ = Thiele modulus, dimensionless
$D_{eff,NO\ corr}$ = Corrected effective diffusion coefficient in m^2/sec
$k_{NO,int}$ = Intrinsic rate constant in m^3/kg sec

The simplification that η = 1/ Λ is valid for Λ >>1 and the values for $D_{eff,NO}$ and $k_{NO,int}$ are obtained from experimental data (9).

Since the diffusion coefficient was determined at atmospheric pressure, the value must be corrected for the elevated pressure within the reactor.

$$D_{eff,NO\ corr} = \frac{D_{eff,NO}}{P_{exh}/100000} \qquad \text{Eq. 78}$$

Where:

$D_{eff,NO}$ = Effective diffusion coefficient in m^2/sec

The effects of external mass transfer are accounted for by the mass transfer conductance. The mass transfer conductance is obtained from the Sherwood number which is determined, by analogy, from the expression for Nusselt number for laminar flow in square channels (41).

$$Sh = 2.977 + 8.827(1000 * z^*)^{-0.545} * exp(-48.2 * z^*) \qquad \text{Eq. 79}$$

Where:

Sh = Sherwood number, dimensionless

And:

$$z^* = \frac{L * D_{NO,Air}}{d_h * v_{max}} \qquad \text{Eq. 80}$$

Where:

z^* = Dimensionless mass transfer length
$D_{NO,Air}$ = Diffusion coefficient of NO in air in m^2/sec

The length L is an assumed length which is corrected in further iterations of the design and the diffusion coefficient $D_{NO,Air}$ is calculated in Module 5 and is different from the effective diffusion coefficient which is used to determine the Thiele modulus.

The mass transfer conductance is determined from the definition of the Sherwood number:

$$k_m = \frac{Sh\rho_{exh}D_{NO,Air}}{d_h} \qquad \text{Eq. 81}$$

Where:

k_m = Mass transfer conductance in kg/m^2 sec

Finally, the Arrhenius equation is used to determine the overall rate of the reaction. The activation energy and pre-exponential factor have been determined from experimental data (33).

$$k_{SCR,emp} = Ae^{\left(\frac{-E_a}{RT_{exh}}\right)} \qquad \text{Eq. 82}$$

Where:

$k_{SCR,emp}$ = Empirical rate coefficient in m^3/kg sec
A = Pre-exponential coefficient in m^3/kg sec
E_a = Activation energy in J/mol

The rate coefficient is corrected so as to have units which match the mass transfer coefficient.

$$k_{SCR} = k_{SCR,emp} * \rho_{cat} * \left(\frac{1}{S_a}\right) * \rho_{NO} \qquad \text{Eq. 83}$$

Where:

k_{SCR} = Rate of reaction in kg/m^2 sec
ρ_{cat} = Density of the catalyst in kg/m^3
S_a = Specific surface area of catalyst in m^2/m^3
ρ_{NO} = Density of NO in kg/m^3

The overall mass transfer conductance is therefore:

$$\frac{1}{k_m^{oa}} = \frac{1}{k_{SCR}\eta} + \frac{1}{k_m \rho_{exh}} \qquad \text{Eq. 84}$$

Where:

k_m^{oa} = Overall mass transfer conductance in kg/m^2 sec

The mass flow rate of exhaust through a single channel is given by:

$$\dot{m}_{exh,ch} = \frac{\dot{m}_{ehx}}{n_{ch}} \qquad \text{Eq. 85}$$

Where:

$\dot{m}_{exh,ch}$ = Mass flow exhaust through a single channel in kg/sec

The conversion of NO$_X$ in a single channel is described by the following equations [Mills]:

$$\varepsilon = 1 - e^{\frac{-k_m^{oa}\mathcal{P}L}{\dot{m}_{exh,ch}}} \qquad \text{Eq. 86}$$

And:

$$\varepsilon = \frac{\dot{m}_{NOx\,Tier\,I} - \dot{m}_{NOx\,Tier\,III}}{\dot{m}_{NOx\,Tier\,I}} \qquad \text{Eq. 87}$$

The equation is solved by determining the number of transfer units:

$$N_{TU} = ln\left(\frac{1}{1-\varepsilon}\right) = \frac{-k_m^{oa}\mathcal{P}L}{\dot{m}_{exh,ch}} \qquad \text{Eq. 88}$$

Where:

N_{TU} = Number of transfer units, dimensionless

And the length of the reactor is given by:

$$L_{calc} = \frac{N_{TU}\dot{m}_{exh,ch}}{-k_m^{oa}\mathcal{P}} \qquad \text{Eq. 89}$$

5 RESULTS

The model that was developed in the course of this work was used to investigate the size and relevant operating parameter of an SCR installation for an MAN 11 K90 MC-C engine. Using the values the previously described values, the program was able to calculate the cross-sectional area and channel length that would be required to achieve a minimum conversion of 80% when the engine was operating at full load.

The program was also evaluated at a second case in which a 90% reduction in NOx emissions was required. This reduction rate corresponds to the reduction that would be required to reduce the NOx emissions as derived from the work of Miller et al. to levels which would satisfy the IMO Tier III requirements.

For both cases, the calculations were further extended to investigate the case the length required in the case of an assumed rate of catalyst deactivation of 5% per 10,000 hrs.

In addition, the model calculated a number of the significant operating parameters, including velocity through the channels, urea consumption and storage requirements, and the pressure drop across the unit.

The results of the calculation are summarized in Figure 12 and presented in detail in Appendix D.

Given the base condition, and without accounting for the effects of catalyst deactivation, it was determined that the reactor would have to be 1.7 meters long to achieve a required reduction of 80% and 2.4 meters to achieve a reduction of 90%. The required length of the unit found to increase slightly by taking the expected deactivation of the catalyst into consideration. The minimum lengths required for a reactor that was experiencing some deactivation increase to 1.8 m for 80% reduction and 2.5 meters for 90% reduction.

Given a flow velocity of 6.1 m/s, and assuming a maximum Reynolds number of 2000, the minimum required cross-sectional area of the channels was 10.64 m^2. Taking into account the geometry of the catalyst blocks, the cross-sectional area of the catalyst elements was determined to be 14.72 m^2 with a total of 121 catalyst blocks arranged in a square configuration. Assuming that the catalyst blocks were .5 meters, the required height of the catalyst would be 2.5 meters for an 80% reduction and 3.5 meters for a 90% reduction. Given the assume catalyst height, this corresponds to a total catalyst volume of either 36.80 m^3 or 51.52 m^3.

Given a maximum allowable slip of 5 ppm by volume, the consumption of 40% urea water solution for the 80% case is 1718 kg/hr and 3706 kg/hr for the 90% reduction case. Based upon the assumed operating profile of the vessel and not including any safety factors, i.e. 350 days of operation a year with 40% of the time spent in ECA areas including 70 days in port per year, the expected storage requirements for a month's worth of solution is 217 cubic meters for the 80% reduction case and 469 m^3 per month for the 90% reduction case.

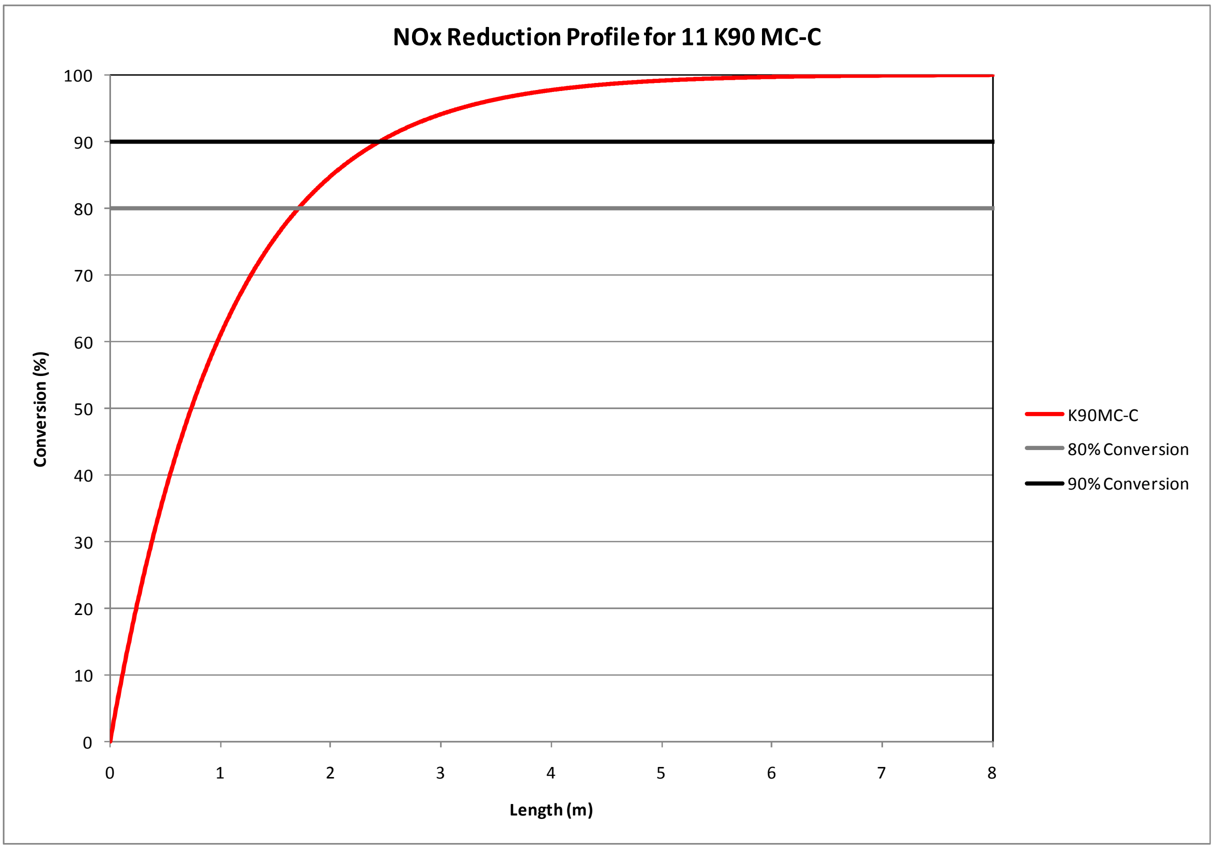

FIGURE 12 - NO_X REDUCTION PROFILE FOR AN 11K90MC-C MARINE LOW-SPEED DIESEL ENGINE.

These values are summarized in Table 2 which also presents a comparison of the values that were obtained from the sizing of an SCR unit for a 14 cylinder, 98 cm bore 14 K98 MC-C engine, which is the largest engine currently being manufactured.

The application of SCR to the 14 K98 MC-C engine chosen for investigation because it represents the extreme case with regards to the maximum size unit that one might expect to see installed on a ship.

In comparing the results obtained in the two calculations, it should be noted that there is very little difference in reactor length between the engine, but that the surface area of the unit is scaled proportionately with the increase in mass flow. The consumption and storage requirements of urea water solution, especially with regards to the K98 engine.

The application of SCR to this particular engine is chosen for investigation because it represents the extreme case with regards to the maximum sized unit that could reasonably be expected to be installed on a ship.

Value	11 K90 MC-C	14 K98 MC-C	Units
Power	52,000	87,220	kW
Rpm	104	97	r/min
Bore	900	.98	m
Mass flow exhaust	466,159	811,722	kg/hr
Length 80% reduction	1.71	1.60	m
Length 80% w/deact	1.78	1.67	m
Length 90% reduction	2.41	2.29	m
Length 90% w/deact	2.51	2.39	m
Velocity of flow	6.06	6.06	m/s
Surface area catalyst	14.72	27.37	m^2
Number of elements	121	225	
Number of layers 80%	4	4	
Number of layers 90%	5	5	
Volume of catalyst 80%	58.88	109.48	m^3
Volume of catalyst 90%	73.6	136.85	m^3
UWS consumption 80%	1717	2882	kg/hr
UWS consumption 90%	3706	6480	kg/hr
UWS storage 80%	218	365	m^3/month
UWS storage 90%	469	820	m^3/month

TABLE 2 - COMPARISON OF NO_X REDUCTION CHARACTERISTICS FOR TWO ENGINE MODELS.

The program was also used to investigate the relevant operating characteristics of the SCR systems. The results of these investigations are presented below.

Figure 13 illustrates the effect of reduced exhaust flow rate due to decreased engine load on the operation of an SCR unit which has been sized for the maximum load case. The figure indicates that decreased flow rate has the effect of increasing the conversion of NO along the length of the channel; however, since the exhaust gas temperature decreases at decrearsing loads, it is expected that the effects illustrated in this figure will be counteracted by the effect of reduced catalyst reactivity due to lower gas temperature.

The effect of temperature upon catalyst activity is illustrated in Figure 14 in which decreasing exhaust temperature is clearly shown to have an adverse effect on the ability of the catalyst to reduce NO concentration. This behavior is consistent with the exponential relation between temperature and rate constant.

Figure 15 shows the effect of Reynolds number upon NO_X conversion rate. The figure shows that Reynolds number shorter channel lengths are required for smaller Reynolds numbers, however this is misleading because this effect is actually a result of the reduced flow rate through the channel, which must be compensated for my increasing the number of channels. This is illustrated by the comparison in Table 3 which shows that summarizes the output values for a series of calculations that were performed for the same conditions, but with different Reynolds numbers. In comparing the product of the number of channels multiplied by the length of the channel, in channel-meters, it is evident that the value of channel-meter does not change across the range of Reynolds number.

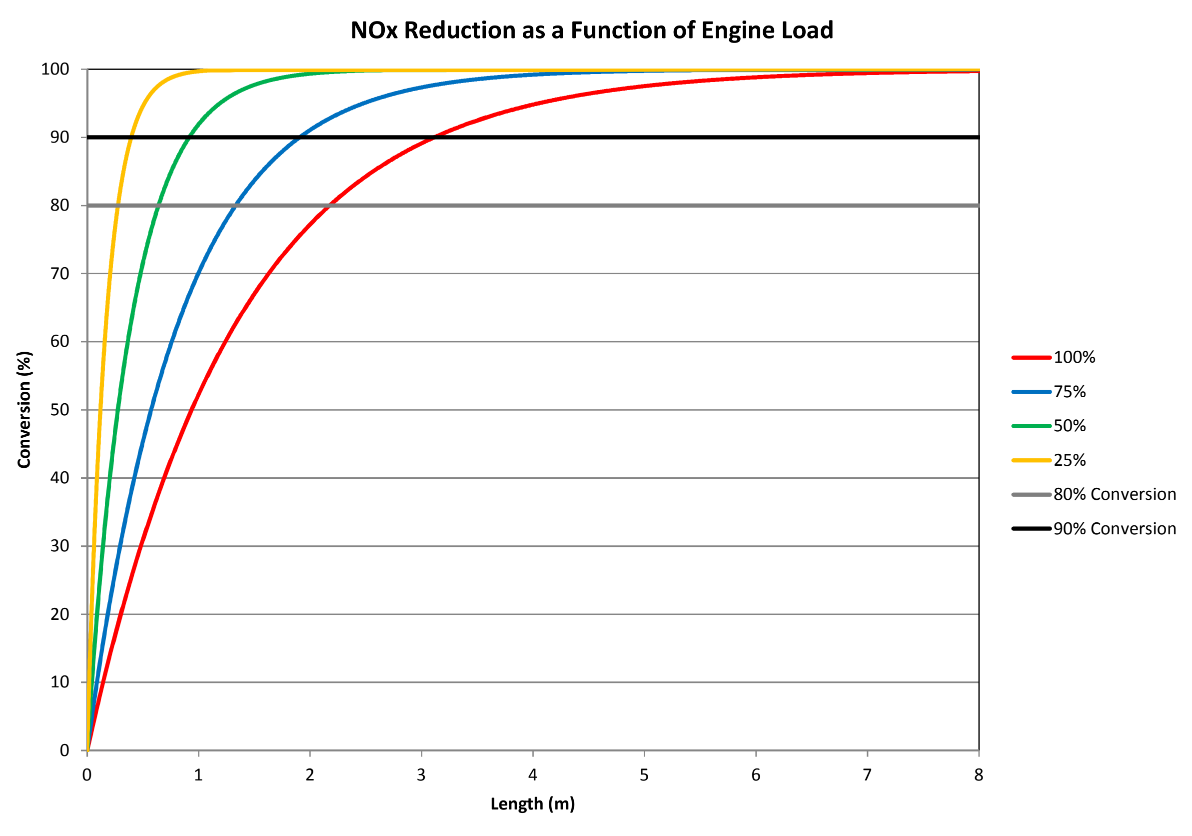

FIGURE 13 - NO_X REDUCTION AS A FUNCTION OF ENGINE LOAD.

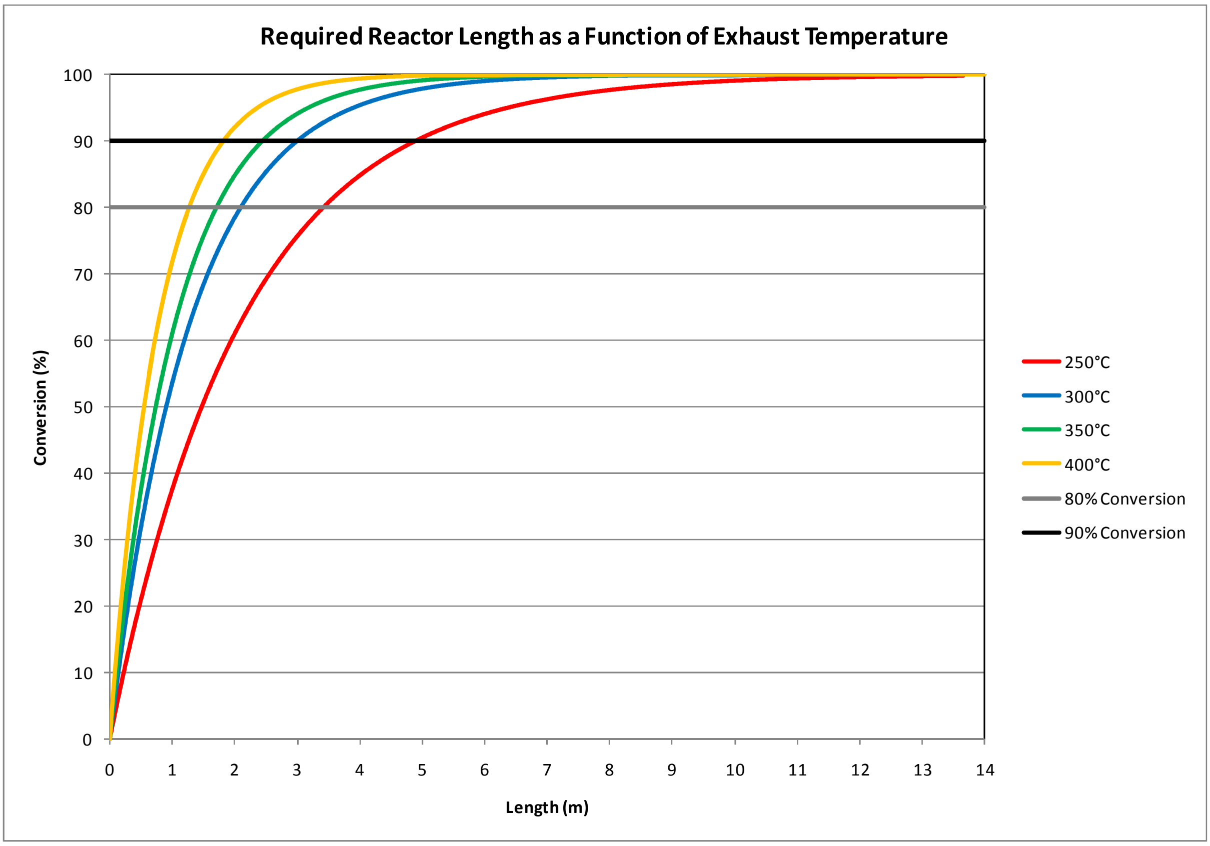

FIGURE 14 - REQUIRED REACTOR LENGTH AS A FUNCTION OF EXHAUST TEMPERATURE.

This is an interesting observation, because it shows that mutual effects of channel length and flow on overall conversion rate.

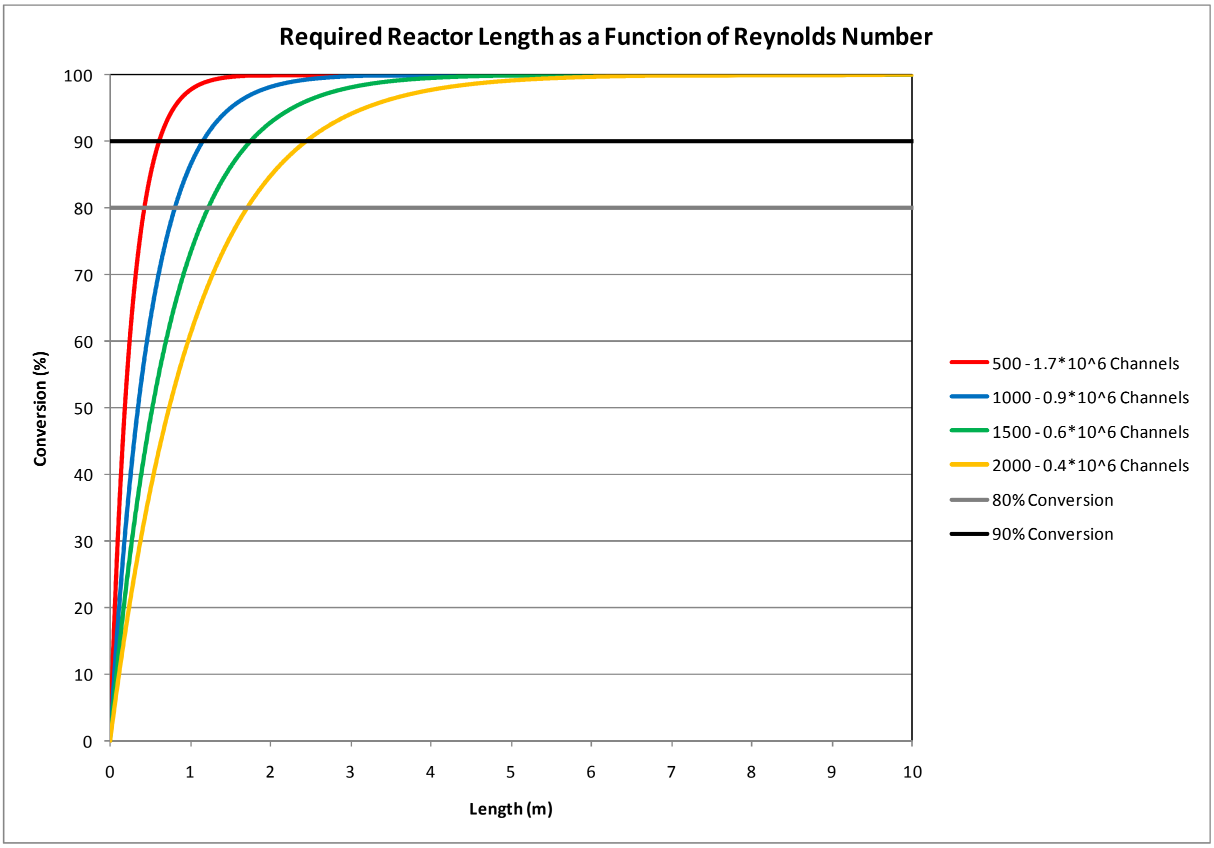

FIGURE 15 - REQUIRED REACTOR LENGTH AS A FUNCTION OF REYNOLDS NUMBER.

Reynolds Number	Number of Blocks	Number of Channels	Block Length (m)	Channel-meters to reach 90% Reduction
500	484	1742400	0.61	1,067,254
1000	256	921600	1.16	1,067,254
1500	169	608400	1.75	1,067,254
2000	121	435600	2.45	1,067,254

TABLE 3 - COMPARISON OF SCR UNIT CHARACTERISTICS AS A FUNCTION OF REYNOLDS NUMBER.

Figure 16 shows the effect of channel width on NO_X conversion. As expected, channels with smaller widths have a higher conversion rate than those with larger widths. In this simulation, the width of the channel wall was kept unchanged. This can be explained by the fact that if Sherwood number is kept at the same value, an increase in the width of the channel will result in a corresponding decrease in the value of the mass transfer coefficient.

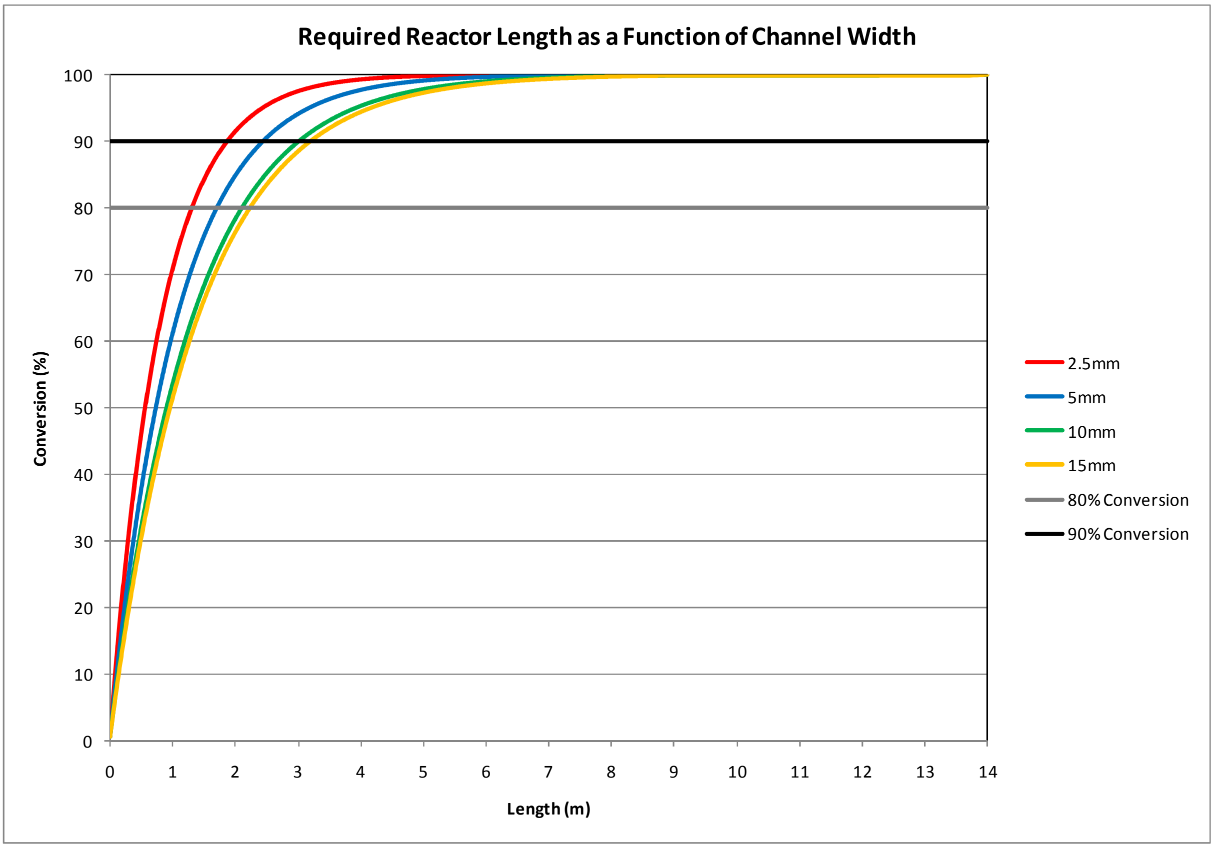

FIGURE 16 - REQUIRED REACTOR LENGTH AS A FUNCTION OF CHANNEL WIDTH.

6 DISCUSSION

The model was used to evaluate the required size and urea consumption for an SCR react for a 52,000 kW main propulsion low speed diesel engine of the type that would be typical for a post-Panamax containership. The engine in question was an 11 cylinder 90 centimeter - bore 11 K90 MC-C engine that was designed by MAN Diesel and delivered in 1995. The model was applied to this particular engine because of the availability of published experimental emissions data for this engine.

The calculations were executed using a combination of experimentally determined data and with representative values that were obtained from literature. Although the rate coefficient and effective diffusion coefficients were specific to an SCR catalyst from Haldor Topsøe, other dimensions of the catalyst were chosen so as to be representative of a typical square-channeled monolithic catalyst. A channel width of 5 mm was chosen for the application as this was considered typical for SCR catalysts for the treatment of diesel exhaust (40).

The exhaust flow calculation module was used to estimate the exhaust flow rate on the basis of air, fuel, and cylinder lube oil flow through the engine. The calculated exhaust flow rate was determined to be 466,159 kg/hr on a mass basis or 213,950 m^3/hr on a volumetric basis, which are equivalent to 129.5 kg/sec or 64.5 m^3/sec. and These results were later compared with the published data from the manufacturer’s engine selection project guide, which stated that the design flow rate for an 11 K90 MC-C engine was 480,000 kg/hr. Given height of the scavenge ports was only approximated, this agreement between the output of the module and the published data was very good.

The exhaust gas module was also used to approximate the exhaust flow rate from the engine at less than full load, i.e. 25%, 50%, and 75% of the full loads. The purpose these calculations to determine the NO_X reductions that could be expected for a unit that was operating at less than full engine load.

A secondary purpose of the partial load calculations was to obtain comparison values for evaluating whether the exhaust flow rates calculated in the work of Miller et al. (1) are reasonable. The exhaust flow rate reported in this work for the same engine was 170,672 scfm at 71% load. Since this value was later used to correlate NO_X measurements that were obtained in ppm by volume, it was assumed that the volumetric flow rate determined was for the same conditions as the location of the sample probe. From the photographs and description included in the report, it was evident that exhaust gas was sampled at a location after the outlet of the turbocharger. Therefore, it was assumed that the temperature and pressure used for the work are approximately 250°C and 1 bar which are the typical temperature and pressure of the exhaust at the outlet of the (37) (38).

In comparing the exhaust gas flow rate obtained by Miller et. al with the flow rate that was obtained from the calculations in this work, the exhaust flow rates obtained by Miller et al. were found to be significantly lower. Corrected to units of m^3/sec, the exhaust flow rate from Miller et al. was 80.6 m^3/sec. At the same temperature and pressure, and for the same engine load, the value obtained from this work was 189.3 m^3/sec. Given that the mass flow rates found in this work agree with the manufacturer's data, the quantity calculated in this work was taken as the more correct value.

The data from Miller et. al is, however, still useful because the measurements were done in parts per million by volume. Since a reasonable approximation of the actual exhaust gas flow rate was known, it was therefore to determine the correct emissions rate by scaling the report values relative to exhaust gas flow rate. In light of this, the value of 20.2 g/kW-hr that was originally reported by Miller et al. was corrected to 32.8 g/kW-hr.

The corrected value is considered to be reasonable because the engine from which the measurements were taken was delivered before the Tier I regulations came into effect. This is therefore an interesting case because the elevated emissions suggest that the engine has not been tuned ultra-low NO_X emissions conditions and thereby should also have a lower specific fuel consumption rate than a similar Tier I compliant engine. One of the possible benefits of running a vessel with an SCR system would be the ability to return the engine to its basic, i.e. higher, fuel efficiency.

Another of the interesting features of the model was the ability to compare the relative influence of the various mass transfer mechanisms in determining the overall mass transfer coefficient.

We have already discussed how each of the individual mass transfer mechanisms are accounted for in the overall mass transfer coefficient. By comparing the calculated values of each of these variables relative to the calculated overall mass transfer coefficient, it is possible to draw some conclusions regarding the relative importance of the individual steps.

To review, the overall mass transfer coefficient is obtained from the following equation:

$$\frac{1}{k_{m1}^{oa}} = \frac{1}{k_{SCR}\eta} + \frac{1}{k_m}$$

Table 4summarizes the values that were obtained for relevant mass transfer quantities during the calculation applied to the K90 engine.

Variable	k_m	k_{SCR}	η	$k_{SCR}\eta$	k_{m1}^{oa}
Value	0.053	0.1677	0.1156	0.0194	0.0140
Quantity	Convective	Reaction rate	Intraporous	Reaction & Intraporous	Overall

TABLE 4 - MASS TRANSFER QUANTITIES CALCULATED AND APPLIED TO THE K90 ENGINE.

From Table 4, it is evident that the rate of reaction is fast relative to the rate of convective mass transfer from the bulk fluid flow to the wall. However, when the rate coefficient is corrected for the effects of intraporous mass transfer, the overall rate is decreased significantly. As such, it is possible to conclude that rate of reaction is much faster three times faster than the rate of convective mass transfer, but that the overall mass transfer is governed by the diffusion of species through the pore structure of the catalyst. These observations are consistent with those that have been reported elsewhere in literature (40)

6.1 FEASIBILITY OF APPLICATION OF SCR

The purpose of this project was to investigate the feasibility of applying selective catalytic reduction to low speed marine diesel engines. A model was formulated and then used to determine the main operating parameters for two large low speed diesel engines in order to quantify the size of the units that would need to be installed.

The results of these calculations are discussed in the results section, but needless to say, the required sizes that were determined were quite large. The K90 engine required a reactor with a surface area of 14.72 m^2 and the K98 engine required a surface area of 27.4 m^2, with these being the surface areas of the catalytic material within the unit and not the entire unit itself.

Additionally, the associated urea storage requirements are also quite large, with approximately 218 m^3 being required for the K90 engine and 365 m^3 for the K98 engine for the lower of the two reduction rates that were evaluated.

The size requirements are considerable, and it is certainly a challenge to fit an SCR unit within current standard ship designs. However, recently there have been a number of other regulations which have also had the effect of necessitating alterations to standard ship configurations, so this challenge is nothing new.

The extreme case is that there are some ships currently in service which have adopted twin engine room arrangements in the name of environmental safety and stewardship. If it is possible to add a whole other engine room to a ship, then it should certainly be possible to find room for an SCR unit that has a surface area of between 14.72 and 27.4 m^2 at the extreme.

In the course of this work we also have identified a number of advantages and disadvantages to the SCR system.

Major advantages include the high rates of NOx reduction that can be achieved and the relatively simple operating principle of the system. Additionally, since SCR units are very effective at reducing NOx, there is a possible fuel savings that can be achieve since the previously employed methods of engine tuning are no longer required.

Another significant advantage of the system is that is does not appreciably affect the actual conditions within the combustion chamber. From an operating standpoint, the conditions within the combustion chamber can be very difficult to predict and with miscalculations have potentially hefty consequences. An important advantage of the SCR system is the fact that it, unlike many of the other available systems, does not introduce additional variables into the combustion chamber.

The major disadvantages to the system are is the sensitivity of the system to the sulfur content of the fuel and the potential for corrosion of components downstream of the reactor. However, for vessels that expect to spend a significant portion of their time operating in current or proposed ECA areas, this concern is mitigated by the fact that maximum NO reduction regulation, i.e. Tier III standards, are also accompanied by the requirement to burn low sulfur fuels.

Ultimately, the best way to mitigate the concern of size requirements is to adopt a proactive approach and to work with ship designers to develop a machinery arrangement that can successfully incorporate the unit.

7 CONCLUSIONS

The goal of this project was to investigate the application of a Urea base selective catalytic reduction system to a large bore marine diesel engine. The work presented a comprehensive review of the topics relating to the application of SCR units, including a discussion of the theory behind NOx generation and selective catalytic reduction, a review of pertinent legislation regarding the reduction of NOx, and practical discussion regarding the application of the SCR units to low speed marine diesel engines.

A model was developed to described the reduction of NOx from a selective catalytic reactor. The model was based upon the considerations and limitations that were identified in the course of the literature survey, and utilized a combination of published experimental data and feasible values and correlations that were obtained from a variety of sources in literature.

The model was developed so as to have maximum flexibility with respect to engine types, catalyst properties, configurations, and assumptions and the development of the model was described in detail.

The model was used to evaluate the required sizes of SCR units for a MAN 11 K90 MC-C engine and for the 14 cylinder MAN 14 K98 MC-C engine, which is the largest engine currently in production.

It was found that the required length of an SCR reactor for the 11K90 engine was 1.71 meters for an 80% reduction in NOx and 2.41 meters for a 90% reduction in NOx. These values corresponded to a flow rate of 6.1 m/s and a reactor surface area of 14.72 m^2.

For the 14 K98 engine, the required length was found to be 1.60meter for and 80% reduction and 1.67 meters for a 90% reduction in NOx emissions. These values correspond to a reactor surface area of 27.37 m^2 and a flow velocity of 6.1 m/s.

The model was also exercised to investigate effect of various parameters on the behavior of the unit.

Finally, conclusions were drawn relative to the feasibility of applying the unit to a marine application. It was determined that with the coupling of fuel sulfur content and NOx reduction requirements in emissions control areas (ECAs), that SCR was a promising method for NOx reduction aboard vessels with low speed diesel propulsion plants. However, the relatively large footprint of the unit and the associated Urea storage requirements presented significant challenges relative to current machinery arrangement practices. In order to successfully apply the SCR unit, it would be necessary to take a proactive approach to the design and configuration of the machinery arrangement.

8 RECOMMENDATIONS FOR FUTURE WORK

Since regulations are scheduled to come into effect in 2016 that will limit the allowable emission of NOx from marine vessels by 80%, there is no shortage of future work that can and should be undertaken. Important topics that require further investigation is the need for a similar study that evaluates the feasibility of apply exhaust gas recirculation as the primary means of NOx reduction for the purposes of presenting a comparison to the conclusions that were drawn from this work. It would also be valuable to undertake a study regarding the redesign of the vessel's machinery arrangement in order to successfully accommodate such systems as SCR.

SELECTED BIBLIOGRAPHY

1. **J.W. Miller, H. Agrawal, and B. Welch.** *Measurement of Emissions from the Main Propulsion Engine (MAN B&W 11K90 MC-C) on a Panamax Class Containership.* Riverside, CA : University of California, Riverside, 2009.

2. **MARISEC.** Environmental Performance. [Online] naked ideas, den 20 November 2010. http://www.marisec.org/shippingfacts/environmental/atmospheric-pollution.php.

3. **UNCTAD.** *Review of Maritime Transport 2009.* Geneva : United Nations Conference on Trade and Development, 2009.

4. *Mortality from Ship Emissions: A Global Assessment.* **J. Corbett, J. Winebrake, E. Green, P. Kasibhatla, V. Eyring, and A. Lauer.** 24, Newark, Delaware : American Chemical Society, 2007, Environmental Science and Technology, Vol. 41, ss. 8512-8518.

5. *Modeling Energy Use and Emissions from North American Shipping: Application of Ship Traffice, Energy, and Environment Model.* **C. Wang, J. Corbett, and J. Firestone.** 9, Newark, Delaware : American Chemical Society, 2007, Environmental Science and Technology, Vol. 41, ss. 3226-3232.

6. *Measurements of NOx Emissions and In-Service Duty Cycle from a Towboat Operating on the Inland River System.* **Corbett, J. J. och Robinson, A. L.** 7, Pittsburgh, Pennsylvania : American Chemical Society, 2001, Environmental Science & Technology, Vol. 35, ss. 1343-1349.

7. **CIMAC.** *Guide to Diesel Exhaust Emissions Control of NOx, SOx, Particulates, Smoke, and CO2.* Frankfurt : CIMAC, 2008.

8. **EPA.** *EPA-456/F-98-005.* Research Triangle Park, NC : United States Environmental Protection Agency, 1998.

9. **Turns, Stephen R.** *Introduction to Combustion: Concepts and Applications.* Singapore : McGraw-Hill Higher Education, 2006.

10. **K. Verbiezen, A.J. Donkerbroek, R.J.H. Klein-Douwel, A.P. van Vliet,.** Diesel combustion: In-cylinder NO concentrations. *Combustion and Flame.* 2007, Vol. 151.

11. **Y. H. Li, S. -C. Kong.** Diesel combustion modelling using LES turbulence model with detailed. *Combustion Theory and Modelling.* 2008, Vol. 12, 2.

12. **Dara D. Torkzadeh, Wolfgang Lhgst, Uwe Kiencke.** *Engine Modeling and Exhaust Gas Estimation for DI-Diesel Engines.* Arlington, VA : u.n., 2001.

13. *Reduced Kinetics Schemes for Oxides of Nitrogen Emissions from a Slow-Speed Marine Diesel Engine.* **Goldsworthy, Laurie.** 2, Launceston, Tasmania : American Chemical Society, 2003, Energy & Fuels, Vol. 17.

14. **Jean Arregle, J. Javier Lopez, Carlos Guardiola, and Christelle Monin.** On Board NOx Prediction in Diesel Engines: A.

15. **Hong, S., o.a.** Modeling of Diesel Combustion, Soot and NO Emissions Based on a Modified Eddy Dissipation Concept. *Combustion Science and Technology.* 2008, Vol. 180.

16. **Aithal, S.M.** Modeling of NOx formation in diesel engines using finite-rate chemical kinetics. *Applied Energy.* 2010, Vol. 87.

17. *Prediction of NOx Emissions from a Transiently Operating Diesel Engine Using an Artificial Neural Network.* **H. Krijnsen, W. van Kooten, H. Calis, R. Verbeek, C van den Bleek.** 1999, Chemical Engineering Technology, ss. 601-607.

18. **CIMAC.** *Guide to Diesel Exhaust Emissions Control of NOx, SOx, Particulates, Smoke, and CO2.* 2008 : CIMAC, 2008.

19. **MEPC.** *AMENDMENTS TO THE ANNEX OF THE PROTOCOL OF 1997 TO AMEND THE.* London : International Maritime Organization, 2008.

20. **Jacobsen, Henrik Trolle.** *SCR DeNOx Catalyst and Technology.* [PowerPoint Presentation] Copenhagen : Haldor Topsøe, 2010.

21. *CFD-Modelling of Selective Non-Catalytic Reduction of NOx in Grate Kiln Plants.* **P.E. Burstrom, T. S. Lundstrom, B. D. Marjavaara, and S. Toyra.** Melbourne : CSIRO, 2009.

22. **C. M. Schar, C. H. Onder, and H. P. Geering.** Control of an SCR Catalytic Converter System for a Mobile Heavy-Duty Application. *IEEE Transactions on Control Systems Technology.* 2006, Vol. 14, 4.

23. **Tronconi.** *Chapter from Book.*

24. **Topsoe, N.Y.** Catalysis for NOx Abatement: Selective catalytic reduction of NOx by ammonia: fundamental and industrial aspects. *CATTECH.* 1997.

25. **Fogler, F. S.** *Elements of Chemical Reaction Engineering, 4th Edition.* Upper Saddle River : Pearson Education, 2006.

26. **Mills, Anthony.** *Heat and Mass Transfer.* u.o. : CRC Press, 1994.

27. **J. C. Fu, and C.J. Pereira.** Design of Monolith Catalyst for Fouling Resistance. *Ind. Eng. Chem. Res.* 1998, Vol. 37.

28. **Reid.** *Properties of Liquids and Gases.*

29. **M. Koebel, and M. Elsener.** Selective Catalytic Reuction of NO over Commercial DeNOx Catalysts Comparison fo the Measured and Calcualted Performance. *Ind. Eng. Chem. Res.* 1998, Vol. 37.

30. **E. Tronconi, P. Forzatti, J.P. Gomez Martin, S. Mallogi.** Selective Catalytic Removal of NOx: A Mathematical Model for Design of Catalysts and Reactors. *Chemical Engineering Science.* 1992, Vol. 47, 9-11.

31. **E. Tronconi, and P. Forzatti.** Adequacy of Lumped Parameter Models for SCR Reactors. *American Institute of Chemical Engineers.* 1992, Vol. 38, 2.

32. **Berg, Camilla och Andersen, Maria Friberg.** *Kinetics and Diffusion in DeNOx Catalysts.* Copenhagen : Technical University of Denmark, 2007.

33. **Haldor Topsoe.** *The Topsøe SCR DeNOx unit for reduction of NOx in diesel engine exhaust gas.* Copenhagen : Haldor Topsøe, 2003.

34. **Crane Valves.** *Flow of Fluids Through Valves, Fittings, and Pipe.* Long Beach, CA : Crane Co., 1999.

35. **MAN Diesel.** *Exhaust Gas Emission Control Today and Tomorrow.* Copenhagen : MAN Diesel, 2009.

36. **Haldor Topsoe.**

37. **MAN B&W.** *Project Guide: K90MC-C6.* Copenhagen : MAN Diesel, 2010.

38. —. *Project Guide: K98MC-C7.* Copenhagen : MAN Diesel, 2010.

39. **Chladova, Lenka.** *Transient Diffusion of Corrosive Species through Cylinder Lubricating Oil in Low Speed Diesel Engines.* Aalborg : Aalborg University, 2010.

40. **Reid, Robert C.** *Properties of Liquids and Gases.* u.o. : McGraw-Hill Companies, 1987.

41. *The role of inter- and intra-phase mas transfer in the SCR-DeNOx reaction over catalysts of different shapes.* **Tronconi, Enrico och Beretta, Alessandra.** 249-258, Milan : Catalysis Today, 1999, Vol. 52.

APPENDICES

Appendix A	Model Module Input Parameters
Appendix B	Model Matlab Scripts
Appendix C	Model Module Output Files
Appendix D	Summary of Calculations for a K90MC-C Engine
Appendix E	Excerpt from UCI Data

APPENDIX A - MODEL MODULE INPUT PARAMETERS

Module 1 Input

```
Stroke Bore Height_scavport Ideal_gas_const MW_air Num_cyl Rpm KW SFOC SLOC
MW_exh_calc
2.300 0.900 0.2 8.314472 28.966 11 104 52000 177 0.15 30.0281
```

Module 2 Input

```
Backpress_exh_avg Visc_dyn_exh
1500 0.00003050
```

Module 3 Input

```
NOx_gkwh_TierI NOx_gkwh_TierIII MW_NO2 SCFM_exh_UCI Mass_flow_NOx_UCI_gh
P_UCI T_UCI
17 3.4 46.0055 170672 726331 100000 523
```

Module 4 Input

```
Slip MW_NH3 MW_NO MW_Urea Percent_urea SG_Urea_soln Days_op_year
Days_year_port Percent_ECA
5 17.031 30.006 60.06 40 1.107 350 70 .40
```

Module 5 Input

```
Epsilon_air Sigma_air Epsilon_NO Sigma_NO Epsilon_NH3 Sigma_NH3
78.6 3.711 116.7 3.492 558.3 2.90
```

Module 6 Input

```
Width_ch Thick_wall Num_channel_x Num_channel_y Height_element Rho_cat
0.005 0.0008 60 60 0.5 1111
```

Module 7 Input

```
P_cat_exp T_cat_exp D_eff_NO K_NO_Int Lenth_cat Ea_SCR A_pre_exp_SCR Re
Fact_deact Num_years
100000 623 0.00000493 .579 2.0 56920 35075 2000 0.05 5
```

APPENDIX B - MODEL MODULE MATLAB SCRIPTS

Module 1 – Calculate exhaust flow rate

```
% CLEAR ALL AND CLOSE ALL
clear all
close all



% IMPORT NEW VARIABLES FOR MODULE
% Stroke Bore Height_scavport Ideal_gas_const MW_air Num_Cyl Rpm KW SFOC
% SLOC MW_exh_calc
fid = fopen('C:\Matlab NOx\Mod1_Input.txt');
Mod1_Input = textscan(fid, '%s %s %s %s %s %s %s %s %s %s %s',
'Headerlines', 3);
fclose(fid);

% Inport load dependent values for module
% Load P_int T_int Total_excess Comb_excess P_exh T_exh
fid = fopen('C:\Matlab NOx\Mod1_Input_VectorData.txt');
Mod1_Input_VectorData = textscan(fid, '%s %s %s %s %s %s %s',
'Headerlines', 3);
fclose(fid);



% DEFINE VARIABLES FOR MODULE
% define cylinder stroke in meters
Stroke = Mod1_Input{1};
Stroke = str2double(cell2mat(Stroke));

% define cylinder bore in meters
Bore = Mod1_Input{2};
Bore = str2double(cell2mat(Bore));

% define height of scavenge air ports in meters
Height_scavport = Mod1_Input{3};
Height_scavport = str2double(cell2mat(Height_scavport));

% define ideal gas constant in m^3 Pa/mol K
Ideal_gas_const = Mod1_Input{4};
Ideal_gas_const = str2double(cell2mat(Ideal_gas_const));

% define molecular weight of air in g/mol
MW_air = Mod1_Input{5};
MW_air = str2double(cell2mat(MW_air));

% define number of cylinders - dimensionless
Num_cyl = Mod1_Input{6};
Num_cyl = str2double(cell2mat(Num_cyl));

% define engine rpm in revs/min
Rpm = Mod1_Input{7};
Rpm = str2double(cell2mat(Rpm));

% define engine kW in kW
KW = Mod1_Input{8};
KW = str2double(cell2mat(KW));

% define specific fuel oil consumption in g/kW-hr
SFOC = Mod1_Input{9};
```

```
SFOC = str2double(cell2mat(SFOC));

% define specific lube oil consumption in g/kW-hr
SLOC = Mod1_Input{10};
SLOC = str2double(cell2mat(SLOC));

% define molecular weight of undiluted exhaust in g/mol
MW_exh_calc = Mod1_Input{11};
MW_exh_calc = str2double(cell2mat(MW_exh_calc));

% define load vector in percent
Load_25 = Mod1_Input_VectorData{1}(1);
Load_25 = str2double(cell2mat(Load_25));
Load_50 = Mod1_Input_VectorData{1}(2);
Load_50 = str2double(cell2mat(Load_50));
Load_75 = Mod1_Input_VectorData{1}(3);
Load_75 = str2double(cell2mat(Load_75));
Load_100 = Mod1_Input_VectorData{1}(4);
Load_100 = str2double(cell2mat(Load_100));

% define scavenge air pressure in Pa
P_scav_25 = Mod1_Input_VectorData{2}(1);
P_scav_25 = str2double(cell2mat(P_scav_25));
P_scav_50 = Mod1_Input_VectorData{2}(2);
P_scav_50 = str2double(cell2mat(P_scav_50));
P_scav_75 = Mod1_Input_VectorData{2}(3);
P_scav_75 = str2double(cell2mat(P_scav_75));
P_scav_100 = Mod1_Input_VectorData{2}(4);
P_scav_100 = str2double(cell2mat(P_scav_100));

% define scavenge air temperature in K
T_scav_25 = Mod1_Input_VectorData{3}(1);
T_scav_25 = str2double(cell2mat(T_scav_25));
T_scav_50 = Mod1_Input_VectorData{3}(2);
T_scav_50 = str2double(cell2mat(T_scav_50));
T_scav_75 = Mod1_Input_VectorData{3}(3);
T_scav_75 = str2double(cell2mat(T_scav_75));
T_scav_100 = Mod1_Input_VectorData{3}(4);
T_scav_100 = str2double(cell2mat(T_scav_100));

% define total excess air ratio - dimensionless
Total_excess_25 = Mod1_Input_VectorData{4}(1);
Total_excess_25 = str2double(cell2mat(Total_excess_25));
Total_excess_50 = Mod1_Input_VectorData{4}(2);
Total_excess_50 = str2double(cell2mat(Total_excess_50));
Total_excess_75 = Mod1_Input_VectorData{4}(3);
Total_excess_75 = str2double(cell2mat(Total_excess_75));
Total_excess_100 = Mod1_Input_VectorData{4}(4);
Total_excess_100 = str2double(cell2mat(Total_excess_100));

% define combustion excess air vector - dimensionless
Comb_excess_25 = Mod1_Input_VectorData{5}(1);
Comb_excess_25 = str2double(cell2mat(Comb_excess_25));
Comb_excess_50 = Mod1_Input_VectorData{5}(2);
Comb_excess_50 = str2double(cell2mat(Comb_excess_50));
Comb_excess_75 = Mod1_Input_VectorData{5}(3);
Comb_excess_75 = str2double(cell2mat(Comb_excess_75));
Comb_excess_100 = Mod1_Input_VectorData{5}(4);
Comb_excess_100 = str2double(cell2mat(Comb_excess_100));
```

```
% define exhaust pressure in Pa
P_exh_25 = Mod1_Input_VectorData{6}(1);
P_exh_25 = str2double(cell2mat(P_exh_25));
P_exh_50 = Mod1_Input_VectorData{6}(2);
P_exh_50 = str2double(cell2mat(P_exh_50));
P_exh_75 = Mod1_Input_VectorData{6}(3);
P_exh_75 = str2double(cell2mat(P_exh_75));
P_exh_100 = Mod1_Input_VectorData{6}(4);
P_exh_100 = str2double(cell2mat(P_exh_100));

% define exhaust temperature in K
T_exh_25 = Mod1_Input_VectorData{7}(1);
T_exh_25 = str2double(cell2mat(T_exh_25));
T_exh_50 = Mod1_Input_VectorData{7}(2);
T_exh_50 = str2double(cell2mat(T_exh_50));
T_exh_75 = Mod1_Input_VectorData{7}(3);
T_exh_75 = str2double(cell2mat(T_exh_75));
T_exh_100 = Mod1_Input_VectorData{7}(4);
T_exh_100 = str2double(cell2mat(T_exh_100));



% CREATE VECTORS TO STORE LOAD DEPENDENT DATA
Load = [ Load_25; Load_50; Load_75; Load_100 ];

P_scav = [P_scav_25; P_scav_50; P_scav_75; P_scav_100 ];

T_scav = [T_scav_25; T_scav_50; T_scav_75; T_scav_100 ];

Total_excess = [Total_excess_25; Total_excess_50; Total_excess_75;
Total_excess_100 ];

Comb_excess = [Comb_excess_25; Comb_excess_50; Comb_excess_75;
Comb_excess_100 ];

P_exh = [P_exh_25; P_exh_50; P_exh_75; P_exh_100 ];

T_exh = [T_exh_25; T_exh_50; T_exh_75; T_exh_100 ];



% PERFORM CALCULATIONS
% calculate revolutions per second in revs/sec
Rps = (Rpm * Load)/60;

% calculate volume of cylinder in m^3
Cyl_vol = .25 * pi * Bore^2 * (Stroke - Height_scavport);

% calculate mols of combustion air in mols/cylinder
Mols_comb_air = (P_scav./T_scav) * (Cyl_vol /Ideal_gas_const);

% calculate mass of combustion air in kg/cyl
Mass_comb_air = (Mols_comb_air * MW_air)/1000;

% correct mass of air for cylinder scavenging in kg/cyl
Mass_intake_air = Mass_comb_air.* (Total_excess./Comb_excess);

% calculate mass flow of intake air in kg/sec-cyl
Mass_flow_air = (Mass_intake_air.* Rps);
```

```
% calculate mass flow of fuel in kg/sec-cyl
Mass_flow_fuel = (SFOC * Load * KW)/(Num_cyl * 3600 * 1000);

% calculate mass flow of cylinder lube oil in kg/sec-cyl
Mass_flow_CLO = (SLOC * Load * KW)/(Num_cyl * 3600 * 1000);

% calculate mass flow of exhaust gas in kg/sec-cyl
Mass_flow_exh_cyl = Mass_flow_air + Mass_flow_fuel + Mass_flow_CLO;

% calculate exhaust gas flow in kg/sec
Mass_flow_exh = Mass_flow_exh_cyl * Num_cyl;

% calculate exhaust gas flow in kg/hr
Mass_flow_exh_hr = Mass_flow_exh * 3600;

% correct molecular weight of exhaust for scavenge air dilution in g/mol
MW_exh = ((MW_exh_calc * Comb_excess) + (Total_excess - Comb_excess) *
MW_air)./Total_excess;

% calculate molar flow rate of exhaust in mols/sec
Mol_flow_exh = (Mass_flow_exh * 1000)./MW_exh;

% calculate volumetric flow rate of exhaust in m^3/sec
Vol_flow_exh = (Mol_flow_exh.* T_exh.* Ideal_gas_const)./(P_exh);

% calculate volumetric flow rate of exhaust in m^3/min
Vol_flow_exh_min = Vol_flow_exh * 60;

% calculate volumetric flow rate of exhuast in scfm
Vol_flow_exh_scfm = Vol_flow_exh_min * 35.3147;



% WRITE OUTPUTS TO FILE
fid = fopen('C:\Matlab NOx\Mod1_Output.txt','w');
fprintf(fid,'%12.8f %12.8f %12.8f %12.8f %12.8f %12.8f %12.8f %12.8f %12.8f
%12.8f %12.8f', [ Ideal_gas_const MW_exh(4) P_exh(4) T_exh(4)
Mass_flow_exh(4) Mol_flow_exh(4) Vol_flow_exh(4) Load(4) KW
Mass_flow_exh_hr(4) MW_air ]);
status = fclose(fid);



% WRITE DATA TO DESIGN SUMMARY FILE
fid = fopen('C:\Matlab NOx\Summary.txt','w');
fprintf(fid,'Summary\r\r');
fprintf(fid,'Bore:                      %6.2f m\n', Bore);
fprintf(fid,'Stroke:                    %6.2f m\n', Stroke);
fprintf(fid,'Number of cylinders:       %6.2f cyl\n', Num_cyl);
fprintf(fid,'Rpm:                       %6.2f rev/min\n', Rpm);
fprintf(fid,'Power:                     %6.2f kW\n', KW);
fprintf(fid,'Fuel oil consumption:      %6.2f g/kW-hr\n', SFOC);
fprintf(fid,'Lube oil consumption:      %6.2f g/kW-hr\n', SLOC);
fprintf(fid,'Scavenge air press:        %6.2f Pa\n', P_scav(4));
fprintf(fid,'Scavenge air temp:         %6.2f °C\n', T_scav(4) - 273);
fprintf(fid,'Exhaust press:             %6.2f Pa\n', P_exh(4));
fprintf(fid,'Exhaust temp:              %6.2f °C\n', T_exh(4) - 273);
fprintf(fid,'Scavenge air press:        %6.2f Pa\n', P_scav(4));
fprintf(fid,'Scavenge air temp:         %6.2f °C\n', T_scav(4) - 273);
fprintf(fid,'Height of Scavport:        %6.2f m\n', Height_scavport);
```

```
fprintf(fid,'Cylinder volume:                %6.2f m^3\n', Cyl_vol);
fprintf(fid,'MW exhaust:                     %6.2f g/mol\n', MW_exh(4));
fprintf(fid,'MW air:                         %6.2f g/mol\n', MW_air);
fprintf(fid,'Mass flow scav air:             %6.2f kg/sec-cyl\n',
Mass_flow_air(4));
fprintf(fid,'Mass flow fuel:                 %6.2f kg/sec-cyl\n',
Mass_flow_fuel(4));
fprintf(fid,'Mass flow CLO (grams):          %6.2f g/sec-cyl\n',
Mass_flow_CLO(4)*1000);
fprintf(fid,'Mass flow exhaust:              %6.2f kg/sec\n', Mass_flow_exh(4));
fprintf(fid,'Vol flow exhaust:               %6.2f m^3/sec\n', Vol_flow_exh(4));
fprintf(fid,'Mass flow exhaust:              %6.2f kg/hr\n',
Mass_flow_exh_hr(4));
fprintf(fid,'Vol flow exhaust:               %6.2f SCFM\n',
Vol_flow_exh_scfm(4));
fprintf(fid,' \r');
status = fclose(fid);
```

Module 2 – Calculate exhaust gas properties

```
% CLEAR ALL AND CLOSE ALL
clear all
close all



% IMPORT NEW VARIABLES FOR MODULE
% Backpress_exh_avg Visc_dyn_exh
fid = fopen('C:\Matlab NOx\Mod2_Input.txt');
Mod2_Input = textscan(fid, '%s %s', 'Headerlines', 3);
%fclose(fid);



% LOAD VARIABLES FROM PREVIOUS MODULE OUTPUT FILES
% Ideal_gas_const MW_exh(4) P_exh(4) T_exh(4) Mass_flow_exh(4)
Mol_flow_exh(4) Vol_flow_exh(4) Load(4) KW Mass_flow_exh_hr(4) MW_air
fid = fopen('C:\Matlab NOx\Mod1_Output.txt');
Mod1_Output = textscan(fid, ' %s %s %s %s %s %s %s %s %s %s %s');
fclose(fid);



% DEFINE VARIABLES FOR MODULE
% define average exhaust gas pressure in Pa
Backpress_exh_avg = Mod2_Input{1};
Backpress_exh_avg = str2double(cell2mat(Backpress_exh_avg));

% define dynamic viscosity for exhaust gas in kg/m sec
Visc_dyn_exh = Mod2_Input{2};
Visc_dyn_exh = str2double(cell2mat(Visc_dyn_exh));

% define ideal gas constant in m^3 Pa/molK
Ideal_gas_const = Mod1_Output{1};
Ideal_gas_const = str2double(cell2mat(Ideal_gas_const));

% define molecular weight of exhaust in g/mol
MW_exh = Mod1_Output{2};
MW_exh = str2double(cell2mat(MW_exh));

% define exhaust pressure in Pa
P_exh = Mod1_Output{3};
P_exh = str2double(cell2mat(P_exh));

% define exhaust temperature in K
T_exh = Mod1_Output{4};
T_exh = str2double(cell2mat(T_exh));



% PERFORM CALCULATIONS
% calculate average exhaust system pressure in Pa
P_exh_avg = P_exh + (Backpress_exh_avg/2);

% calculate density of exhaust gas in kg/m^3
Rho_exh = (MW_exh * P_exh_avg)/(Ideal_gas_const * T_exh * 1000);

% calculate kinematic viscosity in m^2/sec
```

```
Visc_kin_exh = Visc_dyn_exh/Rho_exh;



% WRITE OUTPUTS TO FILE
fid = fopen('C:\Matlab NOx\Mod2_Output.txt','w');
fprintf(fid,'%12.8f %12.8f %12.8f', [ Rho_exh Visc_dyn_exh Visc_kin_exh ]);
status = fclose(fid);



% WRITE DATA TO DESIGN SUMMARY FILE
fid = fopen('C:\Matlab NOx\Summary.txt','a');
fprintf(fid,'Average backpressure:      %6.2f mmH20\n',
Backpress_exh_avg*.098);
fprintf(fid,'Density exhaust:           %6.2f kg/m^3\n', Rho_exh);
fprintf(fid,'Dynamic viscosity exh:     %6.2e kg/m-sec\n', Visc_dyn_exh);
fprintf(fid,'Kinetic viscosity exh:     %6.2e m^s/sec\n', Visc_kin_exh);
fprintf(fid,' \r');
status = fclose(fid);
```

Module 3 – Calculate NOx parameters and compare with UCI results

```
% CLEAR ALL AND CLOSE ALL
clear all
close all



% IMPORT NEW VARIABLES FOR MODULE
% NOx_gkwh_TierI NOx_gkwh_TierIII MW_NO2 SCFM_exh_UCI Mass_flow_NOx_UCI_gh
P_UCI T_UCI
fid = fopen('C:\Matlab NOx\Mod3_Input.txt');
Mod3_Input = textscan(fid, '%s %s %s %s %s %s %s', 'Headerlines', 3);
%fclose(fid);



% LOAD VARIABLES FROM PREVIOUS MODULE OUTPUT FILES
% Ideal_gas_const MW_exh(4) P_exh(4) T_exh(4) Mass_flow_exh(4)
Mol_flow_exh(4) Vol_flow_exh(4) Load(4) KW Mass_flow_exh_hr(4) MW_air
fid = fopen('C:\Matlab NOx\Mod1_Output.txt');
Mod1_Output = textscan(fid, '%s %s %s %s %s %s %s %s %s %s %s');
fclose(fid);



% DEFINE VARIABLES FOR MODULE
% define specific NOx production in g/kW hr
NOx_gkwh_TierI = Mod3_Input{1};
NOx_gkwh_TierI = str2double(cell2mat(NOx_gkwh_TierI));

% define allowable specific NOx emission in g/kW hr
NOx_gkwh_TierIII = Mod3_Input{2};
NOx_gkwh_TierIII = str2double(cell2mat(NOx_gkwh_TierIII));

% define molecular weight of NO2 in g/mol
MW_NO2 = Mod3_Input{3};
MW_NO2 = str2double(cell2mat(MW_NO2));

% define exhaust gas flow rate as measured by UCI in scfm
SCFM_exh_UCI = Mod3_Input{4};
SCFM_exh_UCI = str2double(cell2mat(SCFM_exh_UCI));

% define NOx mass flow rate from UCI data in g/hr
Mass_flow_NOx_UCI_gh = Mod3_Input{5};
Mass_flow_NOx_UCI_gh = str2double(cell2mat(Mass_flow_NOx_UCI_gh));

% define exhaust pressure for UCI data in Pa
P_UCI = Mod3_Input{6};
P_UCI = str2double(cell2mat(P_UCI));

% define exhaust temperature for UCI data in K
T_UCI = Mod3_Input{7};
T_UCI = str2double(cell2mat(T_UCI));

% define ideal gas constant in m^3 Pa/mol K
Ideal_gas_const = Mod1_Output{1};
Ideal_gas_const = str2double(cell2mat(Ideal_gas_const));

% define molecular weight of exhaust gas in g/mol
```

```
MW_exh = Mod1_Output{2};
MW_exh = str2double(cell2mat(MW_exh));

% define exhaust pressure in Pa
P_exh = Mod1_Output{3};
P_exh = str2double(cell2mat(P_exh));

% define exhaust temperature in K
T_exh = Mod1_Output{4};
T_exh = str2double(cell2mat(T_exh));

% define mass flow rate in kg/sec
Mass_flow_exh = Mod1_Output{5};
Mass_flow_exh = str2double(cell2mat(Mass_flow_exh));

% define molar flow rate in mol/sec
Mol_flow_exh = Mod1_Output{6};
Mol_flow_exh = str2double(cell2mat(Mol_flow_exh));

% define volumetric flow rate in m^3/sec
Vol_flow_exh = Mod1_Output{7};
Vol_flow_exh = str2double(cell2mat(Vol_flow_exh));

% define engine load as load factor - dimensionless
Load = Mod1_Output{8};
Load = str2double(cell2mat(Load));

% define engine rated power in kW
KW = Mod1_Output{9};
KW = str2double(cell2mat(KW));



% PERFORM CALCULATIONS
% calculate Tier I mass flow of NOx in kg/s
Mass_flow_NOx_TierI = (NOx_gkwh_TierI * KW * Load)/(3600 * 1000);

% calculate NOx content by mass of exhaust gas in ppm
Ppm_mass_NOx_TierI = (Mass_flow_NOx_TierI/Mass_flow_exh) * (1000000);

% calculate Tier I volumetric flow of NOx in m^3/sec
Vol_flow_NOx_TierI = (Mass_flow_NOx_TierI * Ideal_gas_const * T_exh *
1000)/(MW_NO2 * P_exh);

% calculate NOx content by volume of exhaust gas in ppm
Ppm_vol_NOx_TierI = (Vol_flow_NOx_TierI/Vol_flow_exh) * 1000000;

% calculate NOx content as mol fraction of exhaust gas - dimensionless
Mol_fract_NO_exh_TierI = ((Mass_flow_NOx_TierI *
1000)/MW_NO2)/Mol_flow_exh;

% calculate IMO Tier III permissible NOx flow in kg/s
Mass_flow_NOx_TierIII = (NOx_gkwh_TierIII * KW * Load)/(3600 * 1000);

% calculate Tier III NOx content by mass of exhaust gas in ppm
Ppm_mass_NOx_TierIII = (Mass_flow_NOx_TierIII/Mass_flow_exh) * (1000000);

% calculate Tier III volumetric flow of NOx in m^3/sec
Vol_flow_NOx_TierIII = (Mass_flow_NOx_TierIII * Ideal_gas_const * T_exh *
1000)/(MW_NO2 * P_exh);
```

```
% calculate NOx content by volume of exhaust gas in ppm
Ppm_vol_NOx_TierIII = (Vol_flow_NOx_TierIII/Vol_flow_exh) * 1000000;

% calculate Tier III NOx content as mol fraction - dimensionless
Mol_fract_exh_TierIII = ((Mass_flow_NOx_TierIII *
1000)/MW_NO2)/Mol_flow_exh;

% calculate design effectiveness of SCR unit
Effect_TierI = (NOx_gkwh_TierI - NOx_gkwh_TierIII)/NOx_gkwh_TierI;



% PERFORM CALCULATIONS BASED ON UCI EXPERIMENTAL DATA
% calculate volumetric flow rate of exhaust from UCI study in m^3/sec
Vol_UCI = (SCFM_exh_UCI/(35.3147 * 60));

% correct calculated volumetric flow rate to UCI conditions in m^3/sec
Vol_calc_corr =  (Mol_flow_exh * Ideal_gas_const * T_UCI)/(P_UCI);

% calculate corrected mass emission rate in g/hr
Mass_NOx_ghr_UCI_corr = (Mass_flow_NOx_UCI_gh/Vol_UCI) * Vol_calc_corr;

% calculate corrected NOx flow rate in ppm by mass
Ppm_mass_NOx_UCI = ((Mass_NOx_ghr_UCI_corr/(1000*3600))/(Mass_flow_exh *
Load)) * (1000000);

% calculate corrected UCI specific NOx emissions in g/kW-hr
NOx_gkwh_UCI_corr = Mass_NOx_ghr_UCI_corr/(KW * Load);

% calculate design effectiveness based on UCI data - dimensionles
Effect_UCI = (NOx_gkwh_UCI_corr - NOx_gkwh_TierIII)/NOx_gkwh_UCI_corr;



% WRITE OUTPUTS TO FILE
fid = fopen('C:\Matlab NOx\Mod3_Output.txt','w');
fprintf(fid,'%12.8f %12.8f %12.8f %12.8f %12.8f', [ Effect_TierI Effect_UCI
Ppm_mass_NOx_TierI Ppm_mass_NOx_UCI MW_NO2 ]);
status = fclose(fid);



% WRITE DATA TO DESIGN SUMMARY FILE
fid = fopen('C:\Matlab NOx\Summary.txt','a');
fprintf(fid,'NOx Tier I:                %6.2f g/kW-hr\n', NOx_gkwh_TierI);
fprintf(fid,'NOx ppm Tier I (mass):     %6.2f ppm\n', Ppm_mass_NOx_TierI);
fprintf(fid,'NOx ppm Tier I (vol):      %6.2f ppm\n', Ppm_vol_NOx_TierI);
fprintf(fid,'NOx Tier III:              %6.2f g/kW-hr\n',
NOx_gkwh_TierIII);
fprintf(fid,'NOx ppm Tier III (mass):   %6.2f ppm\n',
Ppm_mass_NOx_TierIII);
fprintf(fid,'NOx ppm Tier III (vol):    %6.2f ppm\n', Ppm_vol_NOx_TierIII);
fprintf(fid,'Effectiveness:             %6.2f \n', Effect_TierI);
fprintf(fid,'Vol flow UCI data:         %6.2f m^3/sec\n', Vol_UCI);
fprintf(fid,'Vol flow UCI corrected:    %6.2f m^3/sec\n', Vol_calc_corr);
fprintf(fid,'NOx UCI corr:              %6.2f g/kW-hr\n',
NOx_gkwh_UCI_corr);
fprintf(fid,'Effectiveness UCI:         %6.2f \n', Effect_UCI);
fprintf(fid,' \r');
```

```
status = fclose(fid);
```

Module 4 – Calculate Urea solution consumption

```
% CLEAR ALL AND CLOSE ALL
clear all
close all



% IMPORT NEW VARIABLES FOR MODULE
% MW_NO MW_Urea Percent_urea SG_Urea_soln Days_op_year Days_year_port
Percent_ECA
fid = fopen('C:\Matlab NOx\Mod4_Input.txt');
Mod4_Input = textscan(fid, '%s %s %s %s %s %s %s %s %s', 'Headerlines', 3);
%fclose(fid);



% LOAD VARIABLES FROM PERVIOUS MODULE OUTPUT FILES
% % Ideal_gas_const MW_exh(4) P_exh(4) T_exh(4) Mass_flow_exh(4)
Mol_flow_exh(4) Vol_flow_exh(4) Load(4) KW Mass_flow_exh_hr(4) MW_air
fid = fopen('C:\Matlab NOx\Mod1_Output.txt');
Mod1_Output = textscan(fid, '%s %s %s %s %s %s %s %s %s %s %s');
fclose(fid);

% Effect_TierI Effect_UCI Ppm_mass_NOx_TierI Ppm_mass_NOx_UCI MW_NO2
fid = fopen('C:\Matlab NOx\Mod3_Output.txt');
Mod3_Output = textscan(fid, '%s %s %s %s %s');
fclose(fid);



% DEFINE VARIABLES FOR MODULE
% define slip as concentration of HN3 at reactor outlet in ppm by vol (wet)
Slip = Mod4_Input{1};
Slip = str2double(cell2mat(Slip));

% define define molecular weight of ammonia in g/mol
MW_NH3 = Mod4_Input{2};
MW_NH3 = str2double(cell2mat(MW_NH3));

% define molecular weight of NO2 in g/mol
MW_NO = Mod4_Input{3};
MW_NO = str2double(cell2mat(MW_NO));

% define molecular weight of Urea in g/mol
MW_Urea = Mod4_Input{4};
MW_Urea = str2double(cell2mat(MW_Urea));

% define percent urea in solution by mass
Percent_urea = Mod4_Input{5};
Percent_urea = str2double(cell2mat(Percent_urea));

% define specific gravity of urea solution - dimensionless
SG_Urea_soln = Mod4_Input{6};
SG_Urea_soln = str2double(cell2mat(SG_Urea_soln));

% define operational days per year in days/year
Days_op_year = Mod4_Input{7};
Days_op_year = str2double(cell2mat(Days_op_year));
```

```
% define number of days in port per year in days/year
Days_port_year = Mod4_Input{8};
Days_port_year = str2double(cell2mat(Days_port_year));

% define percent of operational time spent in ECA areas
Percent_ECA = Mod4_Input{9};
Percent_ECA = str2double(cell2mat(Percent_ECA));

% define molecular weight of exhaust in g/mol
MW_exh = Mod1_Output{2};
MW_exh = str2double(cell2mat(MW_exh));

% define mass flow rate of exhaust in kg/hr
Mass_flow_exh_hr = Mod1_Output{10};
Mass_flow_exh_hr = str2double(cell2mat(Mass_flow_exh_hr));

% define Tier I effectiveness of SCR unit - dimensionless
Effect_TierI = Mod3_Output{1};
Effect_TierI = str2double(cell2mat(Effect_TierI));

% define Tier I effectiveness of SCR unit - dimensionless
Effect_UCI = Mod3_Output{2};
Effect_UCI = str2double(cell2mat(Effect_UCI));

% define Tier I NOx content in ppm by mass
Ppm_mass_NOx_TierI = Mod3_Output{3};
Ppm_mass_NOx_TierI = str2double(cell2mat(Ppm_mass_NOx_TierI));

% define UCI NOx content in ppm by mass
Ppm_mass_NOx_UCI = Mod3_Output{4};
Ppm_mass_NOx_UCI = str2double(cell2mat(Ppm_mass_NOx_UCI));

% define molecular weight of NO2 in g/mol
MW_NO2 = Mod3_Output{5};
MW_NO2 = str2double(cell2mat(MW_NO2));



% PERFORM CALCULATIONS
% determine mols NO2 in NO/NO2 mixture in mols
Mol_NO2 = .1 * (1/MW_NO2);

% determine mols of NO in NO/NO2 mixture in mols
Mol_NO = (1 - (Mol_NO2 * MW_NO2))/MW_NO;

% determine total mols in mols
Mol_NO_NO2 = Mol_NO2 + Mol_NO;

% determine mols as 100% NO2 in mols
Mol_NO2_ref = 1/MW_NO2;

% determine correction factor in total mols/mol NO2
Corr_mol = Mol_NO_NO2/Mol_NO2_ref;

% calculate ratio of NH3 to NOx dosage for Tier I conditions -
dimensionless
Ratio_NH3_NOx_TierI = (Effect_TierI +((Slip *
(MW_exh/MW_NH3))/Ppm_mass_NOx_TierI));

% calculate ration of NH3 to NOx dosage for UCI conditions - dimensionless
```

```
Ratio_NH3_NOx_UCI = (Effect_UCI +((Slip *
(MW_exh/MW_NH3))/Ppm_mass_NOx_UCI));

% calculate NH3 consumption for TierI conditions in kg/hr
Mass_flow_NH3_TierI_hr = Mass_flow_exh_hr * (Ppm_mass_NOx_TierI/1000000)
*(MW_NH3/MW_NO2) * Corr_mol * Ratio_NH3_NOx_TierI;

% calculate NH3 consumption for UCI conditions in kg/hr
Mass_flow_NH3_UCI_hr = Mass_flow_exh_hr * (Ppm_mass_NOx_UCI/1000000)
*(MW_NH3/MW_NO2) * Corr_mol * Ratio_NH3_NOx_UCI;

% calculate consumption of urea solution for Tier I condition in kg/hr
Mass_flow_urea_soln_TierI = (Mass_flow_NH3_TierI_hr/Percent_urea) *
(MW_Urea/MW_NH3) * (100/2);

% calculate mass flow of urea solution for UCI condition in kg/hr
Mass_flow_urea_soln_UCI = (Mass_flow_NH3_UCI_hr/Percent_urea) *
(MW_Urea/MW_NH3) * (100/2);

% calculate volumetric flow of urea solution for TierI condition in m^3/hr
Vol_flow_urea_hr_TierI = (Mass_flow_urea_soln_TierI)/(SG_Urea_soln * 1000);

% calculate volumetric flow of urea solution for UCI condition in m^3/hr
Vol_flow_urea_hr_UCI = (Mass_flow_urea_soln_UCI)/(SG_Urea_soln * 1000);

% calculate monthly consumption of urea for TierI condition in m^3
Vol_month_urea_TierI = (((Days_op_year * Percent_ECA) - Days_port_year) *
24 * Vol_flow_urea_hr_TierI)/12;

% calculate monthly consumption of urea for UCI condition in m^3
Vol_month_urea_UCI = (((Days_op_year * Percent_ECA) - Days_port_year) * 24
* Vol_flow_urea_hr_UCI)/12;



% WRITE OUTPUTS TO FILE
fid = fopen('C:\Matlab NOx\Mod4_Output.txt','w');
fprintf(fid,'%12.8f %12.8f %12.8f %12.8f %12.8f', [ MW_NH3 MW_NO
Days_op_year Days_port_year Percent_ECA ]);
status = fclose(fid);

% WRITE DATA TO SUMMARY FILE
fid = fopen('C:\Matlab NOx\Summary.txt','a');
fprintf(fid,'Urea soln:                    %6.0f percent by mass\n',
Percent_urea);
fprintf(fid,'Maximum slip:                 %6.1f ppm by vol\n', Slip);
fprintf(fid,'Days in operation/yr:         %6.0f days/yrea\n', Days_op_year);
fprintf(fid,'Days in port/yr:              %6.0f days/year\n',
Days_port_year);
fprintf(fid,'Percent time in ECA:          %6.2f percent time in ECA\n',
Percent_ECA);
fprintf(fid,'Mass flow NH3 (TierI):        %6.2f kg/hr\n',
Mass_flow_NH3_TierI_hr);
fprintf(fid,'Mass flow Urea (TierI):       %6.2f kg/hr\n',
Mass_flow_urea_soln_TierI);
fprintf(fid,'Vol flow urea soln (T-I)      %6.2f m^3/hr\n',
Vol_flow_urea_hr_TierI);
fprintf(fid,'Vol flow per month (T-I):     %6.2f m^3/month\n',
Vol_month_urea_TierI);
```

```
fprintf(fid,'Mass flow NH3 (UCI):       %6.2f kg/hr\n',
Mass_flow_NH3_UCI_hr);
fprintf(fid,'Mass flow Urea (UCI):      %6.2f kg/hr\n',
Mass_flow_urea_soln_UCI);
fprintf(fid,'Vol flow urea soln (UCI):  %6.2f m^3/hr\n',
Vol_flow_urea_hr_UCI);
fprintf(fid,'Vol flow per month (UCI:   %6.2f m^3/month\n',
Vol_month_urea_UCI);
fprintf(fid,' \r');
status = fclose(fid);
```

Module 5 – Calculate diffusion coefficients for NO and NH3

```
% CLEAR ALL AND CLOSE ALL
clear all
close all



% IMPORT NEW VARIABLES FOR MODULE
% Epsilon_air Sigma_air Epsilon_NO Sigma_NO Epsilon_NH3 Sigma_NH3
fid = fopen('C:\Matlab NOx\Mod5_Input.txt');
Mod5_Input = textscan(fid, '%s %s %s %s %s %s', 'Headerlines', 3);
%fclose(fid);



% LOAD VARIABLES FROM PREVIOUS MODULE OUTPUT FILES
% Ideal_gas_const MW_exh(4) P_exh(4) T_exh(4) Mass_flow_exh(4)
Mol_flow_exh(4) Vol_flow_exh(4) Load(4) KW Mass_flow_exh_hr(4) MW_air
fid = fopen('C:\Matlab NOx\Mod1_Output.txt');
Mod1_Output = textscan(fid, '%s %s %s %s %s %s %s %s %s %s %s');
fclose(fid);

% MW_NH3 MW_NO Days_op_year Days_port_year Percent_ECA
fid = fopen('C:\Matlab NOx\Mod4_Output.txt');
Mod4_Output = textscan(fid, '%s %s %s %s %s');
fclose(fid);



% DEFINE VARIABLES FOR MODULE
% define epsilon/Boltzman constant for air in K
Epsilon_air = Mod5_Input{1};
Epsilon_air = str2double(cell2mat(Epsilon_air));

% define sigma air in Angstroms
Sigma_air = Mod5_Input{2};
Sigma_air = str2double(cell2mat(Sigma_air));

% define epsilon/Boltzman constant for NO in K
Epsilon_NO = Mod5_Input{3};
Epsilon_NO = str2double(cell2mat(Epsilon_NO));

% define sigma NO in Angstroms
Sigma_NO = Mod5_Input{4};
Sigma_NO = str2double(cell2mat(Sigma_NO));

% define epsilon/Boltzman constant for NH3 in K
Epsilon_NH3 = Mod5_Input{5};
Epsilon_NH3 = str2double(cell2mat(Epsilon_NH3));

% define sigma NH3 in Angstroms
Sigma_NH3 = Mod5_Input{6};
Sigma_NH3 = str2double(cell2mat(Sigma_NH3));

% define exhuast gas pressure in Pa
P_exh = Mod1_Output{3};
P_exh = str2double(cell2mat(P_exh));

% define temperature in K
```

```
T_exh = Mod1_Output{4};
T_exh = str2double(cell2mat(T_exh));

% define molecular weight of air in g/mol
MW_air = Mod1_Output{11};
MW_air = str2double(cell2mat(MW_air));

% define molecular weight of NH3 in g/mol
MW_NH3 = Mod4_Output{1};
MW_NH3 = str2double(cell2mat(MW_NH3));

% define molecular weight of NO in g/mol
MW_NO = Mod4_Output{2};
MW_NO = str2double(cell2mat(MW_NO));



% PERFORM CALCULATIONS
% calculate epsilon NO/air in K
Epsilon_NO_air = (Epsilon_air * Epsilon_NO)^0.5;

% calculate epsilon NH3/air in K
Epsilon_NH3_air = (Epsilon_air * Epsilon_NH3)^0.5;

% calculate sigma NO/air in Angstroms
Sigma_NO_air = (Sigma_air + Sigma_NO)/2;

% calculate sigma NH3/air in Angstroms
Sigma_NH3_air = (Sigma_air + Sigma_NH3)/2;

% calculate molecular weight NO/air in g/mol
MW_NO_air = 2/((1/MW_air) + (1/MW_NO));

% calculate molecular weight NH3/air in g/mol
MW_NH3_air = 2/((1/MW_air) + (1/MW_NH3));

% calculate temperature parameter for NO/air - dimensionless
T_NO_air = T_exh/Epsilon_NO_air;

% calculate temperature parameter for NH3/air - dimensionless
T_NH3_air = T_exh/Epsilon_NH3_air;

% calculate omega NO/air - dimensionless
Omega_NO_Air = (1.06036/(T_NO_air)^0.15610) + (0.193/exp(0.47635 *
T_NO_air)) + (1.03587/exp(1.52996 * T_NO_air)) + (1.76474/exp(3.89411 *
T_NO_air));

% calculate omega NH3/air - dimensionless
Omega_NH3_Air = (1.06036/(T_NH3_air)^0.15610) + (0.193/exp(0.47635 *
T_NH3_air)) + (1.03587/exp(1.52996 * T_NH3_air)) + (1.76474/exp(3.89411 *
T_NH3_air));

% calculate diffusion coefficient of NO in air in cm^2/sec
D_NO_air_cm = (0.00266 * T_exh^(3/2))/((P_exh/100000) * MW_NO_air^0.5 *
Sigma_NO_air^2 * Omega_NO_Air);

% calculate diffusion coefficient of NH3 in air in cm^2/sec
D_NH3_air_cm = (0.00266 * T_exh^(3/2))/((P_exh/100000) * MW_NH3_air^0.5 *
Sigma_NH3_air^2 * Omega_NH3_Air);
```

```
% calculate diffusion coefficient of NO in air in m^2/sec
D_NO_air = D_NO_air_cm/10000;

% calculate diffusion coefficient in NH3 in air in m^2/sec
D_NH3_air = D_NH3_air_cm/10000;



% WRITE OUTPUTS TO FILE
fid = fopen('C:\Matlab NOx\Mod5_Output.txt','w');
fprintf(fid,'%12.8f %12.8f', [ D_NO_air D_NH3_air ]);
status = fclose(fid);



% WRITE DATA TO DESIGN SUMMARY FILE
fid = fopen('C:\Matlab NOx\Summary.txt','a');
fprintf(fid,'Diffusion Coeff NO/Air:    %6.2e m^2/sec\n', D_NO_air);
fprintf(fid,'Diffusion Coeff NH3/Air:   %6.2e m^2/sec\n', D_NH3_air);
fprintf(fid,' \r');
status = fclose(fid);
```

Module 6 – Calculate properties of catalyst

```
% CLEAR ALL AND CLOSE ALL
clear all
close all



% IMPORT NEW VARIABLES FOR MODULE
% Width_ch Thick_wall Num_channel_x Num_channel_y Height_element Rho_cat
fid = fopen('C:\Matlab NOx\Mod6_Input.txt');
Mod6_Input = textscan(fid, '%s %s %s %s %s %s', 'Headerlines', 3);
%fclose(fid);



% DEFINE VARIABLES FOR MODULE
% define channel width in m
Width_ch = Mod6_Input{1};
Width_ch = str2double(cell2mat(Width_ch));

% define wall thickness in m
Thick_wall = Mod6_Input{2};
Thick_wall = str2double(cell2mat(Thick_wall));

% define number of channels in x direction for element - dimensionless
Num_element_x = Mod6_Input{3};
Num_element_x = str2double(cell2mat(Num_element_x));

% define number of channels in y direction for element - dimensionless
Num_element_y = Mod6_Input{4};
Num_element_y = str2double(cell2mat(Num_element_y));

% define height of catalyst element in m
Height_element = Mod6_Input{5};
Height_element = str2double(cell2mat(Height_element));

% define density of catalyst in kg/m^3
Rho_cat = Mod6_Input{6};
Rho_cat = str2double(cell2mat(Rho_cat));



% PERFORM CALCULATIONS
% calculate area of channel in m^2
Area_ch = Width_ch^2;

% calculate perimenter of channel in m
Perimeter_ch = 4 * Width_ch;

% calculate hydraulic diameter in m
Diam_hydraulic = (4 * Area_ch)/Perimeter_ch;

% calculate number of channels in monolith element
Num_element = Num_element_x * Num_element_y;

% calculate surface area of channel in m^2
Surf_area_ch = 4 * Width_ch * Height_element;

% calculate active surface area for catalyst element in m^2
```

```
Surf_area_element = Surf_area_ch * Num_element;

% calculate width of element in x direction in m
Width_element_x = (Num_element_x * Width_ch + (Num_element_x + 1) *
Thick_wall);

% calculate width of element in y direction in m
Width_element_y = (Num_element_y * Width_ch + (Num_element_y + 1) *
Thick_wall);

% calculate cross sectional area of element in m^2
Area_element = Width_element_x * Width_element_y;

% calculate nominal volume of catalyst element in m^3
Vol_element = Area_element * Height_element;

% calculate volume of catalyst in element in m^3
Vol_cat_element = Height_element * (Area_element - (Num_element *
Area_ch));

% calculate volume of catalyst per channel
Vol_cat_ch = Vol_cat_element/Num_element;

% calculate specific surface area in m^2/m^3
Surf_area_spec = Surf_area_ch/Vol_cat_ch;

% calculate mass of catalyst in element in kg
Mass_cat_element = Rho_cat * Vol_cat_element;



% WRITE OUTPUTS TO FILE
fid = fopen('C:\Matlab NOx\Mod6_Output.txt','w');
fprintf(fid,'%12.8f %12.8f %12.8f %12.8f %12.8f %12.8f %12.8f %12.8f %12.8f
%12.8f %12.8f', [ Width_ch Thick_wall Rho_cat Surf_area_spec Area_ch
Perimeter_ch Diam_hydraulic Num_element Surf_area_ch Area_element
Vol_cat_ch ]);
status = fclose(fid);



% WRITE DATA TO DESIGN SUMMARY FILE
fid = fopen('C:\Matlab NOx\Summary.txt','a');
fprintf(fid,'Width of channel:          %6.3f m\n', Width_ch);
fprintf(fid,'Wall thickness:            %6.4f m\n', Thick_wall);
fprintf(fid,'Area of channel:           %6.2e m^2\n', Area_ch);
fprintf(fid,'Perimeter of channel:      %6.3f m\n', Perimeter_ch);
fprintf(fid,'Hydraulic Diameter:        %6.3f m\n', Diam_hydraulic);
fprintf(fid,'Number channels X:         %6.2f \n', Num_element_x);
fprintf(fid,'Number channels Y:         %6.2f \n', Num_element_y);
fprintf(fid,'Number channels:           %6.2f \n', Num_element);
fprintf(fid,'Height of element:         %6.2f m\n', Height_element);
fprintf(fid,'Width of element X:        %6.2f m\n', Width_element_x);
fprintf(fid,'Width of element Y:        %6.2f m\n', Width_element_y);
fprintf(fid,'Area of element:           %6.4f m^2\n', Area_element);
fprintf(fid,'Volume of element:         %6.4f m^3\n', Vol_element);
fprintf(fid,'Surface area of channel:   %6.3f \n', Surf_area_ch);
fprintf(fid,'Surface area per element:  %6.2f \n', Surf_area_element);
fprintf(fid,'Catalyst volume/channel:   %6.2e m^3\n', Vol_cat_ch);
fprintf(fid,'Catalyst volume/element:   %6.4f m^3\n', Vol_cat_element);
```

```
fprintf(fid,'Specific surface area:     %6.2f m^2/m^3\n', Surf_area_spec);
fprintf(fid,'Density of catalyst:       %6.2f kg/m^3\n', Rho_cat);
fprintf(fid,'Mass element:              %6.2f kg\n', Mass_cat_element);
fprintf(fid,' \r');
status = fclose(fid);
```

Module 7 – Calculate size and properties of SCR reactor

```
% CLEAR ALL AND CLOSE ALL
clear all
close all



% IMPORT NEW VARIABLES FOR MODULE
% P_cat_exp T_cat_exp D_eff_NO K_NO_Int Lenth_cat Ea_SCR A_pre_exp_SCR Re
Fact_deact Num_years
fid = fopen('C:\Matlab NOx\Mod7_Input.txt');
Mod7_Input = textscan(fid, '%s %s %s %s %s %s %s %s %s %s', 'Headerlines',
3);
%fclose(fid);



% LOAD VARIALBES FROM PREVIOS MODULE OUTPUT FILES
% Ideal_gas_const MW_exh(4) P_exh(4) T_exh(4) Mass_flow_exh(4)
Mol_flow_exh(4) Vol_flow_exh(4) Load(4) KW Mass_flow_exh_hr(4) MW_air
fid = fopen('C:\Matlab NOx\Mod1_Output.txt');
Mod1_Output = textscan(fid, '%s %s %s %s %s %s %s %s %s %s %s');
fclose(fid);

% Rho_exh Visc_dyn_exh Visc_kin_exh
fid = fopen('C:\Matlab NOx\Mod2_Output.txt');
Mod2_Output = textscan(fid, '%s %s %s');
fclose(fid);

% Effect_TierI Effect_UCI Ppm_mass_NOx_TierI Ppm_mass_NOx_UCI MW_NO2
fid = fopen('C:\Matlab NOx\Mod3_Output.txt');
Mod3_Output = textscan(fid, '%s %s %s %s %s');
fclose(fid);

% MW_NH3 MW_NO Days_op_year Days_port_year Percent_ECA
fid = fopen('C:\Matlab NOx\Mod4_Output.txt');
Mod4_Output = textscan(fid, '%s %s %s %s %s');
fclose(fid);

% D_NO_air D_NH3_air
fid = fopen('C:\Matlab NOx\Mod5_Output.txt');
Mod5_Output = textscan(fid, '%s %s');
fclose(fid);

% Width_ch Thick_wall Rho_cat Surf_area_spec Area_ch Perimeter_ch
Diam_hydraulic Num_element Surf_area_ch Area_element Vol_cat_ch
fid = fopen('C:\Matlab NOx\Mod6_Output.txt');
Mod6_Output = textscan(fid, '%s %s %s %s %s %s %s %s %s %s %s');
fclose(fid);



% DEFINE VARIABLES FOR MODULE
% define pressure at which DTU experimental data was determined in Pa
P_cat_exp = Mod7_Input{1};
P_cat_exp = str2double(cell2mat(P_cat_exp));

% define temperature at which DTU experimental data was determined in K
T_cat_exp = Mod7_Input{2};
```

```
T_cat_exp = str2double(cell2mat(T_cat_exp));

% define effective diffusion coefficient for NO in m^2/sec
D_eff_NO = Mod7_Input{3};
D_eff_NO = str2double(cell2mat(D_eff_NO));

% define intrinsic rate constant in m^3/kg sec
K_NO_Int = Mod7_Input{4};
K_NO_Int = str2double(cell2mat(K_NO_Int));

% define length of catalyst in m
Length_cat = Mod7_Input{5};
Length_cat = str2double(cell2mat(Length_cat));

% define activation energy of catalytic reaction J/mol
Ea_SCR = Mod7_Input{6};
Ea_SCR = str2double(cell2mat(Ea_SCR));

% define pre-exponential factor of catalytic reaction in m^3/kg sec
A_pre_exp_SCR = Mod7_Input{7};
A_pre_exp_SCR = str2double(cell2mat(A_pre_exp_SCR));

% define maximum Reynold number - dimensionless
Re_max = Mod7_Input{8};
Re_max = str2double(cell2mat(Re_max));

% define deactivation factor in 1/10000 hours
Fact_deact = Mod7_Input{9};
Fact_deact = str2double(cell2mat(Fact_deact));

% define number of years between overhaul in years
Num_years = Mod7_Input{10};
Num_years = str2double(cell2mat(Num_years));

% define ideal gas constant in m^3 Pa/mol K
Ideal_gas_const = Mod1_Output{1};
Ideal_gas_const = str2double(cell2mat(Ideal_gas_const));

% define exhuast gas pressure in Pa
P_exh = Mod1_Output{3};
P_exh = str2double(cell2mat(P_exh));

% define exhuast gas temperature in K
T_exh = Mod1_Output{4};
T_exh = str2double(cell2mat(T_exh));

% define mass flow of exhaust in kg/sec
Mass_flow_exh = Mod1_Output{5};
Mass_flow_exh = str2double(cell2mat(Mass_flow_exh));

% define mol flow of exhaust in mol/sec
Mol_flow_exh = Mod1_Output{6};
Mol_flow_exh = str2double(cell2mat(Mol_flow_exh));

% define volumetric flow of exhaust in m^3/sec
Vol_flow_exh = Mod1_Output{7};
Vol_flow_exh = str2double(cell2mat(Vol_flow_exh));

% define density of exhaust gas in kg/m^3
Rho_exh = Mod2_Output{1};
```

```
Rho_exh = str2double(cell2mat(Rho_exh));

% define kinematic viscosity of exhaust gas in m^2/sec
Visc_kin_exh = Mod2_Output{3};
Visc_kin_exh = str2double(cell2mat(Visc_kin_exh));

% define effectiveness of SCR unit - dimensionless
Effect_TierI = Mod3_Output{1};
Effect_TierI = str2double(cell2mat(Effect_TierI));

% define effectiveness of SCR unit - dimensionless
Effect_UCI = Mod3_Output{2};
Effect_UCI = str2double(cell2mat(Effect_UCI));

% define molecular weight of NO in g/mol
MW_NO = Mod4_Output{2};
MW_NO = str2double(cell2mat(MW_NO));

% define operational days per year in days/year
Days_op_year = Mod4_Output{3};
Days_op_year = str2double(cell2mat(Days_op_year));

% Define days in port per year in days/year
Days_port_year = Mod4_Output{4};
Days_port_year = str2double(cell2mat(Days_port_year));

% Define percent of operational time in ECA including port days
Percent_ECA = Mod4_Output{5};
Percent_ECA = str2double(cell2mat(Percent_ECA));

% define diffusion coefficient of NO in air in m^2/sec
D_NO_air = Mod5_Output{1};
D_NO_air = str2double(cell2mat(D_NO_air));

% define width of channel in m
Width_ch = Mod6_Output{1};
Width_ch = str2double(cell2mat(Width_ch));

% define wall thickness in m
Thick_wall = Mod6_Output{2};
Thick_wall = str2double(cell2mat(Thick_wall));

% define density of catalyst in kg/m^3
Rho_cat = Mod6_Output{3};
Rho_cat = str2double(cell2mat(Rho_cat));

% define specific surface area in m^2/m^3
Surf_area_spec = Mod6_Output{4};
Surf_area_spec = str2double(cell2mat(Surf_area_spec));

% define area of channel in m^2
Area_ch = Mod6_Output{5};
Area_ch = str2double(cell2mat(Area_ch));

% define perimeter of channel in m
Perimeter_ch = Mod6_Output{6};
Perimeter_ch = str2double(cell2mat(Perimeter_ch));

% define hydraulic diameter in m
Diam_hydraulic = Mod6_Output{7};
```

```
Diam_hydraulic = str2double(cell2mat(Diam_hydraulic));

% define number of channels in catalyst element - dimensionless
Num_element = Mod6_Output{8};
Num_element = str2double(cell2mat(Num_element));

% define surface area of channel in m^2
Surf_area_ch = Mod6_Output{9};
Surf_area_ch = str2double(cell2mat(Surf_area_ch));

% define area of SCR element in m^2
Area_element = Mod6_Output{10};
Area_element = str2double(cell2mat(Area_element));

% define volume of catalyst per channel in m^3
Vol_cat_ch = Mod6_Output{11};
Vol_cat_ch = str2double(cell2mat(Vol_cat_ch));


% PERFORM CALCULATIONS
% calculate maximum allowable flow velocity through channel in m/s
V_max_Re = (Re_max * Visc_kin_exh)/Diam_hydraulic;

% Calculate required area for maximum flow rate in m^2
Area_ch_req = Vol_flow_exh/V_max_Re;

% calculate number of channels - dimensionless
Num_channel_prelim = Area_ch_req/Area_ch;

% calculate number of blocks for a square reactor cross-section -
dimensionless
Num_blocks = ceil(sqrt(Num_channel_prelim/Num_element))^2;

% calculate number of channels based on the number of blocks -
dimensionless
Num_channel = Num_blocks * Num_element;

% calculate cross-sectional area of reactor in m^2
Area_cross_sect = Num_blocks * Area_element;

% calculate friction factor - dimensionless
Fm = 14.227/Re_max;

% calculate pressure drop per 1 meter of catalyst monolith in Pa
Delta_P_1m = ((2 * Fm * Rho_exh * V_max_Re^2)/(Diam_hydraulic * 1000)) +
((1.5 * Rho_exh * V_max_Re^2)/2);

% calculate rate coefficient for catalytic reaction in m^3/kg sec
K_SCR_exp = (A_pre_exp_SCR * exp(-Ea_SCR/(Ideal_gas_const * T_exh)));

% correct effective diffusion coefficient for system pressure in m^2/sec
D_eff_NO_corr = D_eff_NO/(P_exh/100000);

% calculate Thiele modulus - dimensionless
Thiele_mod = (Thick_wall/2) * ((K_SCR_exp * Rho_cat)/D_eff_NO_corr)^0.5;

% calculate efficiency in percent
Efficiency = 1/Thiele_mod;

% calculate mass transfer distance z - dimensionless
```

```
Z_ndim = (Length_cat * D_NO_air)/(Diam_hydraulic^2 * V_max_Re);

% calculate Sherwood number - dimensionless
Sherwood = 2.977 + (8.827 * ((1000 * Z_ndim)^-0.545) * exp(-48.2 *
Z_ndim));

% calculate mass transfer coefficient in m/sec
K_mass_trans_in = (Sherwood * D_NO_air)/(Width_ch/2);

% correct mass transfer coefficient for density of exhaust in kg/m^2-sec
K_mass_trans = K_mass_trans_in * Rho_exh;

% calculate density of NO in kg/m^3
Rho_NO = (MW_NO * P_cat_exp)/(Ideal_gas_const * T_cat_exp * 1000);

% correct rate coefficient to kg/m^2-sec
K_SCR = (K_SCR_exp * Rho_cat) * (1/Surf_area_spec) * (Rho_NO);

% calculate overall mass transfer coefficient
K_mass_trans_OA = ((1/(K_SCR * Efficiency)) + (1/K_mass_trans))^-1;

% calculate number of transfer units based on design case
Num_trans_units_TierI = log(1/(1-Effect_TierI));

% calculate number of transfer units based on UCI design case
Num_trans_units_UCI = log(1/(1-Effect_UCI));

% calculate length of reactor based on design case in m
Length_calc_TierI = (Num_trans_units_TierI *
(Mass_flow_exh/Num_channel))/(K_mass_trans_OA * Perimeter_ch);

% calculate length of reactor based on UCI data in m
Length_calc_UCI = (Num_trans_units_UCI *
(Mass_flow_exh/Num_channel))/(K_mass_trans_OA * Perimeter_ch);

% calculate pressure drop across reactor (TierI) in Pa
Delta_P_TierI = ((Length_calc_TierI * ((2 * Fm * Rho_exh *
V_max_Re^2)/(Diam_hydraulic * 1000))) + ((1.5 * Rho_exh * V_max_Re^2)/2));

% calculate pressure drop across reactor (UCI) in Pa
Delta_P_UCI = ((Length_calc_UCI * ((2 * Fm * Rho_exh *
V_max_Re^2)/(Diam_hydraulic * 1000))) + ((1.5 * Rho_exh * V_max_Re^2)/2));

% calculate expected deactivation of catalyst selected period
Deact = (1 - Fact_deact)^((Num_years * ((Days_op_year * Percent_ECA) - 70)
* 24)/10000);

% calculate length of reactor based on design case including deactivation
in m
Length_calc_TierI_deact = Length_calc_TierI/Deact;

% calculate length of reactor based on UCI data including deactivation in m
Length_calc_UCI_deact = Length_calc_UCI/Deact;



% Plot concentration profile
Length = linspace(0, 4 * Length_calc_TierI, 1000);
```

```
plot(Length, 1-exp((-K_mass_trans_OA * Perimeter_ch *
Length)/(Mass_flow_exh/Num_channel)), 'r-', Length, 0.80, 'b-', Length,
Effect_UCI, 'g-')
axis([0, 4*Length_calc_TierI, 0, 1])
title('NOx Conversion')
xlabel('Length (m)')
ylabel('Conversion')
legend('5mm ch')


% Plot concentration profile
%Length = linspace(0, 4 * Length_calc_TierI, 1000);
%plot(Length, exp((-K_mass_trans_OA * Perimeter_ch *
Length)/(Mass_flow_exh/Num_channel)), Length, (exp((-K_mass_trans_OA *
Perimeter_ch * Length)/(Mass_flow_exh/Num_channel))/Deact), 'r-', Length,
0.20, 'b-', Length, 1-Effect_UCI, 'g-')
%axis([0, 4*Length_calc_TierI, 0, 1])
%title('NOx Conversion')
%xlabel('Length (m)')
%ylabel('Conversion')
%legend('5mm ch')


% WRITE DATA TO DESIGN SUMMARY FILE
fid = fopen('C:\Matlab NOx\Summary.txt','a');
fprintf(fid,'Re max:                    %6.0f \n', Re_max);
fprintf(fid,'Velocity max:              %6.2f m/sec\n', V_max_Re);
fprintf(fid,'Required channel area:     %6.2f m^2\n', Area_ch_req);
fprintf(fid,'Min number channels:       %6.0f \n', Num_channel);
fprintf(fid,'Min number of blocks:      %6.0f \n', Num_blocks);
fprintf(fid,'Min cross sect SCR:        %6.2f m^2\n', Area_cross_sect);
fprintf(fid,'Friction factor:           %6.4f \n', Fm);
fprintf(fid,'Delta P per meter:         %6.2f Pa/m\n', Delta_P_1m);
fprintf(fid,'Effect Diff Coeff NO:      %6.2e m^2/sec\n', D_eff_NO);
fprintf(fid,'Effect Diff Coeff NO Corr: %6.2e m^2/sec\n', D_eff_NO_corr);
fprintf(fid,'Activation Energy (Ea):    %6.2f J/mol\n', Ea_SCR);
fprintf(fid,'Pre-exponential factor:    %6.2f m^3/kg-sec\n',
A_pre_exp_SCR);
fprintf(fid,'Rate const calc:           %6.4f m^3/kg-sec\n', K_SCR);
fprintf(fid,'Intrinsic rate (exp):      %6.4f m^3/kg-sec\n', K_NO_Int);
fprintf(fid,'Thiele mod:                %6.2f \n', Thiele_mod);
fprintf(fid,'Efficiency:                %6.2f \n', Efficiency);
fprintf(fid,'Sherwood:                  %6.2f \n', Sherwood);
fprintf(fid,'Mass trans coeff:          %6.4f kg/m^s-sec\n', K_mass_trans);
fprintf(fid,'Overall mass trans coeff:  %6.4f kg/m^s-sec\n',
K_mass_trans_OA);
fprintf(fid,'Transfer units (TI):       %6.2f \n', Num_trans_units_TierI);
fprintf(fid,'Length calculated (TI):    %6.3f m\n', Length_calc_TierI);
fprintf(fid,'Pressure drop (TI):        %6.2f Pa\n', Delta_P_TierI);
fprintf(fid,'Transfer units (UCI):      %6.2f \n', Num_trans_units_UCI);
fprintf(fid,'Length calculated (UCI):   %6.3f m\n', Length_calc_UCI);
fprintf(fid,'Pressure drop (UCI):       %6.2f Pa\n', Delta_P_UCI);
fprintf(fid,'Years between overahaul:   %6.1f years\n', Num_years);
fprintf(fid,'Expected deactivation:     %6.2f \n', Deact);
fprintf(fid,'Length (TI) w/deact:       %6.2f m\n',
Length_calc_TierI_deact);
fprintf(fid,'Length (UCI) w/deact:      %6.2f m\n', Length_calc_UCI_deact);
fprintf(fid,' \r');
%status = fclose(fid);
```

APPENDIX C - MODEL MODULE OUTPUT PARAMETERS

Module 1 Output

```
8.31447200  29.74179706 350000.00000000 623.00000000 129.48855731
4353.75700520  64.43455947   1.00000000 52000.00000000 466158.80630869
28.96600000
```

Module 2 Output

```
2.01391976   0.00003050   0.00001514
```

Module 3 Output

```
0.80000000   0.89643747 1896.34945865 3662.23097436  46.00550000
```

Module 4 Output

```
17.03100000  30.00600000 350.00000000  70.00000000   0.40000000
```

Module 5 Output

```
0.00002097   0.00002453
```

Module 6 Output

```
0.00500000   0.00080000 1111.00000000 2274.05955004   0.00002500
0.02000000   0.00500000 3600.00000000   0.01000000   0.12166144
0.00000440
```

Module 7 Output

```
5.00000000  25.00000000  20.00000000   5.00000000
```

APPENDIX D - SUMMARY OF CALCULATIONS FOR A 11 K90 MC-C ENGINE

Summary

```
Bore:                        0.90 m
Stroke:                      2.30 m
Number of cylinders:        11.00 cyl
Rpm:                       104.00 rev/min
Power:                     52000.00 kW
Fuel oil consumption:      177.00 g/kW-hr
Lube oil consumption:        0.15 g/kW-hr
Scavenge air press:        350000.00 Pa
Scavenge air temp:          62.00 °C
Exhaust press:             350000.00 Pa
Exhaust temp:              350.00 °C
Scavenge air press:        350000.00 Pa
Scavenge air temp:          62.00 °C
Height of Scavport:          0.20 m
Cylinder volume:             1.34 m^3
MW exhaust:                 29.74 g/mol
MW air:                     28.97 g/mol
Mass flow scav air:         11.54 kg/sec-cyl
Mass flow fuel:              0.23 kg/sec-cyl
Mass flow CLO (grams):       0.20 g/sec-cyl
Mass flow exhaust:         129.49 kg/sec
Vol flow exhaust:           64.43 m^3/sec
Mass flow exhaust:         466158.81 kg/hr
Vol flow exhaust:          136529.23 SCFM

Average backpressure:      147.00 mmH20
Density exhaust:             2.01 kg/m^3
Dynamic viscosity exh:     3.05e-005 kg/m-sec
Kinetic viscosity exh:     1.51e-005 m^s/sec

NOx Tier I:                 17.00 g/kW-hr
NOx ppm Tier I (mass):     1896.35 ppm
NOx ppm Tier I (vol):      1225.96 ppm
NOx Tier III:                3.40 g/kW-hr
NOx ppm Tier III (mass):   379.27 ppm
NOx ppm Tier III (vol):    245.19 ppm
Effectiveness:               0.80
Vol flow UCI data:          80.55 m^3/sec
Vol flow UCI corrected:    189.32 m^3/sec
NOx UCI corr:               32.83 g/kW-hr
Effectiveness UCI:           0.90

Urea soln:                       40 percent by mass
Maximum slip:                   5.0 ppm by vol
Days in operation/yr:           350 days/yrea
Days in port/yr:                 70 days/year
Percent time in ECA:         0.40 percent time in ECA
Mass flow NH3 (TierI):     389.67 kg/hr
Mass flow Urea (TierI):    1717.71 kg/hr
Vol flow urea soln (T-I)     1.55 m^3/hr
Vol flow per month (T-I):  217.24 m^3/month
Mass flow NH3 (UCI):       840.65 kg/hr
Mass flow Urea (UCI):      3705.68 kg/hr
Vol flow urea soln (UCI):    3.35 m^3/hr
Vol flow per month (UCI:   468.65 m^3/month

Diffusion Coeff NO/Air:    2.10e-005 m^2/sec
Diffusion Coeff NH3/Air:   2.45e-005 m^2/sec
```

```
Width of channel:           0.005 m
Wall thickness:            0.0008 m
Area of channel:           2.50e-005 m^2
Perimeter of channel:       0.020 m
Hydraulic Diameter:         0.005 m
Number channels X:          60.00
Number channels Y:          60.00
Number channels:           3600.00
Height of element:           0.50 m
Width of element X:          0.35 m
Width of element Y:          0.35 m
Area of element:           0.1217 m^2
Volume of element:         0.0608 m^3
Surface area of channel:    0.010
Surface area per element:   36.00
Catalyst volume/channel:   4.40e-006 m^3
Catalyst volume/element:   0.0158 m^3
Specific surface area:     2274.06 m^2/m^3
Density of catalyst:       1111.00 kg/m^3
Mass element:               17.59 kg

Re max:                      2000
Velocity max:                6.06 m/sec
Required channel area:      10.64 m^2
Min number channels:       435600
Min number of blocks:         121
Min cross sect SCR:         14.72 m^2
Friction factor:           0.0071
Delta P per meter:          55.61 Pa/m
Effect Diff Coeff NO:      4.93e-006 m^2/sec
Effect Diff Coeff NO Corr: 1.41e-006 m^2/sec
Activation Energy (Ea):    56920.00 J/mol
Pre-exponential factor:    35075.00 m^3/kg-sec
Rate const calc:           0.1677 m^3/kg-sec
Intrinsic rate (exp):      0.5790 m^3/kg-sec
Thiele mod:                  8.65
Efficiency:                  0.12
Sherwood:                    2.98
Mass trans coeff:          0.0503 kg/m^s-sec
Overall mass trans coeff:  0.0140 kg/m^s-sec
Transfer units (TI):         1.61
Length calculated (TI):     1.709 m
Pressure drop (TI):         55.75 Pa
Transfer units (UCI):        2.27
Length calculated (UCI):    2.408 m
Pressure drop (UCI):        55.90 Pa
Years between overahaul:      5.0 years
Expected deactivation:       0.96
Length (TI) w/deact:         1.78 m
Length (UCI) w/deact:        2.51 m
```

APPENDIX E - EXCERPT FROM UCI DATA

Appendix C – Test Data and Calculations

C.1 Detailed Engine Operational Results

Test ID	Date	Time	Load%	Load KW	Speed rpm	Manifold Pres. bar	Intake Temp. °C	Displacement liter	Std Correction (Pa*Tstd)/(Pstd*Ta)	Calc. Exh. Flow scfm
MEISO8-1	09/25/2006	22:01:00	8.03%	4036	49.2	0.28	44	16095.2	1.180	32989
MEISO8-2	09/25/2006	22:13:00	8.03%	4035	49.3	0.29	44	16095.2	1.189	33312
MEISO8-3	09/25/2006	22:27:00	7.55%	3796	48.6	0.29	44	16095.2	1.189	32839
MEISO8-4	09/25/2006	22:43:00	7.85%	3948	49.6	0.29	44	16095.2	1.189	33515
MEISO50 1	09/26/2006	5:50:00	51.66%	25970	90.8	1.4	38	16095.2	2.244	115810
MEISO50-2	09/26/2006	6:03:00	51.60%	25940	90.1	1.45	38	16095.2	2.291	117299
MEISO50-3	09/26/2006	6:27:00	51.58%	25930	89.8	1.43	38	16095.2	2.272	115959
MEISO50-4	09/26/2006	6:41:00	51.46%	25870	89.7	1.4	38	16095.2	2.244	114408
MEISO60-1	09/26/2006	9:06:00	60.57%	30450	97.9	1.93	42	16095.2	2.702	150359
MEISO60-2	09/26/2006	9:22:00	61.73%	31030	97.8	1.94	42	16095.2	2.712	150716
MEISO60-3	09/26/2006	9:38:00	64.75%	32550	97.8	1.94	42	16095.2	2.712	150716
MEISO70-1	09/26/2006	11.05.00	69.13%	34750	101.3	2.21	44	16095.2	2.941	169309
MEISO70-2	09/26/2006	11:19:00	69.78%	35080	101.4	2.15	44	16095.2	2.886	166321
MEISO70-3	09/26/2006	11:38:00	71.45%	35920	101.5	2.15	44	16095.2	2.886	166485
MEISO70-4	09/26/2006	11:56:00	71.59%	35990	101.8	2.22	44	16095.2	2.950	170672
MEISO25 1	09/26/2006	12:54:00	28.80%	14480	73.2	0.62	42	16095.2	1.500	62381
MEISO25-2	09/26/2006	13:08:00	27.73%	13940	73.1	0.62	43	16095.2	1.495	62099
MEISO25-3	09/26/2006	13:24:00	27.15%	13650	73	0.61	42	16095.2	1.490	61830
MEISO25-4	09/26/2006	13:45:00	26.14%	13140	73.5	0.69	43	16095.2	1.559	65115

Emissions from the Main Propulsion Engine on a Pamamax Class Ship

			Exhaust	Mass Emission Rates						Load-Specific Emission Factors	ISO Corr.			calc
Test	Date	Time	Flow Rate dscfm[1]	g/hr NO	g/hr NOx	g/hr CO	g/hr CO2	g/hr SO2[2]	Load kW	g/kW-hr NOx	g/kW-hr NOx	g/kW-hr CO	g/kW-hr CO2	g/kW-hr SO2[2]
MEISO8-1	09/25/2006	22:01	32989		84962	7118	2648237	34485	4036	21.1	21.1	1.76	656	8.5
MEISO8-2	09/25/2006	22:13	33312		83948	7188	2664371	34695	4035	20.8	20.8	1.78	660	8.6
MEISO8-3	09/25/2006	22:27	32839		77055	6717	2468563	32145	3796	20.3	20.3	1.77	650	8.5
MEISO8-4	09/25/2006	22:43	33515		85038	7195	2660922	34650	3948	21.5	21.6	1.82	674	8.8
MEISO50-1	09/26/2006	5:50	115810		455087	22046	15781988	205510	25970	17.5	16.3	0.85	608	7.9
MEISO50-2	09/26/2006	6:03	117299		455857	22330	15883969	206838	25940	17.6	16.3	0.86	612	8.0
MEISO50-3	09/26/2006	6:27	115959		461561	22262	15988940	208205	25930	17.8	16.5	0.86	617	8.0
MEISO50-4	09/26/2006	6:41	114408		458674	23206	15958661	207810	25870	17.7	16.5	0.90	617	8.0
MEISO60-1	09/26/2006	9:06	150359		615434	26076	20346706	264951	30450	20.2	18.6	0.86	668	8.7
MEISO60-2	09/26/2006	9:22	150716		608488	25406	20160004	262520	31030	19.6	18.1	0.82	650	8.5
MEISO60-3	09/26/2006	9:38	150716		595212	24982	19933123	259565	32550	18.3	16.9	0.77	612	8.0
MEISO70-1	09/26/2006	11:05	169309		718194	27693	23391551	304600	34750	20.7	19.3	0.80	673	8.8
MEISO70-2	09/26/2006	11:19	166321	654968	699593	26335	22753774	296295	35080	19.9	18.6	0.75	649	8.4
MEISO70-3	09/26/2006	11:38	166485		718921	27216	23485665	305826	35920	20.0	18.7	0.76	654	8.5
MEISO70-4	09/26/2006	11:56	170672		726331	27900	23631453	307724	35990	20.2	18.9	0.78	657	8.6
MEISO25-1	09/26/2006	12:54	62381		223490	21575	7794101	101493	14480	15.4	14.7	1.49	538	7.0
MEISO25-2	09/26/2006	13:08	62099		227176	24410	8135143	105934	13940	16.3	15.6	1.75	584	7.6
MEISO25-3	09/26/2006	13:24	61830	217689	227323	25949	8095452	105417	13650	16.7	15.9	1.90	593	7.7
MEISO25-4	09/26/2006	13:45	65115		235739	27533	8394885	109316	13140	17.9	17.1	2.10	639	8.3

[1] Exhaust flow calculated from engine rpm, intake press./temp and displacement

[2] Per ISO 8178, SO2 mass emissions calculated from fuel S% and BSFC